

VARIABILITY AND CONTROLS OF PRODUCTION, PARTITIONING, AND  
UTILIZATION OF ORGANIC MATTER IN THE NORTH PACIFIC SUBTROPICAL GYRE

A DISSERTATION SUBMITTED TO THE OFFICE OF GRADUATE EDUCATION OF THE  
UNIVERSITY OF HAWAI'I AT MĀNOA IN PARTIAL FULFILLMENT OF THE  
REQUIREMENTS FOR THE DEGREE OF

DOCTOR OF PHILOSOPHY

IN

OCEANOGRAPHY

May 2016

By

Donn Andrew Viviani

Dissertation Committee:

Matthew J. Church, Chairperson

David M. Karl

Craig E. Nelson

Grieg F. Steward

Megan J. Donahue, outside member

Keywords: primary productivity, dissolved organic carbon, bacterial production, ocean  
acidification, North Pacific Subtropical Gyre, Station ALOHA



© Copyright 2016 Donn A. Viviani

All rights reserved.

## DEDICATION

This dissertation is dedicated to my parents and grandparents for the value they placed on education and on figuring things out, my siblings for their love and support, and to Aurora.

## ACKNOWLEDGEMENTS

This work would not have been possible without the assistance of many people and organizations. I would like to acknowledge the financial support of the American taxpayer, through the National Science Foundation, via grants to Matthew J. Church (OCE-0850827 and OCE-1260164) and to the Center for Microbial Oceanography: Research and Education (EF-0424599). I would also like to acknowledge the financial support of the Simons Foundation via the Simons Collaboration on Ocean Processes and Ecology (SCOPE) and the Gordon and Betty Moore Foundation. I would also like to acknowledge the financial support of the Department of Oceanography, as well as the administrative and logistical support of the Department of Oceanography, especially from Kristin Momohara, Anne Lawyer, and Catalpa Kong.

I would like to thank my adviser, Matthew Church, for his unwavering support, as well as for bringing me to UH Manoa to study in his lab. It has been a privilege and an education to observe his trajectory as a scientist and a principal investigator. I have deeply appreciated his wisdom, conscientiousness, insight, and friendship. I am also indebted to David Karl for his support, encouragement, and consistent ability to provide new insight on any question. I would like to acknowledge the encouragement, wisdom, and insight of the other members of my committee, Grieg Steward, Craig Nelson, and Megan Donahue.

This work would not have been possible without the assistance and fellowship of the personnel of the Hawaii Ocean Time-series (HOT) program. I am deeply grateful to the physical oceanography team, including Fernando Santiago-Mandujano, Jeffrey Snyder, Paul Lethaby, Daniel McCoy, Walt Deppe, Joseph Gum, Craig Nosse, and Cammy Fumar. Much of what I know about being an oceanographer, I learned on HOT cruises, and I am indebted to the BEACH

team for their friendship, encouragement, and assistance. I want to recognize Susan Curless, Dan Sadler, Lance Fujieki, Blake Watkins, Brett Updyke, Karin Björkman, Brenner Wai, Ken Doggett, Eric Grabowski, Adriana Harlan, Jay Wheeler, and Alex Nelson for their support and fellowship. I also want to acknowledge the leadership of Roger Lukas and Dave Karl, as well as the assistance I have received from HOT co-PI's, particularly Bob Bidigare, John Dore, and Ricardo Letelier. I am also deeply grateful to members of the Church lab for collecting samples for me during the summer 2012 occupation of Station ALOHA, including Brenner Wai, Shimi Rii, Daniela Böttjer, Christina Johnson, and Sara Thomas. I am also indebted to my partner in ocean acidification experiments, Daniela Böttjer, for being flexible, friendly, and an extremely outstanding scientist. I also thank the captains, crew, and OTG technicians from the R/V Kilo Moana and R/V Kaimikai-o-Kanaloa for providing a safe and welcoming environment in which to do science.

I have also been fortunate that my graduate career coincided with the Center for Microbial Oceanography: Research and Education. I am grateful for the support provided by CMORE, and the assistance and fellowship of CMORE personnel, including Tara Clemente, Sam Wilson, Georgia Tanaka, Sharon Sakamoto, and Steve Poulos. I am also thankful for the encouragement provided by CMORE faculty, including Barb Bruno and Rosie Alegado. I am grateful to UH Oceanography professors Mike Mottl and Niklas Schneider for serving on my qualifying exam committee. I am appreciative of the many thoughtful comments and suggestions from UH Oceanography professors Mark Merrifield and Anna Neuheimer. I am also indebted to many graduate students and postdoctoral scholars for their support and friendship, including Shimi Rii, Chris Schvarz, Anela Choy, Thomas Kilpatrick, Benedetto Barone, Allyn Fetherolf, Scott Grant, Kristen Fogaren, and Hilary Close.

The support of my family and friends was invaluable. I am deeply grateful to my local ohana for their love and support, particularly Wendy Gibson, Debora Halbert, Bruce Guard, Gail and Bob Woliver, the extended Ho family, the extended Kagawa family, the Wong family, and the Revestir family. I could not have done this without my siblings Anne Viviani, Frank Holland, Will Viviani, and Tony Viviani. I also want to thank Eldred Kagawa, Merry Chris Ho, Donn Viviani, Anne Viviani, and Aurora Kagawa-Viviani for their love and support.

## ABSTRACT

Oceans account for approximately half of global primary production, and oligotrophic gyres account for a large fraction of this production. Understanding of time-varying changes to ocean ecosystems largely derives from time-series observations. Since 1988, the Hawaii Ocean Time-series (HOT) program has conducted near-monthly sampling at Station ALOHA (22° 45'N, 158° 00'W), providing information on the magnitude and pathways of carbon cycling in the North Pacific Subtropical Gyre (NPSG). These observations have identified microbial production and consumption of organic matter as major processes catalyzing upper ocean carbon fluxes. In this dissertation, I quantified rates of dissolved and particulate organic carbon production over daily to annual time scales in this ecosystem. Measured rates of primary production (PP) demonstrated significant depth-dependence, unlike rates of dissolved organic carbon (DOC) production. On average, depth-integrated (0–75 m) rates of DOC production were equivalent to  $18 \pm 10\%$  of total (particulate and dissolved) productivity. My findings indicate that in this oligotrophic ecosystem, rates of dissolved and particulate production appear temporally decoupled over daily to monthly time scales. In addition, over a ~2-year period, I quantified rates of bacterial production (BP) at near-monthly time scales, to evaluate potential coupling between photosynthetic production of organic matter and its consumption by heterotrophic bacteria. There was no temporal correlation between rates of bacterial growth and primary production across daily to seasonal time scales, with BP lagging rates of PP by 1 to 2 months. Moreover, in the well-lit (<45 m) upper ocean, there was a significant relationship between seawater temperatures and bacterial production. In the lower euphotic zone (>75 m), there was no significant relationship between temperature and bacterial production. My results suggest photosynthetic production varies seasonally with changes in light, while bacterial production appears more

sensitive to variations in upper ocean temperature. I also experimentally evaluated the effects of abrupt changes to the seawater carbonate system on rates of primary and bacterial production at Station ALOHA. These experiments revealed that abrupt changes in the partial pressure of seawater CO<sub>2</sub> ( $p\text{CO}_2$ ) had little effect on rates of primary and bacterial production in this persistently oligotrophic ecosystem.

## TABLE OF CONTENTS

Acknowledgements.....	v
Abstract.....	viii
List of Tables .....	xiii
List of Figures.....	xiv
<b>Chapter 1: An introduction to the production and consumption of organic matter in the open ocean.....</b>	<b>1</b>
Introduction.....	1
Dissolved organic material in the marine environment.....	1
Partitioning of recently fixed carbon into particulate and dissolved pools .....	3
Bacterial production in the marine environment.....	5
Changes to the seawater carbonate system and its potential impacts on rates of production ..	6
Overall objectives of this research .....	10
Literature cited .....	13
<b>Chapter 2: Variability in photosynthetic production of dissolved and particulate organic carbon in the North Pacific Subtropical Gyre .....</b>	<b>24</b>
Abstract .....	24
Introduction.....	26
Materials and methods .....	29
Chlorophyll <i>a</i> and <sup>14</sup> C-based productivity measurements .....	29
Measurements of <sup>14</sup> C-DOC production .....	31
Diel variability in productivity .....	32
Filter retention characteristics .....	32
Contextual biogeochemical analyses .....	34
Data analyses and statistics .....	35
Results.....	36
Biogeochemical context .....	36
Measurements of <sup>14</sup> C-productivity and chlorophyll <i>a</i> .....	37
Temporal variability in rates of <sup>14</sup> C-based productivity .....	39
Diel variability in rates of productivity .....	41
<sup>14</sup> C-DOC retention by filter type.....	42
Discussion .....	43

Literature cited .....	53
<b>Chapter 3: Temporal variability in bacterial production in the North Pacific Subtropical Gyre</b> .....	<b>72</b>
Abstract .....	72
Introduction .....	74
Methods .....	76
<sup>14</sup> C-primary production and <sup>3</sup> H-leucine incorporation measurements .....	76
Time-course experiments to evaluate linearity of <sup>3</sup> H-leucine incorporation.....	79
Contextual measurements of light, cell abundances, and nutrients.....	81
Statistics and data analysis .....	82
Results .....	83
Time-course experiments to evaluate linearity of <sup>3</sup> H-leucine incorporation.....	84
Monthly and seasonal scale variability in rates of <sup>3</sup> H-leucine incorporation.....	84
Daily and diel scale variability .....	86
Proportion of BP to <sup>14</sup> C-PP and cell-specific rates of production.....	87
Statistical relationships between <sup>3</sup> H-Leu, <sup>14</sup> C-PP, temperature, and PAR.....	88
Discussion .....	89
Literature cited .....	96
<b>Chapter 4: The influence of abrupt increases in seawater <i>p</i>CO<sub>2</sub> on rates of microbial production in the subtropical North Pacific Ocean</b> .....	<b>113</b>
Abstract .....	113
Introduction .....	115
Methods.....	118
Experimental design .....	118
Total alkalinity, dissolved inorganic carbon, and pH.....	119
Measurements of <sup>14</sup> C-primary production.....	120
<sup>3</sup> H-leucine incorporation measurements.....	121
Statistics and data analysis .....	123
Results .....	123
The response in rates of <sup>14</sup> C-PP and <sup>3</sup> H-Leu to elevated seawater <i>p</i> CO <sub>2</sub> .....	124
Depth-dependent responses in <sup>14</sup> C-PP and <sup>3</sup> H-Leu to carbonate perturbations .....	126

Discussion .....	129
Literature cited .....	135
<b>Chapter 5: Conclusion</b> .....	152
Literature cited .....	158

## LIST OF TABLES

Table 2.1. Seasonally averaged rates of productivity and irradiance for the two time periods of this study .....	60
Table 2.2: Mean of <sup>14</sup> C-DOC concentrations measured at the beginning and end of incubation period at six euphotic zone depths evaluated in this study .....	61
Table 2.3: Descriptive characteristics of production-irradiance curve fitting results based on the Platt et al. (1980) model.....	62
Table 3.1: Depth-integrated (mean and standard deviation) rates of <sup>3</sup> H-leucine incorporation, <i>Prochlorococcus</i> and non-pigmented bacteria abundances, and rates of per-cell <sup>3</sup> H-leucine incorporation .....	102
Table 3.2: Linear regression analyses evaluating temporal coupling among rates of <sup>3</sup> H-leucine incorporation, <sup>14</sup> C-PP, and variation in temperature, PAR, and bacterial abundances.....	103
Table 4.1: Near-surface (5 m) temperatures, chlorophyll <i>a</i> concentrations, rates of <sup>14</sup> C-PP, nutrient concentrations, and seawater carbonate system properties during those months when experiments were initiated .....	140
Table 4.2: Percent differences between <i>p</i> CO <sub>2</sub> elevated treatments (1100 ppm unless noted) and controls ([CO <sub>2</sub> perturbed - control] / control) in bubbling experiments for <sup>14</sup> C-PP, <sup>3</sup> H-Leu <sub>Dark</sub> , and <sup>3</sup> H-Leu <sub>Light</sub> .....	141
Table 4.3: Depth-integrated rates of <sup>14</sup> C-PP measured under both ambient (<390 ppm at depths shallower than 45 m) and enhanced <i>p</i> CO <sub>2</sub> (750 ppm) conditions in both upper (0–45 m) and lower euphotic zones (75–125 m) for three plankton size fractions (10, 2, and 0.2 μm).....	142
Table 4.4: Depth-integrated rates of <sup>3</sup> H-Leu (light and dark) incubated under both ambient (390 ppm) and enhanced <i>p</i> CO <sub>2</sub> (750 ppm) for both the upper (0–45 m), lower (75–125 m), and full euphotic zone (0–125 m) .....	143

## LIST OF FIGURES

Figure 1.1: Schematic outlining pathways through which recently photosynthesized organic matter may flow through an open ocean food web.....	20
Figure 1.2: Time-averaged (1988–2014) nitrate + nitrite, chlorophyll <i>a</i> , <sup>14</sup> C-PP, and photosynthetically available radiation (PAR) at Station ALOHA.....	21
Figure 1.3: Monthly binned incident PAR and depth-integrated <sup>14</sup> C-PP at Station ALOHA .....	22
Figure 1.4: Schematic depicting <sup>14</sup> C-PP and currently constrained at Station ALOHA along with rates to be constrained as part of this dissertation.....	23
Figure 2.1: Depth profiles of mean upper ocean properties at Station ALOHA during the period of study (2004–2013).....	63
Figure 2.2: Vertical profiles of rates of <sup>14</sup> C-GFF, <sup>14</sup> C-PC, and <sup>14</sup> C-DOC .....	64
Figure 2.3: Contour plots showing <sup>14</sup> C-GFF, <sup>14</sup> C-PC, and <sup>14</sup> C-DOC over the time periods of this study (October 2004–October 2007 and April 2010–October 2012) .....	65
Figure 2.4: Comparison of measurements of chlorophyll <i>a</i> and <sup>14</sup> C-PP on either glass fiber or polycarbonate filters.....	66
Figure 2.5: Relationship between downwelling photosynthetically active radiation and rates of <sup>14</sup> C-GFF, <sup>14</sup> C-PC, and <sup>14</sup> C-DOC .....	67
Figure 2.6: Time-series measurements of depth-integrated (0–75 m) rates of <sup>14</sup> C-GFF, <sup>14</sup> C-PC, <sup>14</sup> C-delta, and <sup>14</sup> C-DOC .....	68
Figure 2.7: Results from experiments examining daytime and nighttime changes in hourly rates of carbon fixation.....	69
Figure 2.S1: Results from experiments comparing retention of <sup>14</sup> C organic matter onto either glass fiber or polycarbonate membrane filters.....	70
Figure 2.S2: Differences between <sup>14</sup> C-activity on glass fiber and polycarbonate filters ( <sup>14</sup> C-delta = <sup>14</sup> C-GFF - <sup>14</sup> C-PC) where different volumes of seawater were filtered .....	71
Figure 3.1: Mixed layer depth, sea surface temperatures, photosynthetically available radiation, and <sup>14</sup> C-PP at Station ALOHA during the period of study (2011–2013) .....	105
Figure 3.2: Representative time-course experiment showing incorporation of <sup>3</sup> H-leucine as a function of incubation time.....	106
Figure 3.3: Vertical profiles of <sup>3</sup> H-Leu <sub>Dark</sub> and <sup>3</sup> H-Leu <sub>Light</sub> and the ration of <sup>3</sup> H-Leu <sub>Light</sub> to <sup>3</sup> H-Leu <sub>Dark</sub> .....	107

Figure 3.4: Time-series of depth-integrated rates of $^{14}\text{C}$ -PP, $^3\text{H}$ -Leu <sub>Dark</sub> , and $^3\text{H}$ -Leu <sub>Light</sub> .....	108
Figure 3.5: Daily and monthly time-series of $^3\text{H}$ -Leu <sub>Dark</sub> , and $^3\text{H}$ -Leu <sub>Light</sub> at 25 m.....	109
Figure 3.6: Daily and monthly time-series of $^{14}\text{C}$ -PP at 25 m .....	110
Figure 3.7: Diel measurements of $^3\text{H}$ -Leu <sub>Dark</sub> , and $^3\text{H}$ -Leu <sub>Light</sub> .....	111
Figure 3.8: Cell specific $^3\text{H}$ -leucine incorporation and bacterial production to primary production ratios.....	112
Figure 4.1: Distributions of near-surface ocean chlorophyll concentrations and locations of stations occupied during August 2010.....	144
Figure 4.2: Surface ocean $p\text{CO}_2$ (detrended), sea surface temperature, chlorophyll $a$ , and nitrate + nitrate binned by month at Station ALOHA.....	145
Figure 4.3: Comparison of seawater carbonate system properties during the time course experiments conducted for this study .....	146
Figure 4.4: Percent differences between control and perturbed treatments from $p\text{CO}_2$ bubbling experiments for $^{14}\text{C}$ -PP, $^3\text{H}$ -Leu <sub>Dark</sub> , and $^3\text{H}$ -Leu <sub>Light</sub> .....	147
Figure 4.5: Ratio of calculated $p\text{CO}_2$ versus target $p\text{CO}_2$ from <i>in situ</i> array experiments .....	148
Figure 4.6: Depth-resolved measurements of size fractionated $^{14}\text{C}$ -PP during cruises in August 2010 and March 2011 .....	149
Figure 4.7: Percent differences between control (<390 ppm) and elevated $p\text{CO}_2$ (750 ppm) treatments from depth-resolved $^{14}\text{C}$ -PP experiments during cruises in August 2010 and March 2011.....	150
Figure 4.8: Rates of $^3\text{H}$ -leucine incorporation at both ambient and enhanced (750 ppm $p\text{CO}_2$ ) in both light and dark for cruises in August 2010 and March 2011.....	151
Figure 5.1: Schematic depicting $^{14}\text{C}$ -primary production at Station ALOHA along with rates constrained as part of this dissertation .....	159

## **Chapter 1 - An introduction to the production and consumption of organic matter in the open ocean**

Marine primary production accounts for approximately  $50 \text{ Pg C yr}^{-1}$ , or nearly half of the net organic matter production on Earth (Behrenfeld & Falkowski 1997, Field et al. 1998). Much of this productivity occurs in the vast, low nutrient subtropical ocean gyres. In these ecosystems the reduction of inorganic carbon to organic carbon is fueled predominately by photosynthetic plankton. Hence, quantifying photosynthetic carbon fixation and identifying the fate of this material are central to our understanding of the cycling of carbon on this planet.

### **Dissolved organic material in the marine environment**

Organic matter in the marine environment is chemically and structurally diverse, including both dissolved and particulate phases. Dissolved organic matter (DOM), operationally defined as reduced carbon substrates small enough to pass through filters (typically either glass fiber filters with a nominal pore size of  $0.7 \mu\text{m}$  or  $0.2 \mu\text{m}$  pore size polycarbonate membrane filters), constitutes the largest pool of reduced carbon in the sea, equivalent to  $\sim 700 \text{ Pg C}$  or  $>90\%$  of the total oceanic organic matter inventory (Hedges 1992). The bulk DOM pool turns over slowly (century to millennia time scales), which suggests that the dominant components of this pool are biologically unreactive (Druffel et al. 1992, Kaiser & Benner 2009). Although a major fraction (approximately 80-85% of the total; Hansell et al. 2009) of the DOM pool resists degradation over ecologically meaningful time scales (daily to annual scales), the flux of carbon through this pool is large ( $\sim 30 \text{ Pg C yr}^{-1}$ ; Williams 2000), forming one of the largest pathways for the movement of C through ocean ecosystems.

Despite its relevance to carbon cycling, to date we know relatively little about rates of DOM production, consumption, or the factors controlling its cycling in the open sea. Production of DOM is an integral part of the microbial food web, and is known to occur through a variety of trophodynamic processes (Figure 1.1) including direct exudation by phytoplankton (Lignell 1990), viral-mediated cell lysis (Evans et al. 2009), and zooplankton feeding and excretion (Lampert 1978, Banse 1995). It is unclear how much each of these processes contributes to DOM production, and whether their relative contributions to DOM production vary with time, changes in plankton community structure, or alterations in habitat. Early work examined whether DOM exudation from phytoplankton was a process that occurred in natural communities or was instead an artifact of field and laboratory methods (Sharp 1977). Other work has confirmed the existence and importance of algal production of DOM (Hellebust 1965, Mague et al. 1980), but ranges of DOM production as a percentage of total primary production (percent extracellular release; PER) reported from phytoplankton show large variability (Fogg 1966, Lancelot 1979, Karl et al. 1998, Morán & Estrada 2001).

The major sink for DOM is through heterotrophic bacterial metabolism, including bacterial production of cell biomass (anabolism) and respiratory catabolism (Ducklow et al. 2000, Williams 2000). Bacterial production of cell biomass from DOM is a central component of the microbial food web (Pomeroy 1974, Azam et al. 1983). However, in the open ocean, bacterial growth efficiencies (defined as the proportion of cell biomass produced relative to carbon consumed to support both biomass production and cell respiratory demands) are estimated to be between 10 and 15% (del Giorgio & Cole 1998, Carlson et al. 1999), implying that a large fraction (85–90%) of the DOC consumed by these organisms is catabolized for energy. This process is accompanied by consumption of oxygen and remineralization of organic carbon into

CO<sub>2</sub>. Hence, quantifying the rates at which photosynthetically fixed carbon enters the DOM pool, together with measurements of bacterial metabolism and growth, provide important information on major pathways for biological carbon cycling in the sea.

### **Partitioning of recently fixed carbon into particulate and dissolved pools**

Variability in the partitioning of photosynthetically fixed carbon between dissolved and particulate phases has important implications for the fate of carbon in the marine ecosystem. Production of particulate organic carbon (POC) supports particle-feeding organisms, ranging from micrograzers such as ciliates and flagellates (Sherr & Sherr 2002, Pasulka et al. 2013) to larger predators such as copepods (Turner 2004). Not only does recently produced POC form the base of the food web, it also contributes to carbon export, a process known as the biological pump, where particles derived from larger organisms or aggregations of phytoplankton sink into the deep ocean due to gravitational settling (Turner 2002, Robison et al. 2005, Karl et al. 2012). In contrast, DOM is not accessible to these larger organisms, and thus would be lost to the food web, were it not for the presence of osmotrophic bacteria, that can take up DOM and use it to fuel their metabolic needs (Kirchman 2004). Once the heterotrophic bacteria consume DOM and assimilate some fraction of this material into cell biomass, the carbon becomes part of the POC pool, and thus subject to trophic exchange through a predation-based food web (Pomeroy 1974, Azam et al. 1983). In this way, microbial consumption of DOM makes this material available to the food web, with the potential for export as sinking particles.

Our current understanding of the processes that influence how photosynthetic production is partitioned between dissolved and particulate phases remains poor. For example, we know relatively little about how episodic- to seasonal-scale changes to the ocean habitat – for example

alteration of nutrient concentrations, light availability, and/or plankton community composition – influence the partitioning of recently fixed organic carbon between dissolved and particulate phases. Moreover, it remains unclear how, or even whether, progressive changes to the ocean carbonate system due to anthropogenic CO<sub>2</sub> emissions might alter the partitioning of organic matter between dissolved and particulate phases or influence bacterial consumption of DOM. Similarly there are relatively few data available for gauging the sensitivity of bacterial growth to changes in habitat conditions in the open sea.

Investigation of the factors influencing the partitioning of organic matter between dissolved and particulate phases and its associated time variability would benefit from being conducted in the context of well-resolved contextual environmental measurements, like those of the Hawaii Ocean Time-series (HOT) program. Station ALOHA (A Long Term Oligotrophic Habitat Assessment; 22.75°N, 158°W) is the field site of the HOT program, and is located within the North Pacific Subtropical Gyre (NPSG). Subtropical oceanic gyres make up approximately 40% of the surface of the Earth, with the NPSG comprising one of the largest biomes on the planet, covering an area greater than  $2 \times 10^7$  km<sup>2</sup> (Karl 1999). The 27+ year time-series record from Station ALOHA (Karl & Lukas 1996) has provided valuable information on seasonal to subdecadal variability in nutrient supply, primary production, and microbial community structure in the oligotrophic NPSG (Campbell et al. 1994, Winn et al. 1995, Letelier et al. 1996, 2004, Karl et al. 2001, Dore et al. 2008, Church et al. 2009, Karl & Church 2014). Among the major distinguishing characteristics of the NPSG ecosystem are low concentrations of inorganic nutrients in the upper euphotic zone, deep penetration of sunlight into the water column, and a persistent deep chlorophyll maximum layer (Figure 1.2). In spite of the fact that euphotic zone

nutrients are persistently low, rates of primary production (as estimated by the  $^{14}\text{C}$ -bicarbonate assimilation technique) are relatively high (averaging  $184 \text{ g C m}^{-2} \text{ yr}^{-1}$ ).

The sustained, near-monthly HOT program climatology shows that the upper ocean habitat at Station ALOHA exhibits weak to moderate seasonality in important biogeochemical properties and processes. For example, rates of particulate matter production vary ~2-3-fold seasonally, increasing during the summer months when the upper ocean is warm, stratified, and nutrient-poor, and decreasing during the winter with seasonal declines in irradiance (Figure 1.3). Temporal variability associated with photosynthetic production of dissolved organic matter remains largely unknown in this ecosystem, although the contribution of recently photosynthesized DOC to total primary production appears to be a significant component of the daily rate of carbon fixation (Karl et al. 1998).

### **Bacterial production in the marine environment**

The measurement of bacterial production provides a constraint on the magnitude of DOM flux required to support synthesis of new bacterial biomass. Across diverse aquatic ecosystems, rates of bacterial production are often estimated equivalent to 10–30% of contemporaneous rates of photosynthetic carbon fixation (Cole et al. 1982, Ducklow & Carlson 1992, Ducklow 1999, Kirchman et al. 2009). Assuming bacterial growth efficiencies range between 10 and 15%, bacterial metabolism and production are equivalent to >70% of contemporaneous rates of primary production (Church 2008). Hence, estimates of the magnitude and variability associated with bacterial growth in the sea are critical to understanding ocean carbon cycling. At the Bermuda Atlantic Time-series Study (BATS) in the Sargasso Sea, rates of bacterial production have been shown to demonstrate only weak to moderate seasonality, with rates generally

increasing 2-3-fold during the mid summer and declining into the fall and winter (Carlson et al. 1996, Steinberg et al. 2001). These patterns are temporally decoupled from the relatively strong seasonality demonstrated by primary production at this site, where rates of  $^{14}\text{C}$ -primary production can vary more than 10-fold, with peak rates of primary production occurring in the early spring (Steinberg et al. 2001, Church et al. 2013). This offset suggests that coupling between phytoplankton and bacteria in the open ocean can be complicated and controlled by multiple factors. Thus, significant uncertainties remain in our understanding of upper ocean biological carbon cycling, including rates of productivity and metabolism, and the partitioning between dissolved and particulate material (Figure 1.4).

### **Changes to the seawater carbonate system and its potential impacts on rates of production**

Overlaid upon gaps in our understanding of contemporary planktonic growth and metabolism in the ocean is uncertainty in how future changes to the ocean habitat will influence ecological and biogeochemical processes in the sea. Human socioeconomic activities, specifically fossil fuel combustion, cement production, and changes in land use, have resulted in progressive increases in atmospheric and oceanic  $\text{CO}_2$  inventories (IPCC 2014). The ocean is a globally important net sink for  $\text{CO}_2$ , and as such, has already absorbed a significant fraction of anthropogenic carbon (Sabine et al. 2004), resulting in progressive increases the  $p\text{CO}_2$  of seawater, with concomitant decreases in seawater pH (Wolf-Gladrow et al. 1999, Zeebe et al. 2008, Doney et al. 2009, Dore et al. 2009). Such changes have been accompanied by long-term decreases in the saturation state of calcite and aragonite (Orr et al. 2005, Doney et al. 2009).

Studies investigating the effects of changes in seawater carbonate chemistry on coupling between primary and bacterial production in oligotrophic ocean ecosystems are relatively scarce.

While an appropriate null hypothesis could be that ocean acidification may lead to no significant changes in marine microbial contributions to biogeochemical cycling (Joint et al. 2011), testing such a hypothesis will demand rigorous experimental evidence. Previous results and observations suggest that, either as individual species or microbial assemblages, marine microbial physiology may be affected by increases in  $p\text{CO}_2$  (Riebesell et al. 2000, Tortell et al. 2002, 2008, Grossart et al. 2006, Hutchins et al. 2007, Beman et al. 2010). An important question is whether these changes in microbial physiology are large enough to influence ocean biogeochemical cycles; the overall size of these ecosystems implies that even small changes in these rates can have large effects on biogeochemical cycling.

To date, there is relatively little known about the capacity of phytoplankton to adapt or acclimate to changes in the seawater carbonate system. These changes are likely to have complex influences on ocean biology. Major lineages of phytoplankton found in the contemporary oceans evolved during periods in Earth's history when atmospheric and oceanic  $\text{CO}_2$  inventories were considerably greater than found today (Raven 1997a, Tortell 2000). Nonetheless, there is compelling evidence that for some groups of phytoplankton, declines in carbonate ion concentrations that accompany decreases in seawater pH can be detrimental to growth (Riebesell et al. 2000). Improving our predictive knowledge of how such changes in seawater chemistry may influence planktonic organisms will require additional experiments and research.

There are good reasons to believe that growth of phytoplankton may be augmented under higher  $p\text{CO}_2$  conditions. The overall efficiency of phytoplankton metabolism may currently be depressed as a result of limited availability of accessible inorganic carbon. As a result, increasing  $\text{CO}_2$  concentrations could reduce the need for phytoplankton to produce enzymes that transport inorganic carbon or serve as Carbon Concentrating Mechanisms (CCM), for example carbonic

anhydrases (Beardall & Raven 2004, Giordano et al. 2005, Levitan et al. 2010). Ribulose-1,5-bisphosphate carboxylase oxygenase (RuBisCO), the enzyme that initiates CO<sub>2</sub> reduction, appears to have evolved at a time in Earth's history when seawater *p*CO<sub>2</sub> was elevated and O<sub>2</sub> concentrations were low (Bernier 1990, Tortell 2000), and consequently this enzyme acts as either an oxygenase (reducing O<sub>2</sub> to phosphoglycolate, also called photorespiration) or a carboxylase (binding CO<sub>2</sub> into 3-phosphoglycerate and from there to larger organic molecules; Raven 1997b). Phytoplankton appear to have evolved a number of ways to deal with potential undersaturation of RuBisCO with respect to CO<sub>2</sub> (Badger et al. 2002, Falkowski & Raven 2007), thus avoiding the wasteful photorespiratory pathway. These strategies include increasing intracellular CO<sub>2</sub> concentrations via uptake of inorganic carbon, and maintaining concentrations many times greater within the cell than outside the cell (Badger 2003) thus minimizing the oxygenase activity of RuBisCO (Badger et al. 2002, 2006, Price et al. 2002, Badger 2003). In addition to active transport of HCO<sub>3</sub><sup>-</sup>, phytoplankton may utilize several enzymatic pathways to concentrate HCO<sub>3</sub><sup>-</sup> to CO<sub>2</sub>; for example, carbonic anhydrases supply CO<sub>2</sub> to the active site of RuBisCO (Raven et al. 2011). Several strains of marine cyanobacteria belonging to the genus *Synechococcus* sp. take up both CO<sub>2</sub> and HCO<sub>3</sub><sup>-</sup> and actively transport both forms of inorganic carbon (Badger & Andrews 1982, Price et al. 2002). In contrast, *Prochlorococcus* sp. appear to lack the ability to take up CO<sub>2</sub> directly (Badger et al. 2006, Price 2011), with the marine cyanobacterium *Prochlorococcus* MED4 relying on only one or two efficient HCO<sub>3</sub><sup>-</sup> transporters (Hopkinson et al. 2014). *Prochlorococcus* MED4 is notable for its minimal genome size, and differs from other cyanobacteria in that it apparently does not utilize a carbonic anhydrase (Rocap et al. 2003). *Prochlorococcus* is an important phototroph at Station ALOHA in terms of both abundance and production (Campbell et al. 1994, Liu et al. 1997).

The vast majority of  $p\text{CO}_2$  manipulation studies have examined the response of specific organisms to changes in seawater carbonate chemistry in the laboratory, where growth conditions are controlled and organisms are generally examined in isolation. Few studies have looked at interactive planktonic community scale dynamics, and as a result, the feedbacks that normally exist in open ocean communities have not generally been investigated. Recent experiments conducted in coastal waters found that enhanced  $p\text{CO}_2$  shifted the partitioning of carbon fixed during primary production from the particulate to the dissolved phase (Kim et al. 2011); while other mesocosm experiments conducted in fjords revealed increased bacterial growth (Grossart et al. 2006, Piontek et al. 2013) and elevated polysaccharide degradation (Piontek et al. 2010) in treatments in which seawater  $p\text{CO}_2$  was increased. These interesting results highlight the need to perform such experimental manipulations in the open ocean, where a major fraction of global productivity occurs.

Increasing seawater  $p\text{CO}_2$  could also influence heterotrophic bacterial growth, through both direct changes in metabolism (*i.e.* alteration in seawater pH influencing enzymatic reactions) or via indirect interactions (*i.e.* changes in organic matter production, partitioning, or substrate lability). Because of the magnitude of the carbon flux through heterotrophic bacteria, even small changes in rates of respiration or in bacterial growth efficiencies could have a major effect on carbon cycling. Likewise, the importance of the microbial loop to maintaining rates of primary production in oligotrophic waters suggests that changes in heterotrophic metabolic rates would alter community metabolism.

The relative partitioning of primary production between particulate and dissolved phases has important implications for the carbon cycling of the open ocean, and therefore, because of the size of the open ocean, for global carbon cycling. Similarly the degree of coupling between

the metabolic activity of bacteria and primary producers is important for understanding processes controlling carbon cycling through the microbial loop. In order to understand the potential effects of anthropogenic derived changes to the seawater carbonate system on primary and bacterial production, a better understanding of partitioning of primary production between dissolved and particulate phases, the time variability of rates of bacterial production, and the coupling between these processes in the contemporary ocean is required.

### **Overall objectives of this research**

The overall objectives of my doctoral research were to measure the magnitude and time-variability of dissolved primary production, particulate primary production, and bacterial production in the NPSG at monthly scales; examine how these rates co-vary in the contemporary ocean; and also explore how changes to the seawater carbonate system might affect these rates. In addition, I sought to examine how bacterial and primary production varied over a range of nested scales, including diel, daily, monthly, and seasonal. By estimating rates of bacterial production and constraining the relative partitioning of primary production between particulate and dissolved pools, my work contributes to our understanding of the flow of recently photosynthesized carbon through the microbial loop in the surface waters of the NPSG. This dissertation was organized around three major questions:

- How time-variable are rates of carbon fixation, in particular, the partitioning of fixed organic carbon between dissolved and particulate phases?
- How time-variable are rates of bacterial production and do these rates co-vary in time with rates of carbon fixation?

- How sensitive are primary production and bacterial growth to abrupt and large-scale variations in  $p\text{CO}_2$ ?

Research presented as part of this dissertation was conducted in the NPSG, at or near Station ALOHA. This dissertation consists of five chapters. This first chapter introduces the topics explored throughout the thesis and defines the major objectives of the study. Chapter 2 examines the time- and depth- variability of the partitioning of primary production (as measured via the incorporation of  $^{14}\text{C}$ -labeled bicarbonate into biomass) between particulate and dissolved phases at near monthly time scales at Station ALOHA. Chapter 2 also examines shorter, quasi-diel scale variability primary production of both dissolved and particulate organic matter, as well as comparisons of two types of filters (glass fiber and polycarbonate membrane) used to measure primary productivity. Chapter 2 has been published (Viviani et al. 2015). Chapter 3 examines depth- and time-variability in bacterial production (as measured by the incorporation of  $^3\text{H}$ -leucine into biomass) at near monthly scales in both light and dark, in order to account for photostimulation of bacterial production (Church et al. 2006, Björkman et al. 2015). I also compare this variability to contemporaneous rates of primary production. Chapter 3 also examines near-surface (25 m) rates of bacterial production and primary production at nested time scales of variability. Chapter 4 explores the short-term effects of abrupt changes of the seawater carbonate system (from ambient conditions to seawater with target  $p\text{CO}_2$  of 750 or 1100 ppm) on rates of primary production and bacterial production. Two kinds of experiments are presented in Chapter 4; one type consisted of short-term (up to 96 hour) perturbations of near-surface (5 m) seawater, bubbled with either air or a mixture of air and  $\text{CO}_2$ , in order to increase seawater  $p\text{CO}_2$  to levels projected to occur over the next 50 to 100 years. In addition, Chapter 4 presents results from a second type of experiment examining the effects of elevated  $p\text{CO}_2$  on rates of bacterial

production and primary production at different depths through the euphotic zone over the duration of the photoperiod. For these experiments, the seawater carbonate system was manipulated via the addition of acid and bicarbonate to change the seawater  $p\text{CO}_2$  while maintaining a consistent alkalinity. Finally, Chapter 5 provides some general conclusions to the work presented here, including an overall synthesis of this work, as well as the significance of the results presented herein, and some potential future research directions suggested by this work.

## Literature cited

- Azam F, Fenchel T, Field J, Gray J, Meyer-Reil L, Thingstad F (1983) The ecological role of water-column microbes in the sea. *Mar Ecol Prog Ser* 10:257–263
- Badger M (2003) The roles of carbonic anhydrases in photosynthetic CO<sub>2</sub> concentrating mechanisms. *Photosynth Res* 77:83–94
- Badger MR, Andrews TJ (1982) Photosynthesis and inorganic carbon usage by the marine cyanobacterium, *Synechococcus* sp. *Plant Physiol* 70:517–523
- Badger M, Hanson D, Price G (2002) Evolution and diversity of CO<sub>2</sub> concentrating mechanisms in cyanobacteria. *Funct Plant Biol* 29:161–173
- Badger M, Price G, Long B, Woodger F (2006) The environmental plasticity and ecological genomics of the cyanobacterial CO<sub>2</sub> concentrating mechanism. *J Exp Bot* 57:249–265
- Banase K (1995) Zooplankton: Pivotal role in the control of ocean production. *ICES J Mar Sci* 52:265–277
- Beardall J, Raven JA (2004) The potential effects of global climate change on microalgal photosynthesis, growth and ecology. *Phycologia* 43:26–40
- Behrenfeld MJ, Falkowski PG (1997) Photosynthetic rates derived from satellite-based chlorophyll concentration. *Limnol Oceanogr* 42:1–20
- Beman JM, Chow C-E, King AL, Feng Y, Fuhrman JA, Andersson A, Bates NR, Popp BN, Hutchins DA (2010) Global declines in oceanic nitrification rates as a consequence of ocean acidification. *Proc Natl Acad Sci USA* 108:208–213
- Berner R (1990) Atmospheric carbon dioxide levels over Phanerozoic time. *Science* 249:1382–1386
- Björkman KM, Church MJ, Doggett JK, Karl DM (2015) Differential assimilation of inorganic carbon and leucine by *Prochlorococcus* in the oligotrophic North Pacific Subtropical Gyre. *Front Microbiol* 6:1401
- Campbell L, Nolla HA, Vaultot D (1994) The importance of *Prochlorococcus* to community structure in the central North Pacific Ocean. *Limnol Oceanogr* 39:954–961
- Carlson CA, Bates NR, Ducklow HW, Hansell DA (1999) Estimation of bacterial respiration and growth efficiency in the Ross Sea, Antarctica. *Aquat Microb Ecol* 19:229–244
- Carlson CA, Ducklow HW, Sleeter TD (1996) Stocks and dynamics of bacterioplankton in the northwestern Sargasso Sea. *Deep Sea Res II* 43:491–515

- Church MJ (2008) Resource control of bacterial dynamics in the sea. In: Kirchman DL, Mitchell, R (eds) *Microbial Ecology of the Oceans*. John Wiley & Sons, Inc., Hoboken, NJ, USA, p 335–382
- Church M, Ducklow H, Letelier R, Karl D (2006) Temporal and vertical dynamics in picoplankton photoheterotrophic production in the subtropical North Pacific Ocean. *Aquat Microb Ecol* 45:41–53
- Church MJ, Lomas MW, Muller-Karger F (2013) Sea change: Charting the course for biogeochemical ocean time-series research in a new millennium. *Deep Sea Res II* 93:2–15
- Church MJ, Mahaffey C, Letelier RM, Lukas R, Zehr JP, Karl DM (2009) Physical forcing of nitrogen fixation and diazotroph community structure in the North Pacific subtropical gyre. *Global Biogeochem Cycles* 23:GB2020
- Cole J, Likens G, Strayer D (1982) Photosynthetically produced dissolved organic-carbon - an important carbon source for planktonic bacteria. *Limnol Oceanogr* 27:1080–1090
- del Giorgio P, Cole J (1998) Bacterial growth efficiency in natural aquatic systems. *Ann Rev Mar Sci* 29:503–541
- Doney SC, Fabry VJ, Feely RA, Kleypas JA (2009) Ocean acidification: the other CO<sub>2</sub> problem. *Ann Rev Mar Sci* 1:169–192
- Dore J, Letelier R, Church M, Lukas R, Karl D (2008) Summer phytoplankton blooms in the oligotrophic North Pacific Subtropical Gyre: Historical perspective and recent observations. *Prog Oceanogr* 76:2–38
- Dore J, Lukas R, Sadler D, Church M, Karl D (2009) Physical and biogeochemical modulation of ocean acidification in the central North Pacific. *Proc Natl Acad Sci USA* 106:12235–12240
- Druffel E, Williams P, Bauer J, Erel J (1992) Cycling of dissolved and particulate organic matter in the open ocean. *J Geophys Res* 97:15639–15659
- Ducklow H (1999) The bacterial component of the oceanic euphotic zone. *FEMS Microbiol Ecol* 30:1–10
- Ducklow H, Carlson C (1992) Oceanic bacterial production. In: *Advances in Microbial Ecology*. Springer, USA, p 113–181
- Ducklow HW, Dickson M-L, Kirchman DL, Steward G, Orchardo J, Marra J, Azam F (2000) Constraining bacterial production, conversion efficiency and respiration in the Ross Sea, Antarctica, January–February, 1997. *Deep Sea Res II* 47:3227–3247

- Evans C, Pearce I, Brussaard CPD (2009) Viral-mediated lysis of microbes and carbon release in the sub-Antarctic and Polar Frontal zones of the Australian Southern Ocean. *Environ Microbiol* 11:2924–2934
- Falkowski PG, Raven JA (2007) *Aquatic photosynthesis*. Princeton University Press, New Jersey, USA
- Field CB, Behrenfeld MJ, Randerson JT, Falkowski P (1998) Primary production of the biosphere: Integrating terrestrial and oceanic components. *Science* 281:237–240
- Fogg GE (1966) The extracellular products of algae. *Oceanogr Mar Biol* 4:195–212
- Giordano M, Beardall J, Raven JA (2005) CO<sub>2</sub> concentrating mechanisms in algae: Mechanisms, environmental modulation, and evolution. *Ann Rev Plant Biol* 56:99–131
- Grossart H, Allgaier M, Passow U, Riebesell U (2006) Testing the effect of CO<sub>2</sub> concentration on the dynamics of marine heterotrophic bacterioplankton. *Limnol Oceanogr* 51:1–11
- Hansell DA, Carlson CA, Repeta DJ, Schlitzer R (2009) Dissolved organic matter in the ocean: A controversy stimulates new insights. *Oceanography* 22:202–211
- Hedges JJ (1992) Global biogeochemical cycles: progress and problems. *Mar Chem* 39:67–93
- Hellebust JA (1965) Excretion of some organic compounds by marine phytoplankton. *Limnol Oceanogr* 10:192–206
- Hopkinson BM, Young JN, Tansik AL, Binder BJ (2014) The minimal CO<sub>2</sub>-concentrating mechanism of *Prochlorococcus* spp. MED4 is effective and efficient. *Plant Physiol* 166:2205–2217
- Hutchins D, Fu F, Zhang Y, Warner M, Feng Y, Portune K, Bernhardt P, Mulholland M (2007) CO<sub>2</sub> control of *Trichodesmium* N<sub>2</sub> fixation, photosynthesis, growth rates, and elemental ratios: Implications for past, present, and future ocean biogeochemistry. *Limnol Oceanogr* 52:1293–1304
- IPCC (2014) Summary for Policymakers. In: Field CB, Barros VR, Dokken DJ, Mach KJ, Mastrandrea MD, Bilir TE, Chatterjee M, Ebi KL, Estrada YO, Genova RC, Girma B, Kissel ES, Levy AN, MacCracken S, Mastrandrea PR, White LL (eds) *Climate Change 2014: Impacts, Adaptation, and Vulnerability. Part A: Global and Sectoral Aspects. Contribution of Working Group II to the Fifth Assessment Report of the Intergovernmental Panel on Climate Change*. Cambridge University Press, Cambridge, United Kingdom, and New York, NY, USA, p 1–32
- Joint I, Doney SC, Karl DM (2011) Will ocean acidification affect marine microbes? *ISME J* 5:1–7
- Kaiser K, Benner R (2009) Biochemical composition and size distribution of organic matter at the Pacific and Atlantic time-series stations. *Mar Chem* 113:63–77

- Karl D (1999) A sea of change: Biogeochemical variability in the North Pacific Subtropical Gyre. *Ecosystems* 2:181–214
- Karl D, Bidigare R, Letelier R (2001) Long-term changes in plankton community structure and productivity in the North Pacific Subtropical Gyre: The domain shift hypothesis. *Deep Sea Res II* 48:1449–1470
- Karl DM, Church MJ (2014) Microbial oceanography and the Hawaii Ocean Time-series programme. *Nat Rev Microbiol* 12:699–713
- Karl DM, Church MJ, Dore JE, Letelier RM, Mahaffey C (2012) Predictable and efficient carbon sequestration in the North Pacific Ocean supported by symbiotic nitrogen fixation. *Proc Natl Acad Sci USA* 109:1842–1849
- Karl D, Hebel D, Björkman K, Letelier R (1998) The role of dissolved organic matter release in the productivity of the oligotrophic North Pacific Ocean. *Limnol Oceanogr* 43:1270–1286
- Karl D, Lukas R (1996) The Hawaii Ocean Time-series (HOT) program: Background, rationale and field implementation. *Deep Sea Res II* 43:129–156
- Kim J-M, Lee K, Shin K, Yang EJ, Engel A, Karl DM, Kim H-C (2011) Shifts in biogenic carbon flow from particulate to dissolved forms under high carbon dioxide and warm ocean conditions. *Geophys Res Lett* 38:L08612
- Kirchman DL (2004) A primer on dissolved organic material and heterotrophic prokaryotes in the oceans. In: Follows M, Oguz T (eds) *The Ocean Carbon Cycle and Climate*. Springer Netherlands, p 31–63
- Kirchman DL, Hill V, Cottrell MT, Gradinger R, Malmstrom RR, Parker A (2009) Standing stocks, production, and respiration of phytoplankton and heterotrophic bacteria in the western Arctic Ocean. *Deep Sea Res II* 56:1237–1248
- Lampert W (1978) Release of dissolved organic carbon by grazing zooplankton. *Limnol Oceanogr* 23:831–834
- Lancelot C (1979) Gross excretion rates of natural marine phytoplankton and heterotrophic uptake of excreted products in the Southern North Sea, as determined by short-term kinetics. *Mar Ecol Prog Ser* 1:179–186
- Letelier R, Dore J, Winn C, Karl D (1996) Seasonal and interannual variations in photosynthetic carbon assimilation at Station ALOHA. *Deep Sea Res II* 43:467–490
- Letelier R, Karl D, Abbott M, Bidigare R (2004) Light driven seasonal patterns of chlorophyll and nitrate in the lower euphotic zone of the North Pacific Subtropical Gyre. *Limnol Oceanogr* 49:508–519

- Levitan O, Kranz SA, Spungin D, Prasil O, Rost B, Berman-Frank I (2010) Combined effects of CO<sub>2</sub> and light on the N<sub>2</sub>-fixing cyanobacterium *Trichodesmium* IMS101: A mechanistic view. *Plant Physiol* 154:346–356
- Lignell R (1990) Excretion of organic carbon by phytoplankton: its relation to algal biomass, primary productivity and bacterial secondary production in the Baltic Sea. *Mar Ecol Prog Ser* 68:85–99
- Liu H, Nolla H, Campbell L (1997) *Prochlorococcus* growth rate and contribution to primary production in the equatorial and subtropical North Pacific Ocean. *Aquat Microb Ecol* 12:39–47
- Mague TH, Friberg E, Hughes DJ, Morris I (1980) Extracellular release of carbon by marine phytoplankton; A physiological approach. *Limnol Oceanogr* 25:262–279
- Morán XAG, Estrada M (2001) Short-term variability of photosynthetic parameters and particulate and dissolved primary production in the Alboran Sea (SW Mediterranean). *Mar Ecol Prog Ser* 212:53–67
- Orr JC, Fabry VJ, Aumont O, Bopp L, Doney SC, Feely RA, Gnanadesikan A, Gruber N, Ishida A, Joos F, Key RM, Lindsay K, Maier-Reimer E, Matear R, Monfray P, Mouchet A, Najjar RG, Plattner G-K, Rodgers KB, Sabine CL, Sarmiento JL, Schlitzer R, Slater RD, Totterdell IJ, Weirig M-F, Yamanaka Y, Yool A (2005) Anthropogenic ocean acidification over the twenty-first century and its impact on calcifying organisms. *Nature* 437:681–686
- Pasulka AL, Landry MR, Taniguchi DAA, Taylor AG, Church MJ (2013) Temporal dynamics of phytoplankton and heterotrophic protists at station ALOHA. *Deep Sea Res II* 93:44–57
- Piontek J, Borchard C, Sperling M, Schulz KG, Riebesell U, Engel A (2013) Response of bacterioplankton activity in an Arctic fjord system to elevated *p*CO<sub>2</sub>: results from a mesocosm perturbation study. *Biogeosciences* 10:297–314
- Piontek J, Lunau M, Händel N, Borchard C, Wurst M, Engel A (2010) Acidification increases microbial polysaccharide degradation in the ocean. *Biogeosciences* 7:1615–1624
- Pomeroy LR (1974) The ocean's food web, a changing paradigm. *BioScience* 24:499–504
- Price GD (2011) Inorganic carbon transporters of the cyanobacterial CO<sub>2</sub> concentrating mechanism. *Photosynth Res* 109:47–57
- Price G, Maeda S, Omata T, Badger M (2002) Modes of active inorganic carbon uptake in the cyanobacterium, *Synechococcus* sp PCC7942. *Funct Plant Biol* 29:131–149
- Raven J (1997a) Putting the C in phycology. *Eur J Phycol* 32:319–333
- Raven J (1997b) The role of marine biota in the evolution of terrestrial biota: Gases and genes - Atmospheric composition and evolution of terrestrial biota. *Biogeochemistry* 39:139–164

- Raven JA, Giordano M, Beardall J, Maberly SC (2011) Algal and aquatic plant carbon concentrating mechanisms in relation to environmental change. *Photosynth Res* 109:281–296
- Riebesell U, Zondervan I, Rost B, Tortell PD, Zeebe RE, Morel FMM (2000) Reduced calcification of marine plankton in response to increased atmospheric CO<sub>2</sub>. *Nature* 407:364–367
- Robison B, Reisenbichler K, Sherlock R (2005) Giant larvacean houses: Rapid carbon transport to the deep sea floor. *Science* 308:1609–1611
- Rocap G, Larimer F, Lamerdin J, Malfatti S, Chain P, Ahlgren N, Arellano A, Coleman M, Hauser L, Hess W, Johnson Z, Land M, Lindell D, Post A, Regala W, Shah M, Shaw S, Steglich C, Sullivan M, Ting C, Tolonen A, Webb E, Zinser E, Chisholm S (2003) Genome divergence in two *Prochlorococcus* ecotypes reflects oceanic niche differentiation. *Nature* 424:1042–1047
- Sabine CL, Feely RA, Gruber N, Key RM, Lee K, Bullister JL, Wanninkhof R, Wong CS, Wallace DWR, Tilbrook B, Millero FJ, Peng T-H, Kozyr A, Ono T, Rios AF (2004) The oceanic sink for anthropogenic CO<sub>2</sub>. *Science* 305:367–371
- Sharp JH (1977) Excretion of organic matter by marine phytoplankton: Do healthy cells do it? *Limnol Oceanogr* 22:381–399
- Sherr EB, Sherr BF (2002) Significance of predation by protists in aquatic microbial food webs. *Antonie van Leeuwenhoek* 81:293–308
- Steinberg DK, Carlson CA, Bates NR, Johnson RJ, Michaels AF, Knap AH (2001) Overview of the US JGOFS Bermuda Atlantic Time-series Study (BATS): a decade-scale look at ocean biology and biogeochemistry. *Deep Sea Res II* 48:1405–1447
- Tortell PD (2000) Evolutionary and ecological perspectives on carbon acquisition in phytoplankton. *Limnol Oceanogr* 45:744–750
- Tortell P, DiTullio G, Sigman D, Morel F (2002) CO<sub>2</sub> effects on taxonomic composition and nutrient utilization in an Equatorial Pacific phytoplankton assemblage. *Mar Ecol Prog Ser* 236:37–43
- Tortell PD, Payne CD, Li Y, Trimborn S, Rost B, Smith WO, Riesselman C, Dunbar RB, Sedwick P, DiTullio GR (2008) CO<sub>2</sub> sensitivity of Southern Ocean phytoplankton. *Geophys Res Lett* 35:L04605
- Turner JT (2002) Zooplankton fecal pellets, marine snow and sinking phytoplankton blooms. *Aquat Microb Ecol* 27:57–102
- Turner JT (2004) The importance of small planktonic copepods and their roles in pelagic marine food webs. *Zool Stud* 43:255–266

- Viviani DA, Karl DM, Church MJ (2015) Variability in photosynthetic production of dissolved and particulate organic carbon in the North Pacific Subtropical Gyre. *Front Mar Sci* 2:73
- Williams PJL. (2000) Heterotrophic bacteria and the dynamics of dissolved organic material. In: Kirchman DL, *Microbial ecology of the oceans*. Wiley-Liss, p 153–200
- Winn C, Campbell L, Christian J, Letelier R, Hebel D, Dore J, Fujieki L, Karl D (1995) Seasonal variability in the phytoplankton community of the North Pacific Subtropical gyre. *Global Biogeochem Cycles* 9:605–620
- Wolf-Gladrow DA, Riebesell U, Burkhardt S, Bijma J (1999) Direct effects of CO<sub>2</sub> concentration on growth and isotopic composition of marine plankton. *Tellus B* 51:461–476
- Zeebe RE, Zachos JC, Caldeira K, Tyrrell T (2008) Carbon emissions and acidification. *Science* 321:51–52

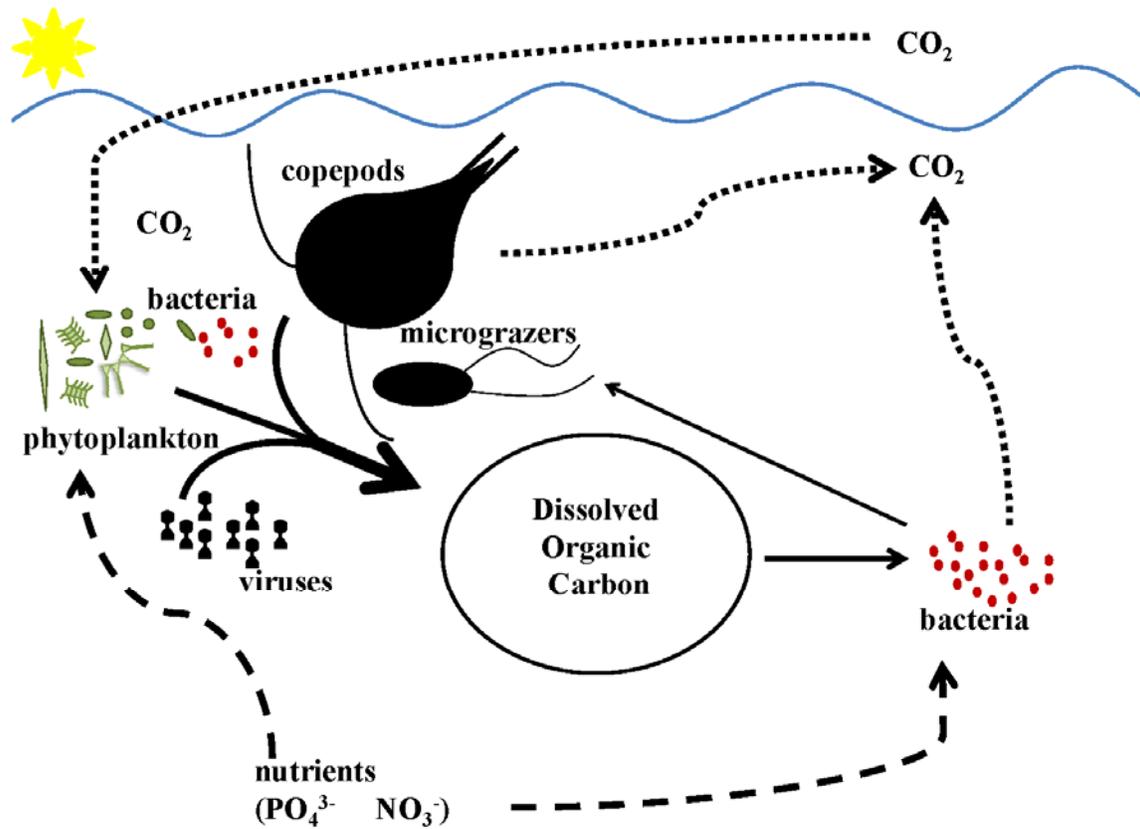


**Figure 1.1.** Schematic outlining the pathways through which recently photosynthesized organic matter may flow through an open ocean food web.

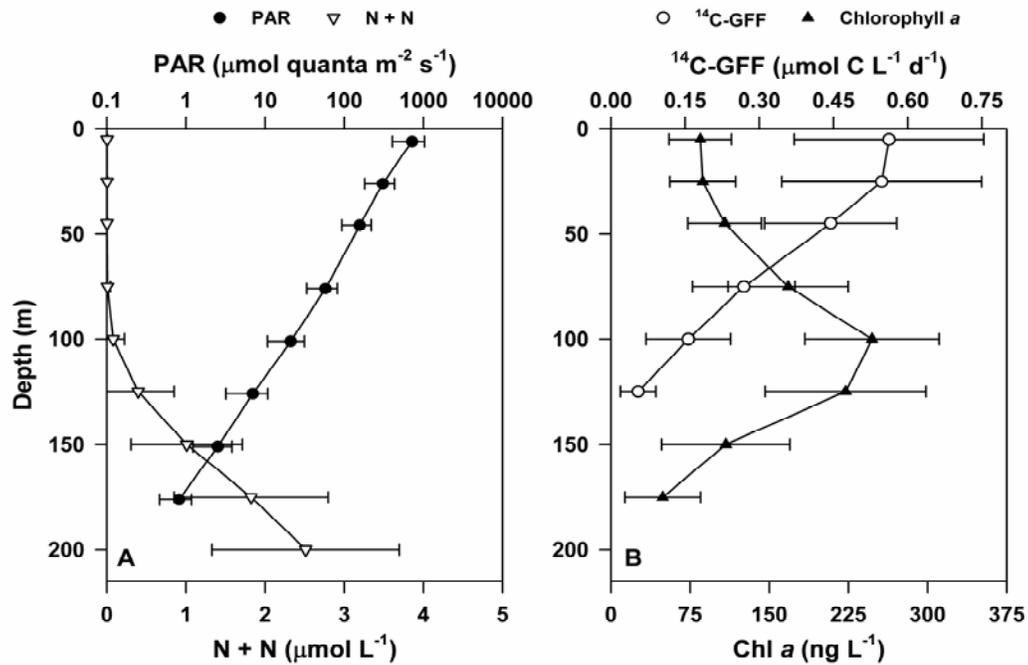


**Figure 1.2.** Time-averaged (1988–2014) concentrations of nitrate + nitrite (N + N) and flux of photosynthetically available radiation (PAR) at Station ALOHA (panel A). Also shown are vertical profiles of the time-averaged mean rates of <sup>14</sup>C-primary production and chlorophyll *a* concentrations at Station ALOHA (panel B). Error bars depict one standard deviation of the mean concentration or rate.

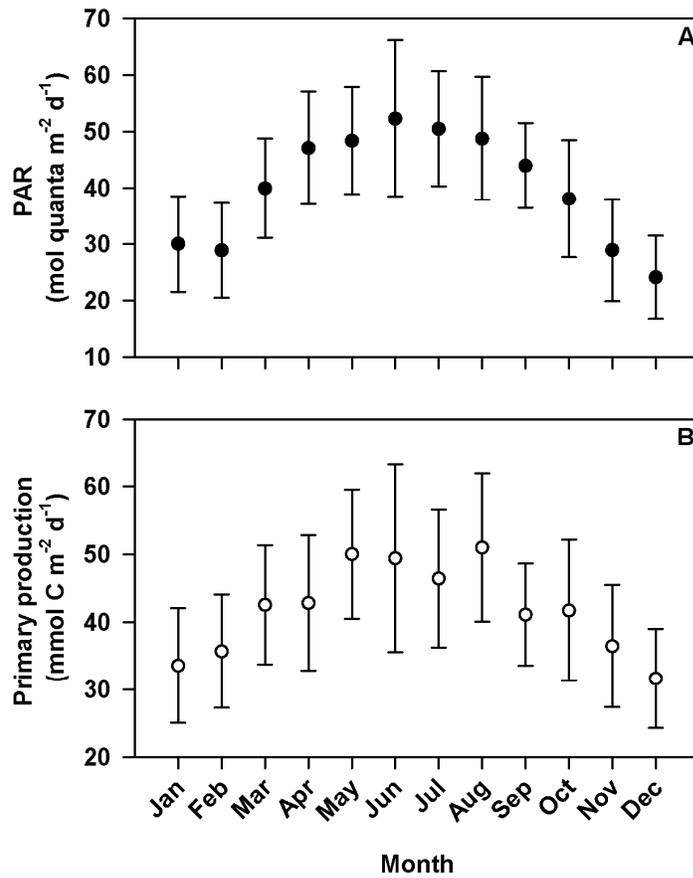


**Figure 1.3.** Monthly binned surface incident PAR (panel A) and depth-integrated (0–125 m) <sup>14</sup>C-primary productivity (panel B) at Station ALOHA.

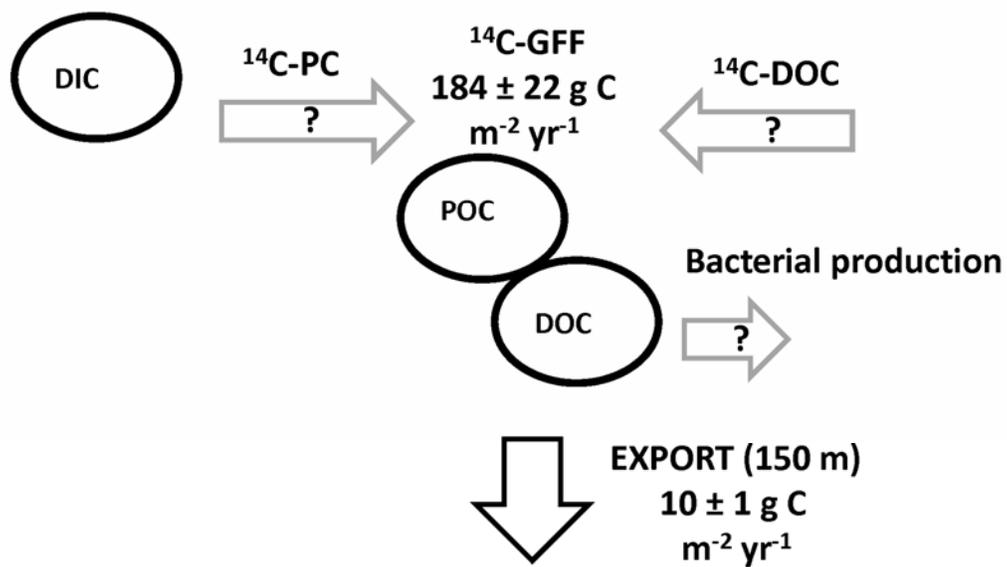


**Figure 1.4.** Schematic depicting rates of  $^{14}\text{C}$ -primary production currently constrained at Station ALOHA. Also depicted are rates constrained as part of the current study ( $^{14}\text{C}$ -particulate carbon production,  $^{14}\text{C}$ -dissolved organic carbon production, and rates of bacterial production).

## CHAPTER 2 - Variability in photosynthetic production of dissolved and particulate organic carbon in the North Pacific Subtropical Gyre

Donn A. Viviani, David M. Karl, and Matthew J. Church (2015) *Front Mar Sci*, 2:73

### Abstract

The partitioning of photosynthetically-derived organic carbon between particulate and dissolved phases has important implications for marine carbon cycling. In this study we utilized  $^{14}\text{C}$ -bicarbonate assimilation to quantify rates of photosynthetic production of both particulate and dissolved organic carbon (DOC) at Station ALOHA ( $22^{\circ}45'\text{N}$ ,  $158^{\circ}\text{W}$ ) in the North Pacific Subtropical Gyre (NPSG). At near-monthly time scales over  $\sim 5$  years, we examined retention of  $^{14}\text{C}$ -labeled organic matter by both glass fiber filters and  $0.2\ \mu\text{m}$  pore size polycarbonate membrane filters that are commonly used for measurements of  $^{14}\text{C}$ -based plankton productivity. Use of polycarbonate filters resulted in significantly lower (averaging 60%) estimates of  $^{14}\text{C}$ -production compared to glass fiber filters. Coincident measurements of chlorophyll *a* concentrations from both  $0.2\ \mu\text{m}$  polycarbonate and glass fiber filters were not significantly different, suggesting the differences in  $^{14}\text{C}$ -productivity between these filter types did not derive from differences in retention of photosynthetic biomass by these filters. Moreover, consistent with previous studies, results from experiments aimed at quantifying retention of organic matter by these filters suggested differences resulted from retention of DOC by glass fiber filters. We also quantified rates of  $^{14}\text{C}$ -DOC production to evaluate the partitioning of photosynthetic production between dissolved and particulate phases over daily to monthly time scales in this ecosystem. Unlike the strong depth dependence observed in measurements of particulate organic

carbon production, measured rates of  $^{14}\text{C}$ -DOC demonstrated no clear depth dependence. On average, depth-integrated (0-75 m) rates of  $^{14}\text{C}$ -DOC production rates were equivalent to  $18 \pm 10\%$  of the total (particulate and dissolved) productivity. Our findings indicate that in this oligotrophic ecosystem, rates of dissolved and particulate production can be temporally decoupled over daily to monthly time scales.

## Introduction

Oceanic net primary production accounts for approximately  $50 \text{ Pg C yr}^{-1}$ , and much of this productivity occurs in the vast, low nutrient subtropical ocean gyres (Behrenfeld and Falkowski, 1997; Field et al., 1998). Dissolved organic carbon (DOC), operationally defined as reduced carbon substrates passing through filters (typical pore sizes ranging  $0.2\text{-}0.7 \mu\text{m}$ ), constitutes  $>90\%$  of total marine organic carbon inventories (Druffel et al., 1992; Hedges, 1992; Kaiser and Benner, 2009). Despite low inorganic nutrient concentrations throughout the upper euphotic zone of the subtropical gyres, concentrations of DOC are enriched in these ecosystems (Hansell et al., 2009). Hence, quantification of rates of DOC production and subsequent utilization are central to constraining carbon cycling in these systems.

A suite of processes can result in DOC production. These include direct release of organic material from phytoplankton cells either passively (Bjørnsen, 1988) or actively (Fogg, 1966; Lignell, 1990; Marañón et al., 2004). High light (Cherrier et al., 2014; Hellebust, 1965) and nutrient limitation (Conan et al., 2007; Lancelot, 1983; López-Sandoval et al., 2011) may also promote phytoplankton DOC release. Processes such as viral lysis and inefficient predation can also constitute major DOC production pathways (Banse, 1995; Evans et al., 2009; Hygum et al., 1997; Lampert, 1978; Møller, 2005; Møller et al., 2003; Saba et al., 2011; Suttle, 2005; Wilhelm and Suttle, 1999). Rates of DOC production are often measured by tracing phytoplankton assimilation of radiolabeled ( $^{14}\text{C}$ ) inorganic carbon and quantifying the subsequent accumulation of  $^{14}\text{C}$ -labelled DOC in seawater (Baines and Pace, 1991; Carlson, 2002; Schindler et al., 1972).

Measurement of  $^{14}\text{C}$  bicarbonate assimilation into autotrophic biomass (Steemann Nielsen, 1952) has proven a sensitive method for estimating primary productivity rates in aquatic

ecosystems and is often reported as approximating net primary productivity (Bender et al., 1987; Marra, 2009; Pei and Laws, 2013; Peterson, 1980). However, studies utilizing this methodology often do not quantify rates of DOC production (hereafter termed  $^{14}\text{C}$ -DOC), or estimate respiratory losses during the incubation period; consequently, organic carbon production may be underestimated by this approach. Direct  $^{14}\text{C}$ -DOC measurements have been made in diverse aquatic ecosystems (Baines and Pace, 1991), with rates in the open oceans typically ranging between 10-40% of particulate carbon production (Carlson et al., 2000; Conan et al., 2007; Karl et al., 1998; Marañón et al., 2004; Morán and Estrada, 2001; Teira et al., 2001, 2003).

The choice of filters utilized for measurements of particulate carbon production is an important consideration. Several studies have compared the retention of organic matter by various types of filters commonly used in aquatic systems (Chavez et al., 1995; Karl et al., 1998; Maske and Garcia-Mendoza, 1994; Morán et al., 1999). Glass fiber filters commonly used for these measurements are known to retain both  $^{14}\text{C}$ -DOC and  $^{14}\text{C}$ -labeled particulate carbon (Karl et al., 1998). However, to date, there are relatively few reports describing how different filter types influence derived rates of  $^{14}\text{C}$ -productivity in the open ocean. In a comparative study of filter retention characteristics, Morán et al. (1999) reported greater retention of  $^{14}\text{C}$ -labeled organic material on glass fiber filters compared to polycarbonate filters. However, the study also observed differences in the retention efficiencies of these filters in different ecosystems, suggesting the structure of planktonic communities and the relative importance of DOC to total organic matter productivity by these communities influences the retention characteristics of these filters (Morán et al. 1999).

The North Pacific Subtropical Gyre (NPSG) is one of the largest open ocean habitats on the planet. Since 1988, the Hawaii Ocean Time-series (HOT) program has sustained near-monthly shipboard measurements at Station ALOHA (A Long-Term Oligotrophic Habitat Assessment; 22°45'N, 158°W) in the NPSG, where oligotrophic upper ocean waters exhibit seasonality in various biogeochemical processes and properties (Campbell et al., 1994; Church et al., 2009; Dore et al., 2008; Karl et al., 2001; Landry et al., 2001; Letelier et al., 2004; Winn et al., 1995). A number of previous studies indicate that rates of primary production at Station ALOHA demonstrate moderate seasonality, with rates higher in summer and lower in winter (Church et al., 2013; Karl et al., 1996; Letelier et al., 1996; Quay et al., 2010). A previous study quantifying  $^{14}\text{C}$ -DOC production rates at Station ALOHA revealed that  $^{14}\text{C}$ -DOC comprised a relatively large fraction (14-51%) of daily photosynthetic production (Karl et al., 1998). However, there is limited information on temporal variability associated with the partitioning of organic carbon production into dissolved and particulate phases in this ecosystem.

In the present study, we assess the magnitude and partitioning of primary production between particulate and dissolved pools at Station ALOHA. We evaluate retention characteristics of glass fiber and polycarbonate filters commonly used for measurements of  $^{14}\text{C}$ -based productivity and concentrations of chlorophyll *a*. Our results confirm that rates of  $^{14}\text{C}$  productivity were significantly greater when derived using glass fiber filters compared to polycarbonate filters, despite no significant differences in the retention of chlorophyll *a* by these filters. We also examined rates of  $^{14}\text{C}$ -DOC production to test the hypothesis that rates of  $^{14}\text{C}$ -DOC production would demonstrate similar time-varying patterns as rates of  $^{14}\text{C}$ -particulate carbon production. However, despite periods of moderate seasonality in photosynthetic

production of particulate carbon,  $^{14}\text{C}$ -DOC production was more temporally variable than coincident rates of  $^{14}\text{C}$ -particulate carbon production.

## **Materials and Methods**

### **Chlorophyll *a* and $^{14}\text{C}$ -based productivity measurements**

Sampling for this study was conducted at near-monthly time scales at Station ALOHA on HOT program cruises during two separate periods, October 2004 to October 2007 and April 2010 to October 2012. During the initial period of the study (2004-2007), we compared retention characteristics of 25 mm diameter 0.2  $\mu\text{m}$  pore size polycarbonate membrane filters (Millipore) and 25 mm diameter glass fiber filters (Whatman GF/F) for subsequent analyses of both chlorophyll *a* concentrations and rates of  $^{14}\text{C}$ -productivity. To compare retention of chlorophyll *a* by these filter types, paired seawater samples were collected from pre-dawn hydrocasts using a conductivity-temperature-density (CTD) rosette sampler equipped with 12 L polyvinyl chloride bottles. Seawater from six discrete depths (5, 25, 45, 75, 100, and 125 m) was sampled from the CTD rosette bottles into 150 ml amber polyethylene bottles. The entire 150 ml sample was filtered onto either polycarbonate or glass fiber filters. Filters were immersed in 5 ml of 100% HPLC grade acetone in 7 ml glass culture tubes and placed at  $-20^{\circ}\text{C}$  to passively extract. After 7 days (Letelier et al., 1996), tubes were removed from the freezer, filters were removed, and extracted chlorophyll in the acetone was quantified using a Turner Designs Model 10-AU fluorometer (Strickland and Parsons, 1972).

Sampling for  $^{14}\text{C}$ -based measurements of particulate production occurred on near-monthly HOT program cruises throughout the study period. We measured rates of  $^{14}\text{C}$ -

assimilation into particulate carbon using polycarbonate filters to harvest plankton biomass (hereafter  $^{14}\text{C}$ -PC), and compared these rates to coincident (in both time and depth) core HOT program measurements of  $^{14}\text{C}$ -assimilation into plankton biomass (Letelier et al., 1996), based on use of glass fiber filters (hereafter  $^{14}\text{C}$ -GFF). During the latter period of observations (2010-2013) we also measured  $^{14}\text{C}$ -DOC production rates. Seawater for the  $^{14}\text{C}$ -based productivity measurements was collected from the same predawn CTD hydrocasts sampled for chlorophyll *a* concentrations. Water for the productivity measurements was sampled from the CTD rosette bottles into acid-cleaned 500-ml polycarbonate bottles. A total of four replicate 500 ml bottles were subsampled per depth and each bottle was spiked with  $\sim 1.85$  MBq  $^{14}\text{C}$ -bicarbonate. One hundred milliliters from one replicate per depth was immediately vacuum filtered through a polycarbonate filter; these “time zero” filtrates provided a  $^{14}\text{C}$ -DOC blank and provided information on background adsorption of inorganic  $^{14}\text{C}$  to the filters. Time zero filters were placed in 20 ml glass scintillation vials (Kimble Chase) and stored at  $-20^{\circ}\text{C}$  until shore-based laboratory processing. The remaining three bottles were hung on a free-drifting array, deployed before dawn, and incubated at their initial collection depths throughout the photoperiod (typically 11-13 hours). After sunset the array was recovered, and 100 ml subsamples of all bottles were filtered under gentle vacuum ( $<50$  mm Hg) onto polycarbonate filters that were then placed in scintillation vials and frozen ( $-20^{\circ}\text{C}$ ). The total radioactivity added to each sample bottle was determined by subsampling 250  $\mu\text{l}$  aliquots into scintillation vials containing 500  $\mu\text{l}$  of  $\beta$ -phenylethylamine. At the shore-based laboratory, filters were acidified by the addition of 1 ml of 2 M hydrochloric acid (HCl) and allowed to passively vent (uncapped) for  $\sim 24$  hours to remove inorganic  $^{14}\text{C}$ . Ten milliliters of Ultima Gold LLT liquid scintillation cocktail was added to all vials (acidified filters and vials for determining total radioactivity) and the resulting

radioactivity was determined using a Perkin Elmer 2600 liquid scintillation counter; glass fiber filters were recounted after 30 days (Karl et al. 1998).

### **Measurements of $^{14}\text{C}$ -DOC production**

Over a ~2.5-year period (April 2010-October 2012), we measured  $^{14}\text{C}$ -DOC production from the same vertical profiles used for determination of  $^{14}\text{C}$ -PC production by utilizing filtrates derived from  $^{14}\text{C}$ -PC rate measurements. These 0.2  $\mu\text{m}$  filtrates were collected from both time zero samples and triplicate bottles incubated *in situ* on the free-drifting array into 125 ml polyethylene amber bottles and stored frozen ( $-20^{\circ}\text{C}$ ) until subsequent processing for determination of  $^{14}\text{C}$ -DOC productivity. In the shore-based laboratory, these samples were processed following the  $^{14}\text{C}$ -DOC methodology described in Karl et al. (1998). Briefly, 100 ml of the  $^{14}\text{C}$ -PC filtrates were thawed, poured into 500 ml polyethylene separatory funnels, and acidified by the addition of 500  $\mu\text{l}$  of 2 M sulfuric acid ( $\text{H}_2\text{SO}_4$ ). Samples were vigorously bubbled with air in a fume hood to remove  $^{14}\text{CO}_2$ . After at least 6 hours of bubbling, a 70 ml subsample was removed from each separatory funnel and poured into a 100 ml glass serum bottle containing 1 ml of 2 M sodium hydroxide ( $\text{NaOH}$ ) and 10 ml of 0.37 M potassium persulfate ( $\text{K}_2\text{S}_2\text{O}_8$ ) in 1 M  $\text{NaOH}$ . Bottles were sealed with rubber stoppers, crimp sealed with an aluminum cap, and autoclaved at  $126^{\circ}\text{C}$  for 200 minutes; oxidizing  $^{14}\text{C}$ -DOC to  $^{14}\text{C}$ -labeled dissolved inorganic carbon ( $^{14}\text{C}$ -DIC) in an alkaline solution. Once cooled to room temperature, samples were uncapped and resealed using rubber sleeve stoppers holding plastic center wells containing ~2 x 2 cm pieces of fluted chromatographic filter paper (Whatman 2) soaked with 0.2 ml of  $\beta$ -phenylethylamine. A syringe was used to inject 4 ml of 9 N  $\text{H}_2\text{SO}_4$  into the solution, converting the  $^{14}\text{C}$ -DIC to  $^{14}\text{CO}_2$ . Samples were stored undisturbed at room temperature, passively trapping the  $^{14}\text{CO}_2$  on the  $\beta$ -phenylethylamine soaked wick. After five days, rubber

sleeve stoppers were removed and center wells and wicks were placed in scintillation vials, followed by the addition of 10 ml of Ultima Gold LLT scintillation cocktail. Samples were subsequently counted on a Perkin Elmer Tri-Carb 2800TR liquid scintillation counter. Rates of  $^{14}\text{C}$ -DOC production were computed for each cruise as the mean of the triplicate bottles from each depth minus the average  $^{14}\text{C}$ -activity of the time zero (blank) samples. We defined a limit of detection for the  $^{14}\text{C}$ -DOC analyses per cruise as the value of the mean time zero ‘blank’ samples for that cruise plus three times the standard deviation of those time zero ‘blank’ samples (Skoog and Leary, 1992). Measurements falling below the detection limit were assigned a value of zero for subsequent analyses, including calculation of mean rates.

### **Diel variability in productivity**

On three separate occasions (April 2013, May 2013, and June 2013), we conducted experiments to examine short-term (diel) variability in production and loss of  $^{14}\text{C}$ -PC,  $^{14}\text{C}$ -GFF, and  $^{14}\text{C}$ -DOC. Triplicate 500 ml samples were collected from 25 m depth from pre-dawn CTD hydrocasts, inoculated with  $\sim 1.85$  MBq  $^{14}\text{C}$ -bicarbonate, and placed in a surface seawater cooled incubator shaded to 50% incident irradiance. Samples were incubated for varying lengths of time: predawn until noon ( $\sim 6$  hours), full photoperiod (predawn to dusk,  $\sim 12$  hours), or over a full day (predawn to predawn,  $\sim 24$  hours). Following incubation, samples were filtered and processed as previously described for determination of  $^{14}\text{C}$ -PC,  $^{14}\text{C}$ -GFF, and  $^{14}\text{C}$ -DOC. Rates of  $^{14}\text{C}$ -DOC below the limit of detection were assigned a value of zero for these analyses.

### **Filter retention characteristics**

We conducted an experiment designed to specifically evaluate retention characteristics of glass fiber and polycarbonate filters for measurements of  $^{14}\text{C}$ -productivity and chlorophyll *a*

(October 2014). For this experiment, 500 ml seawater samples were collected from the near-surface (25 m) ocean, inoculated with  $\sim 1.85$  MBq  $^{14}\text{C}$ -bicarbonate and incubated from dawn to dusk in temperature controlled, shaded (50% incident irradiance) incubators. After sunset, triplicate 100 ml subsamples were vacuum filtered onto both polycarbonate and glass fiber filters individually, and onto these filters in series (*i.e.* glass fiber filters underlain by polycarbonate filter or polycarbonate underlain by glass fiber filter). Filters were placed in scintillation vials, acidified, and processed as previously described for determination of  $^{14}\text{C}$  activities. From the same water sample, we also compared retention of planktonic chlorophyll *a* by glass fiber and polycarbonate filters; 125 ml was collected and filtered onto either a glass fiber filter, a polycarbonate filter, or onto these filters in series (as above). Chlorophyll concentrations were determined via fluorometric analysis as previously described.

An additional experiment (October 2014) was conducted to evaluate trapping of  $^{14}\text{C}$ -organic carbon by glass fiber filters. Replicate 500 ml polycarbonate bottles containing whole seawater from Station ALOHA were inoculated with  $\sim 1.85$  MBq  $^{14}\text{C}$ -bicarbonate and incubated in a temperature controlled and shaded incubator for the duration of the photoperiod. After dusk, incubations were terminated by filtering the sample bottles onto polycarbonate filters. The resulting filtrates were collected and triplicate 100 ml volumes were sequentially filtered onto new glass fiber filters, resulting in a filtrate that had been filtered a total of five separate times through five different glass fiber filters. In addition, triplicate 500 ml samples of the original 0.2  $\mu\text{m}$  filtrate were filtered onto glass fiber filters to evaluate possible volume-dependent differences in the trapping of  $^{14}\text{C}$ -DOC by these filters. The resulting  $^{14}\text{C}$  activities associated with each glass fiber filter were determined as previously described.

We also evaluated the effects of filtering different volumes of the  $^{14}\text{C}$ -productivity samples onto glass fiber and polycarbonate filters. For these comparisons, we examined paired primary production samples collected from the upper ocean (<45 m) at Station ALOHA, where 100 ml of seawater was filtered onto a polycarbonate filter, while varying volumes of seawater (100 ml, 150 ml, 400 ml, or 500 ml) were filtered onto glass fiber filters. These comparative measurements were used to calculate the difference between the derived rates of  $^{14}\text{C}$ -productivity on the glass fiber and polycarbonate filters ( $^{14}\text{C}\text{-}\delta = ^{14}\text{C}\text{-GFF} - ^{14}\text{C}\text{-PC}$ ). Results from this comparison provided information on whether differences in retention of  $^{14}\text{C}$ -organic carbon by glass fiber and polycarbonate filters in our time-series measurements might reflect differences in the volume of seawater filtered for these measurements (*i.e.* 500 ml onto glass fiber versus 100 ml onto polycarbonate filters).

### **Contextual biogeochemical analyses**

Seawater samples for measurements of nutrient concentrations (nitrate + nitrite, N+N; soluble reactive phosphorus, SRP) were collected in 125 or 500 ml acid-washed polyethylene bottles and stored upright in a freezer for analysis on shore. Concentrations of N+N were determined using the high sensitivity chemiluminescent technique (Dore and Karl, 1996; Garside, 1982); SRP concentrations were analyzed using the magnesium-induced co-precipitation (MAGIC) method (Karl and Tien, 1992). Daily fluxes of photosynthetically active radiation (PAR; 400 to 700 nm wavelength) were measured on HOT cruises using a deckboard LI-COR LI-192 cosine collector. Vertical profiles of downwelling PAR were measured daily at noon using a Satlantic HyperPro radiometer. Coincident measurements of incident PAR were collected using a deckboard radiometer (Satlantic); these measurements were used to derive diffuse attenuation coefficients ( $K_{\text{PAR}}$ ) for each cruise. Derived  $K_{\text{PAR}}$  values, together with daily

integrated incident PAR measurements, were utilized to compute daily downwelling flux of PAR at discrete depths.

### **Data analyses and statistics**

We evaluated seasonality in upper ocean properties and rates of  $^{14}\text{C}$ -productivity by binning our data into predefined seasons based on the solstices and equinoxes (*i.e.* Spring: March 20 to June 20; Summer: June 21 to September 22; Fall: September 23 to December 20; and Winter: December 21 to March 19). Analysis of variance (ANOVA) was used to examine possible seasonality in vertically-binned (0-45 m and 75-125 m) volumetric rates of  $^{14}\text{C}$ -GFF,  $^{14}\text{C}$ -PC, and  $^{14}\text{C}$ -DOC. We also examined temporal variability in rates of productivity using various time-series statistical models, including an optimized least squares monthly regression approach described in Llope et al. (2007), and the Lomb-Scargle periodogram for unevenly sampled time-series data (Scargle, 1982). We first used these techniques to test for seasonality in the near-monthly, depth-integrated (0-75 m) HOT  $^{14}\text{C}$ -GFF measurements collected between 1989 and 2013 (see <http://hahana.soest.hawaii.edu/hot/hot-dogs/interface.html>). We then examined the time-series of rate measurements ( $^{14}\text{C}$ -GFF,  $^{14}\text{C}$ -PC, and  $^{14}\text{C}$ -DOC) from the two periods (*i.e.* October 2004 to October 2007 and April 2010 to October 2012) sampled in the current study using these statistical techniques. The Lomb-Scargle periodogram analysis was performed in the R statistical environment (R Development Core Team, 2008) using the “lomb” package (Ruf, 1999). The Llope et al. (2007) model was fit to the data using MATLAB (MathWorks). Depth-integrated rates and stocks were calculated using trapezoidal integration. Data were tested for normality, and if not normally distributed, were  $\log_{10}$  transformed; when transformed data failed to conform to the assumption of normality, nonparametric statistical methods were utilized. For statistical analyses of ratios (*e.g.*  $^{14}\text{C}$ -DOC :  $^{14}\text{C}$ -PC), geometric

rather than arithmetic means and standard deviations were used (Zar, 1999). For computing mean rates of  $^{14}\text{C}$ -DOC, measured rates falling below the limit of detection were designated as having a value of zero.

To evaluate the relationship between *in situ* PAR and measured rates of productivity, the derived daily PAR fluxes and measured rates of production were fitted to photosynthetic-irradiance (P-E) relationships using the equation of Platt et al. (1980):

$$P = P_{\max} [1 - \exp(-\alpha E / P_{\max})] \exp(-\beta E / P_{\max}) \quad (1)$$

where P is the rate of carbon fixation,  $P_{\max}$  is the maximum rate of photosynthesis without photoinhibition, E is the light flux (PAR),  $\alpha$  is the initial slope of the curve (representing the rate of maximum light utilization), and  $\beta$  is the rate of photoinhibition. These relationships were examined for rates of  $^{14}\text{C}$ -GFF,  $^{14}\text{C}$ -PC, and  $^{14}\text{C}$ -DOC. From these relationships values for  $E_k$  (the irradiance necessary to saturate carbon fixation) were calculated as follows:

$$E_k = P_{\max} / \alpha \quad (2)$$

HOT program measurements utilized in this study (nutrients, PAR, chlorophyll a, and rates of  $^{14}\text{C}$ -GFF production) are available via the HOT program data website (<http://hahana.soest.hawaii.edu/hot/hot-dogs/>). Rates of  $^{14}\text{C}$ -DOC and  $^{14}\text{C}$ -PC are available via the Center for Microbial Oceanography: Research and Education (C-MORE) data system (<http://cmore.soest.hawaii.edu/datasearch/data.php>).

## Results

### Biogeochemical context

Consistent with HOT program sampling of Station ALOHA, upper ocean concentrations of inorganic nutrients were very low throughout the period of this study, with near-surface (5 m) concentrations of N+N persistently < 3 nM and SRP averaging 66 nM. In the dimly-lit regions of the lower euphotic zone (100-125 m) concentrations of N+N increased and became more variable, ranging between 0.2 - 3.0  $\mu\text{M}$  (Figure 2.1). The penetration of PAR decreased more than two orders of magnitude through the upper 125 m of the water, with fluxes at the sea surface ranging from  $\sim 11$  to  $57 \text{ mol quanta m}^{-2} \text{ d}^{-1}$  and decreasing to 0.02 to  $0.8 \text{ mol quanta m}^{-2} \text{ d}^{-1}$  by 125 m. Incident PAR also demonstrated significant seasonal variability (one-way ANOVA,  $p < 0.0001$ ), with fluxes ranging between 11 and  $42 \text{ mol quanta m}^{-2} \text{ d}^{-1}$  in the winter, increasing approximately 2-fold (on average) in the summer (ranging from 32 to  $57 \text{ mol quanta m}^{-2} \text{ d}^{-1}$ ; Table 2.1). Concentrations of chlorophyll *a* were consistently elevated in the lower euphotic zone (70-140 m; Figure 2.1).

### **Measurements of $^{14}\text{C}$ -productivity and chlorophyll *a***

We examined vertical variability associated with  $^{14}\text{C}$ - based productivity at Station ALOHA over the two time periods sampled as part of the current study (October 2004-October 2007, and April 2010-October 2012). Rates of  $^{14}\text{C}$ -PC and HOT program measurements of  $^{14}\text{C}$ -GFF demonstrated similar depth-dependent patterns and temporal variability. Average rates of  $^{14}\text{C}$ -PC and  $^{14}\text{C}$ -GFF decreased  $\sim 3$ -fold between the well-lit upper ocean waters (<45 m; average PAR flux at 45 m of  $4.1 \pm 1.7 \text{ mol quanta m}^{-2} \text{ d}^{-1}$ ) and the lower euphotic zone (75-125 m; Figure 2.2). HOT program measurements of  $^{14}\text{C}$ -GFF averaged  $0.52 \pm 0.12 \mu\text{mol C L}^{-1} \text{ d}^{-1}$  in the upper euphotic zone, decreasing and becoming more temporally variable ( $0.17 \pm 0.13 \mu\text{mol C L}^{-1} \text{ d}^{-1}$ ) in the light-limited regions of the lower euphotic zone (Figure 2.2, 2.3). Upper euphotic zone  $^{14}\text{C}$ -PC rates averaged  $0.32 \pm 0.08 \mu\text{mol C L}^{-1} \text{ d}^{-1}$  and decreased to a mean value of  $0.10 \pm 0.07$

$\mu\text{mol C L}^{-1} \text{ d}^{-1}$  near the base of the euphotic zone (Figure 2.2, 2.3). Both volumetric and depth-integrated (0-125 m) rates of  $^{14}\text{C}$ -GFF were significantly greater (by  $\sim 1.7$ -fold, on average) than coincident measurements of  $^{14}\text{C}$ -PC (Figure 2; Kruskal-Wallis,  $p < 0.0001$ ).

By comparing concentrations of chlorophyll *a* and rates of  $^{14}\text{C}$ -productivity measured using polycarbonate filters to coincident HOT program measurements made using glass fiber filters we were able to examine differences in the retention characteristics of these two types of filters (Figure 2.4). This comparison revealed that volumetric concentrations and vertically integrated (0-125 m) inventories of chlorophyll *a* derived from both polycarbonate and glass fiber filters were statistically indistinguishable (Kruskal-Wallis,  $p > 0.05$ ; Figure 2.4).

To examine temporal variability in rates of  $^{14}\text{C}$ -DOC, we utilized the methodology described by Karl et al. (1998). The resulting precision of the derived rates, based on the coefficient of variation of triplicate  $^{14}\text{C}$ -DOC samples, ranged from 2-74% (averaging 29%). In comparison, the precision associated with the  $^{14}\text{C}$ -PC and  $^{14}\text{C}$ -GFF measurements ranged 0.3-70% (averaging 19%) and 0.5-50% (averaging 10%), respectively. More than half of  $^{14}\text{C}$ -DOC samples were above the calculated detection limit (defined as three times the standard deviation values of the mean time zero 'blanks' for each cruise) in the three uppermost depths (5, 25, 45 m), but by 125 m less than 20% of  $^{14}\text{C}$ -DOC measurements were above the detection limit (Figure 2.3, Table 2.2). In contrast, measurements of  $^{14}\text{C}$ -PC and  $^{14}\text{C}$ -GFF were consistently above detection limits, irrespective of the depth sampled.

Rates of  $^{14}\text{C}$ -DOC production were consistently lower than either  $^{14}\text{C}$ -PC or  $^{14}\text{C}$ -GFF (Figure 2.2). Upper ocean rates of  $^{14}\text{C}$ -DOC production averaged  $0.07 \pm 0.05 \mu\text{mol C L}^{-1} \text{ d}^{-1}$  and decreased to  $0.03 \pm 0.04 \mu\text{mol C L}^{-1} \text{ d}^{-1}$  in the lower euphotic zone; however, rates of  $^{14}\text{C}$ -DOC

in the lower euphotic were frequently below detection (Table 2.2). The resulting depth-dependent decreases in rates of  $^{14}\text{C}$ -DOC were slightly less ( $\sim 2.4$ -fold) than observed for either  $^{14}\text{C}$ -PC or  $^{14}\text{C}$ -GFF. Rates of  $^{14}\text{C}$ -DOC in the upper euphotic zone averaged  $\sim 21\%$  of  $^{14}\text{C}$ -PC, while mean rates of  $^{14}\text{C}$ -DOC in the lower euphotic zone were equivalent to  $\sim 33\%$  of  $^{14}\text{C}$ -PC (Figure 2.2). The resulting sum of the  $^{14}\text{C}$ -PC and  $^{14}\text{C}$ -DOC was consistently lower than the HOT program measurements of  $^{14}\text{C}$ -GFF; on average, the  $^{14}\text{C}$ -GFF rates were 1.4-fold greater than the sum of the coincident  $^{14}\text{C}$ -PC and  $^{14}\text{C}$ -DOC measurements.

We evaluated potential relationships between depth-dependent changes in PAR and the various  $^{14}\text{C}$ -based measurements of productivity using a hyperbolic photosynthesis-irradiance model (Platt et al., 1980). Although the model provided information on vertical relationships between  $^{14}\text{C}$ -GFF,  $^{14}\text{C}$ -PC and the downwelling light field, the relationship between light intensity and rates of  $^{14}\text{C}$ -DOC productivity was poorly described using this model (Table 2.3; Figure 2.5). Rates of both  $^{14}\text{C}$ -PC and  $^{14}\text{C}$ -GFF demonstrated similar patterns as a function of irradiance, increasing linearly with increasing light intensity in the lower euphotic zone, and saturating at light intensities ( $E_K$ )  $\sim 1.5$  mol quanta  $\text{m}^{-2} \text{d}^{-1}$  (Table 2.3). Throughout the study, the 1.5 mol quanta  $\text{m}^{-2} \text{d}^{-1}$  isolume varied between 35 m and 97 m. Neither  $^{14}\text{C}$ -GFF nor  $^{14}\text{C}$ -PC demonstrated significant photoinhibition (Table 2.3). The initial slope ( $\alpha$ ) derived from the relationship between  $^{14}\text{C}$ -GFF and PAR was significantly greater than that derived from the relationship of  $^{14}\text{C}$ -PC to PAR (Table 2.3).

### **Temporal variability in rates of $^{14}\text{C}$ -based productivity**

We examined temporal variability in the resulting time-series measurements of  $^{14}\text{C}$ -GFF,  $^{14}\text{C}$ -PC, and  $^{14}\text{C}$ -DOC productivity. As a result of the low detectability of  $^{14}\text{C}$ -DOC production

rates in the lower euphotic zone, we confined our analysis of time variability in productivity to the upper 75 meters. Depth-integrated (0-75 m) rates of  $^{14}\text{C}$ -GFF ranged between 21.8 and 48.7  $\text{mmol C m}^{-2} \text{d}^{-1}$  (Figure 2.6) throughout the study, while rates (0-75 m) of  $^{14}\text{C}$ -PC production ranged between 11.4 and 31.5  $\text{mmol C m}^{-2} \text{d}^{-1}$  (Figure 2.6). Rates of  $^{14}\text{C}$ -DOC productivity ranged from undetectable to 12.6  $\text{mmol C m}^{-2} \text{d}^{-1}$  (Figure 2.6), and did not vary significantly with time-varying changes in  $^{14}\text{C}$ -GFF (Model II linear regression;  $r^2 = 0.01$ ,  $p > 0.2$ ), rates of  $^{14}\text{C}$ -PC (Model II linear regression;  $r = 0.00$ ,  $p > 0.4$ ), or with the resulting differences in derived rates of  $^{14}\text{C}$ -production ( $^{14}\text{C}\text{-delta} = ^{14}\text{C}\text{-GFF} - ^{14}\text{C}\text{-PC}$ ) (Model II linear regression;  $r = 0.06$ ,  $p > 0.15$ ). The resulting depth-integrated rates of  $^{14}\text{C}$ -DOC were temporally variable, with rates varying  $\sim 9$ -fold (1.4 to 12.6  $\text{mmol C m}^{-2} \text{d}^{-1}$ ) over the period of study, while rates of  $^{14}\text{C}$ -delta varied  $\sim 11$ -fold (2.6 to 27.8  $\text{mmol C m}^{-2} \text{d}^{-1}$ ). In contrast, rates of  $^{14}\text{C}$ -GFF and  $^{14}\text{C}$ -PC varied by  $\sim 2$  and  $\sim 3$ -fold, respectively (Figure 2.6).

Binning our measurements by predefined seasons and examining possible seasonality in volumetric rates of  $^{14}\text{C}$ -DOC,  $^{14}\text{C}$ -PC, and  $^{14}\text{C}$ -GFF in both the well-lit, upper ocean (0-45 m) and dimly-lit, lower euphotic zone (75-125 m) highlighted apparent seasonal differences among the measures of productivity. When combining all the data collected for this study (October 2004-October 2007, and April 2010-October 2012), rates of both  $^{14}\text{C}$ -PC and  $^{14}\text{C}$ -GFF in the upper euphotic zone were significantly greater during the summer than during the winter (One-way ANOVA;  $p < 0.01$  and  $p < 0.05$ , respectively), while rates of  $^{14}\text{C}$ -DOC demonstrated no significant seasonality (One-way ANOVA;  $p > 0.05$ ). In the lower euphotic zone, rates of  $^{14}\text{C}$ -GFF were greater in the spring than during fall and winter (One-way ANOVA;  $p < 0.0005$ ), while rates in the summer were greater than rates measured in the fall (One-way ANOVA;  $p < 0.0005$ ). Lower euphotic zone  $^{14}\text{C}$ -PC rates were greater during the spring than during fall and winter,

while rates of  $^{14}\text{C}$ -DOC were not significantly different among seasons (One-way ANOVA;  $p < 0.005$ ). However, when we considered the two periods measured during this study (Table 2.1), seasonal differences were only observed during the first period of this study. These differences were similar to those observed when both periods were considered together. In contrast, no significant differences were seen for any rates measured during the second period of observations (One-way ANOVA;  $p > 0.05$ ).

Results of the seasonal comparisons led us to analyze the resulting time-series measurements of  $^{14}\text{C}$ -DOC,  $^{14}\text{C}$ -delta,  $^{14}\text{C}$ -PC, and  $^{14}\text{C}$ -GFF using two different time-series statistical models. Application of the Lomb-Scargle periodogram (Ruf, 1999) to the full  $^{14}\text{C}$ -GFF time-series (1989 – 2013) revealed a significant periodicity at ~12 months ( $p < 0.0000005$ ; data not shown), consistent with previously described annual cycle of primary productivity at Station ALOHA, where rates increase in summer compared to winter (Church et al., 2013; Karl et al., 1996; Letelier et al., 1996). However, use of the Lomb-Scargle periodogram to analyze the time-series rates ( $^{14}\text{C}$ -DOC,  $^{14}\text{C}$ -PC, and  $^{14}\text{C}$ -GFF) either as a combined record (*i.e.* October 2004-October 2007, and April 2010-October 2012) or either record alone identified no significant periodicity ( $p > 0.05$ ). Use of the model described in Llope et al. (2007) revealed similar results. Results from both the seasonal regression and the Lomb-Scargle periodogram suggested that the measurement records made during this study were of insufficient length to identify recurring temporal patterns.

### **Diel variability in rates of productivity**

We conducted three experiments designed to evaluate short-term (daily scale) variability in the various measures of  $^{14}\text{C}$ -productivity. For these experiments, we varied the incubation

period for the  $^{14}\text{C}$  measurements, including samples incubated during the morning hours only (predawn to noon), the full photoperiod (predawn to dusk), and over a full 24 hour period (predawn to the following predawn). These experiments demonstrated significant overnight losses of particulate  $^{14}\text{C}$ -labeled carbon relative to incubations conducted throughout the photoperiod (Figure 2.7). Hourly rates measured during morning hours only were not significantly different from hourly rates measured during the entire photoperiod for  $^{14}\text{C}$ -PC (One-way ANOVA;  $p>0.5$ ). In contrast, hourly rates measured during the photoperiod were greater than those measured over the full 24 hours for both  $^{14}\text{C}$ -GFF and  $^{14}\text{C}$ -PC (One-way ANOVA;  $p<0.001$ ). The resulting hourly rates of  $^{14}\text{C}$ -PC and  $^{14}\text{C}$ -GFF production measured over a 24 hour period were  $37 \pm 16\%$  and  $43 \pm 17\%$  of rates measured over the photoperiod, hence the amount of carbon fixed over 24 hours averaged  $75 \pm 15\%$  and  $87 \pm 8\%$  of photoperiod carbon fixation for  $^{14}\text{C}$ -PC and  $^{14}\text{C}$ -GFF, respectively. In contrast, hourly rates of  $^{14}\text{C}$ -DOC and  $^{14}\text{C}$ -GFF were significantly greater for incubations during the morning hours (One-way ANOVA;  $p<0.05$ ) than for incubations lasting the full photoperiod; photoperiod rates of  $^{14}\text{C}$ -DOC were  $43 \pm 17\%$  of hourly rates measured during morning hours only. Rates of  $^{14}\text{C}$ -DOC measured over a 24 hour period) were not significantly different from rates measured over the photoperiod (One-way ANOVA;  $p>0.10$ ).

### **$^{14}\text{C}$ -DOC retention by filter type**

We conducted several experiments designed to evaluate possible reasons for the greater retention of  $^{14}\text{C}$ -organic carbon on glass fiber filters relative to polycarbonate filters. The first set of experiments involved stacking polycarbonate and glass fiber filters in series for subsequent filtration of  $^{14}\text{C}$ -labeled whole seawater samples. When a glass fiber filter was stacked on top of a polycarbonate filter, the polycarbonate filter retained a small fraction ( $<5\%$ ) of the total  $^{14}\text{C}$

activity associated with both filters (Supplementary Figure 2.S1). In contrast, when a polycarbonate filter was overlaid on a glass fiber filter, the glass fiber filter retained >33% of the resulting total  $^{14}\text{C}$ -activity. Similar experiments conducted to examine filter retention of chlorophyll *a* through stacked glass fiber and polycarbonate filters revealed that irrespective of which filter type was on top, the bottom filter retained <5% of the measured chlorophyll *a* (Supplementary Figure 2.S1) of the top filter. Another experiment was conducted to evaluate successive retention of  $^{14}\text{C}$ -organic carbon by glass fiber filters. We refiltered 100 ml volumes of  $0.2\ \mu\text{m}$   $^{14}\text{C}$ -PC filtrate onto a succession of glass fiber filters and found that retention of  $^{14}\text{C}$  labeled organic carbon by these filters decreased ~5-fold (to <20% of the first 100 ml filtration) by the second filtration and ~8-fold (to 13% of the first 100 ml filtration) by the fourth filtration (Supplementary Figure 2.S1). Additionally, the amount of  $^{14}\text{C}$ -DOC adsorbed onto the glass fiber filters following filtration of the first 100 ml of sample was not significantly different than the amount of  $^{14}\text{C}$ -DOC adsorbed after filtration of 500 ml (one-way ANOVA;  $p>0.05$ ; Supplementary Figure 2.S1) onto one filter. We also conducted an experiment to evaluate the effects of filtering different volumes of seawater onto both glass fiber and  $0.2\ \mu\text{m}$  polycarbonate filters (Supplementary Figure 2); the resulting differences in derived rates of  $^{14}\text{C}$ -delta did not vary with increasing volume filtered onto glass fiber filters, suggesting that the observed differences between the time-series based rates of  $^{14}\text{C}$ -GFF and  $^{14}\text{C}$ -PC was not an artifact of differences in filtration volumes used for these filters (500 ml versus 100 ml, respectively; Supplementary Figure 2.S2).

## Discussion

The partitioning of organic carbon production between dissolved and particulate phases has important biogeochemical and ecological implications, and numerous hypotheses have been proposed to explain processes regulating the magnitude and variability of this partitioning (see review by (Carlson, 2002). While photosynthetic production of particulate organic carbon (*i.e.* cellular material) can fuel numerous food web pathways (*e.g.* predation, viral lysis) and constitute a pathway for organic carbon export from the upper ocean (via gravitational settling or zooplankton migration), production of DOC subsidizes the energetic and nutritional demands of heterotrophic bacteria, fueling a grazing intensive microbial loop (Azam et al., 1983). Moreover, DOC can constitute an important component of carbon export, via removal through physical processes such as mixing and eddy diffusivity (Carlson et al., 1994; Emerson, 2014). Hence, quantifying the partitioning of organic carbon productivity through these distinct pathways is important for insight into the fate of recently fixed carbon through aquatic ecosystems.

In the current study, we examined rates of dissolved and particulate  $^{14}\text{C}$ -based measures of primary production at Station ALOHA. The resulting time-series measurements yielded insight into methodological considerations underlying application of the  $^{14}\text{C}$ -based production assays, and highlighted vertical and temporal variability in the partitioning of recently fixed carbon between particulate and dissolved pools in this ecosystem. Consistent with previous reports (Karl et al., 1998; Maske and Garcia-Mendoza, 1994; Morán et al., 1999), our study demonstrated greater (1.6-fold on average)  $^{14}\text{C}$ -productivity derived from samples filtered onto glass fiber filters (with a nominal pore size of  $0.7\ \mu\text{m}$ ) relative to productivity rates derived from  $0.2\ \mu\text{m}$  polycarbonate membrane filters. In contrast, but consistent with a previous study (Chavez et al., 1995), simultaneous fluorometric determinations of chlorophyll *a* concentrations filtered onto polycarbonate and glass fiber filters revealed no consistent difference between these

filter types for retention of chlorophyll *a*, suggesting the observed differences between  $^{14}\text{C}$ -GFF and  $^{14}\text{C}$ -PC did not derive from differences in the efficiency with which these filters trap photosynthetic organisms.

Various studies have documented adsorption of DOC by glass fiber filters (Abdel-Moati, 1990; Maske and Garcia-Mendoza, 1994), and our findings largely support the hypothesis that the greater rates of  $^{14}\text{C}$ -GFF relative to  $^{14}\text{C}$ -PC derive from adsorption of  $^{14}\text{C}$ -DOC produced during the incubation to the glass fiber filters (Karl et al., 1998; Morán et al., 1999). Notably, on average, rates of  $^{14}\text{C}$ -GFF productivity exceeded the sum of the independent measurements of  $^{14}\text{C}$ -PC and  $^{14}\text{C}$ -DOC production by ~42%. Such differences between rates of  $^{14}\text{C}$ -PC +  $^{14}\text{C}$ -DOC and  $^{14}\text{C}$ -GFF may reflect incomplete recovery of  $^{14}\text{C}$ -DOC by the oxidation and trapping procedure, loss of volatile  $^{14}\text{C}$ -DOC during the active bubbling procedure in the  $^{14}\text{C}$ -DOC assay, incomplete oxidation of  $^{14}\text{C}$ -DOC by the persulfate oxidation procedure, or incomplete removal of  $^{14}\text{C}$ -DIC from the glass fiber filters (Mague et al., 1980). Moreover, the relatively large methodological uncertainty of the  $^{14}\text{C}$ -DOC assay (coefficient of variation of triplicate measurements averaged 29%) further complicates this comparison. Time zero blanks indicated that the amount of  $^{14}\text{C}$  remaining on glass fiber filters post-acidification was always less than 5% of total  $^{14}\text{C}$  retained on the these filters post-incubation. These results, together with our experiments examining retention of  $^{14}\text{C}$  organic matter onto glass fiber filters using particle-free seawater, suggest the differences between measured  $^{14}\text{C}$ -GFF and  $^{14}\text{C}$ -PC reflect adsorption of  $^{14}\text{C}$ -DOC by glass fiber filters. Hence we computed the difference between the  $^{14}\text{C}$ -GFF and  $^{14}\text{C}$ -PC rate measurements ( $^{14}\text{C}$ -delta) as an additional proxy for  $^{14}\text{C}$ -DOC production. Throughout our study, there was no relationship between depth-integrated rates of  $^{14}\text{C}$ -DOC and  $^{14}\text{C}$ -delta, with  $^{14}\text{C}$ -delta rates greater than  $^{14}\text{C}$ -DOC rates on all but one cruise.

The observed differences between the  $^{14}\text{C}$ -PC and  $^{14}\text{C}$ -GFF rates could derive from differences in the volumes filtered for these analyses (see Huete-Ortega et al., 2012). For the  $^{14}\text{C}$ -PC filtrations, we concentrated 100 ml of seawater sample onto polycarbonate filters, while the HOT program  $^{14}\text{C}$ -GFF measurements rely on filtration of 500 ml volumes of seawater. This difference in volume filtered could result in greater trapping of particles or  $^{14}\text{C}$ -DOC by the glass fiber filters, which could account for the observed discrepancy between  $^{14}\text{C}$ -GFF and  $^{14}\text{C}$ -DOC+ $^{14}\text{C}$ -PC. However, results from experiments we conducted examining adsorption characteristics of glass fiber filters suggest that the majority of  $^{14}\text{C}$ -DOC is adsorbed during filtration of the first 100 ml of sample. Moreover, we observed no significant increases in the volume corrected differences between  $^{14}\text{C}$ -GFF and  $^{14}\text{C}$ -PC ( $^{14}\text{C}$ -delta) with increasing filtration volume above 100 ml. Such results suggest the differences in filtered volumes for the  $^{14}\text{C}$ -PC and  $^{14}\text{C}$ -GFF determinations likely would not account for the observed differences in  $^{14}\text{C}$ -delta and direct quantification of  $^{14}\text{C}$ -DOC. Regardless of the mechanism responsible for the apparent offset between these measurements, the coincident measurements of  $^{14}\text{C}$ -productivity using both glass fiber and polycarbonate filters provided a useful constraint on the partitioning of primary production between dissolved and particulate phases in our study.

The resulting time-series measurements of  $^{14}\text{C}$ -DOC,  $^{14}\text{C}$ -GFF, and  $^{14}\text{C}$ -PC productivity provided insight into vertical- and time-dependent variations in the partitioning of primary production among dissolved and particulate phases at Station ALOHA. Over ~2.5 years (2010-2012), rates of  $^{14}\text{C}$ -DOC production averaged 18% ( $\pm 10\%$ ) of the daytime photosynthetic production (sum of  $^{14}\text{C}$ -DOC and  $^{14}\text{C}$ -PC). Integrated rates (0-75 m) of  $^{14}\text{C}$ -DOC production ranged approximately 8.8-fold over the period of study (1.4 to 12.6  $\text{mmol C m}^{-2} \text{d}^{-1}$ ) and did not appear to co-vary with changes in  $^{14}\text{C}$ -GFF or  $^{14}\text{C}$ -PC primary productivity. Similar to studies in

the oligotrophic Atlantic Ocean (Teira et al., 2001, 2003), rates of  $^{14}\text{C}$ -DOC in the current study were not well correlated (either in depth or in time) with estimates of photosynthetic particulate matter production (based on rates of  $^{14}\text{C}$ -GFF or  $^{14}\text{C}$ -PC). When data from both time periods of this study were combined, in both the upper and lower regions of the euphotic zone, rates of  $^{14}\text{C}$ -GFF and  $^{14}\text{C}$ -PC varied seasonally, with elevated production in the upper euphotic zone during the summer, while rates in the lower euphotic zone were greatest in the spring. We utilized various statistical models (the Lomb-Scargle periodogram and an optimized least squares monthly regression) to evaluate possible recurring temporal patterns in our datasets. However, the relatively limited duration of our near-monthly observations ( $\sim 2.5$  years for  $^{14}\text{C}$ -DOC, and  $\sim 5$  years for  $^{14}\text{C}$ -GFF and  $^{14}\text{C}$ -PC) proved insufficient to derive statistically robust patterns based on these analyses. Use of comparative statistical models (ANOVA) did highlight apparent seasonality in the longer duration time-series measurements of  $^{14}\text{C}$ -PC and  $^{14}\text{C}$ -GFF; however, rates of  $^{14}\text{C}$ -DOC did not demonstrate similar seasonal fluctuations. These analyses confirmed that the latter period of our observations (2010 to 2012) coincided with a period of time where anomalous patterns in productivity were observed (Wilson et al., 2015). Unlike the seasonal climatology observed in the HOT program record of productivity, where rates of  $^{14}\text{C}$ -GFF increase 2-3-fold during the summer months (Karl and Church, 2014), rates of  $^{14}\text{C}$ -GFF were greatest during the winter months of 2011 and 2012. Such anomalous seasonal patterns in productivity likely contributed to the relatively poor fit of the various statistical models we applied to our measurements of  $^{14}\text{C}$ -GFF,  $^{14}\text{C}$ -PC, and  $^{14}\text{C}$ -DOC.

The weak relationship observed between measurements of  $^{14}\text{C}$ -DOC and rates of  $^{14}\text{C}$ -PC and  $^{14}\text{C}$ -GFF may reflect the complex suite of processes that control net production of DOC in this ecosystem, many of which may not be directly coupled in time to photosynthetic production

of particulate carbon and likely vary with depth. Ecosystems dominated by picoplankton such as the NPSG often appear to partition a greater fraction of photosynthetic production toward DOC than do larger phytoplankton (Legendre and Rassoulzadegan, 1995; Malinsky-Rushansky and Legrand, 1996; Teira et al., 2001). The greater partitioning of fixed carbon into the DOC pool is hypothesized to derive from tightly coupled trophodynamic processes, including those linked to the functioning of the microbial loop (predation and/or viral lysis). Several studies have observed that nutrient-limited and light replete systems tend to partition a greater fraction of recently produced photosynthate into the dissolved pool relative to the particulate pool; conversely nutrient-enriched ecosystems appear to partition a greater fraction of the daily net productivity toward cellular (particulate) production (Biddanda et al., 2001; Carlson et al., 1998). Over the course of our study we observed significant production of  $^{14}\text{C}$ -DOC in the persistently oligotrophic, well-lit upper euphotic zone (0-45 m); in contrast, in the light-limited but nutrient-enriched lower euphotic zone (75-125 m), rates of  $^{14}\text{C}$ -DOC were often below our detection limit. Unlike rates of  $^{14}\text{C}$ -DOC, rates of particulate carbon production ( $^{14}\text{C}$ -PC and  $^{14}\text{C}$ -GFF) exhibited strong depth dependence, with rates in the dimly-lit lower euphotic zone averaging ~33% and 34% ( $^{14}\text{C}$ -PC and  $^{14}\text{C}$ -GFF, respectively) of rates measured in the well-lit upper ocean. As a result, the vertical distribution of PER (Percent Extracellular Release;  $^{14}\text{C}$ -DOC / ( $^{14}\text{C}$ -DOC +  $^{14}\text{C}$ -PC)) did not demonstrate clear depth dependence, a finding consistent with previous work in more eutrophic marine systems (*e.g.* Marañón et al., 2004).

Application of a photosynthesis-irradiance model further emphasized the differences between vertical changes in  $^{14}\text{C}$ -DOC compared to particulate production. Rates of  $^{14}\text{C}$ -DOC production demonstrated no significant relationships with downwelling PAR. The observation that rates of  $^{14}\text{C}$ -DOC varied less with depth than rates of  $^{14}\text{C}$ -PC or  $^{14}\text{C}$ -GFF suggests that

unlike cellular production (as estimated from measurements of  $^{14}\text{C}$ -PC and  $^{14}\text{C}$ -GFF), light does not appear to be as strong a control on net photosynthetic production of DOC at Station ALOHA. Such results are consistent with other environmental studies conducted in ocean ecosystems (Lancelot, 1983; Marañón et al., 2004), although studies in the Gulf of Mexico and the Eastern tropical North Pacific revealed a dependence of  $^{14}\text{C}$ -DOC production with vertical changes in irradiance (Cherrier et al., 2014). While we did not evaluate mechanisms that underlie the partitioning of photosynthetically fixed carbon into DOC, such results suggest the potential importance of processes that are light independent.

The time-series rate measurements conducted as part of this study derived from incubations lasting over the full daily photoperiod (11-13 hours); during that time period, a significant fraction of the  $^{14}\text{C}$ -DOC produced during the incubation was likely consumed. Hence our measurements of  $^{14}\text{C}$ -DOC presumably approximate net rates of production. On three occasions, we compared  $^{14}\text{C}$ -productivity during three time periods: morning (predawn to noon), photoperiod (predawn to dusk), and 24-hour (predawn to predawn). These experiments were conducted to provide insight into nighttime removal of the recently fixed  $^{14}\text{C}$ , and to investigate possible differences in partitioning of recently fixed  $^{14}\text{C}$  throughout the daylight period. Rates of  $^{14}\text{C}$ -DOC production were significantly greater during the morning compared to the full photoperiod, suggesting a larger fraction of recently fixed photosynthate is partitioned to DOC in the morning. Alternatively, these results could reflect changes in the coupling between production and consumption throughout the day, and hence the longer duration (photoperiod) rate measurements may approximate net production while the shorter incubation may be more similar to gross  $^{14}\text{C}$ -DOC production (e.g. Lancelot (1979).

Our experiments demonstrated no significant difference between the total amount of  $^{14}\text{C}$ -DOC produced during 24 hour and photoperiod incubations, compared to significant nighttime losses of fixed  $^{14}\text{C}$ -particulate carbon ( $^{14}\text{C}$ -PC and  $^{14}\text{C}$ -GFF, respectively). Such results suggest that  $^{14}\text{C}$ -DOC produced during the photoperiod was consumed at night at lower rates than contemporaneous particulate production; alternatively, there may be sources of  $^{14}\text{C}$ -DOC production at night that offset simultaneous consumption. Previous results from a coastal upwelling system (Marañón et al. 2004) found no significant DOC production at night, and that study attributed DOC production to phytoplankton exudation rather than trophic processes. In contrast, in the oligotrophic NPSG, lack of significant change in  $^{14}\text{C}$ -DOC produced at night could reflect a combination of reinforcing processes. Rapid coupling between production and consumption of  $^{14}\text{C}$ -DOC during daylight hours could leave a relatively less reactive pool of  $^{14}\text{C}$ -DOC to persist through the nighttime. In addition, the diverse pathways that create DOC during the day (grazing, viral lysis, direct exudation/excretion) likely continue during the night (Christaki et al., 2002; Tsai et al., 2005). In contrast, photoperiod photosynthetic production of particulate material presumably reflects net cellular production, and subsequent nighttime losses of the fixed carbon likely reflect phytoplankton respiration together with cellular removal processes (grazing, viral lysis) (Marra and Barber, 2004). Recent studies have reported diel cycle fluctuations in the physiological and transcriptional activities of both phytoplankton and heterotrophic bacteria, that appear tightly coupled (Aylward et al., 2015; Binder and DuRand, 2002; Ottesen et al., 2013, 2014; Poretsky et al., 2009; Vaultot et al., 1995). Results from the short-term productivity experiments in the present study indicate that in addition to the lack of a significant relationship between rates of particulate and dissolved primary productivity observed during our monthly scale sampling, these rates are also decoupled over daily time scales, which

may have important implications for the diel activity cycles of the heterotrophic bacteria that rely on recently produced photosynthate.

The time-series measurements of  $^{14}\text{C}$ -primary production reported here underscore several important features of the NPSG ecosystem. Rates of net  $^{14}\text{C}$ -DOC production appear both vertically and temporally decoupled from variations in rates of  $^{14}\text{C}$ -GFF or  $^{14}\text{C}$ -PC. In particular, over a ~2.5 year period of near-monthly observations, rates of particulate matter productivity were decoupled from  $^{14}\text{C}$ -DOC production over diel to seasonal time scales. Moreover, consistent with a prior report (Karl et al. 1998), we find that photosynthetic production of DOC can be an important, but variable pathway for organic carbon production in the NPSG, accounting for nearly one fifth of the net daytime  $^{14}\text{C}$ -based estimates of productivity. Our results also provide indications of the complexity of interacting processes that control net production and consumption of organic matter in this ecosystem, highlighting the need for future studies quantifying the magnitude and variability of such processes.

### **Conflict of Interest Statement**

The authors declare that the research was conducted in the absence of any commercial or financial relationship that could be construed as a potential conflict of interest.

### **Acknowledgements**

Funding for this study derived from the National Science Foundation, including grants OCE-0850827 (MJC), OCE-1260164 (MJC and DMK), and EF-0424599 (DMK). Additional

support derived from the Simons Foundation via the Simons Collaboration on Ocean Processes and Ecology (SCOPE; DMK and MJC) and the Gordon and Betty Moore Foundation Marine Microbiology Investigator grant 3794 (DMK). We thank the various scientists and staff of the HOT program for their assistance at sea and in the laboratory. We thank Benedetto Barone for his thoughtful comments that improved this manuscript. We extend our gratitude to the officers and crew of the R/V *Kilo Moana* and the R/V *Kaimikai-o-Kanaloa*. Comments by two anonymous reviewers improved the presentation of this work.

### **Author contributions**

All authors contributed substantially to the design of this study, interpretation of results, and preparation of the manuscript.

## Literature Cited

- Abdel-Moati, A. R. (1990). Adsorption of dissolved organic carbon (DOC) on glass fibre filters during particulate organic carbon (POC) determination. *Water Res.* 24, 763–764. doi:10.1016/0043-1354(90)90033-3.
- Aylward, F. O., Eppley, J. M., Smith, J. M., Chavez, F. P., Scholin, C. A., and DeLong, E. F. (2015). Microbial community transcriptional networks are conserved in three domains at ocean basin scales. *Proc. Natl. Acad. Sci.*, 112, 5443-5448. doi:10.1073/pnas.1502883112.
- Azam, F., Fenchel, T., Field, J., Gray, J., Meyer-Reil, L., and Thingstad, F. (1983). The ecological role of water-column microbes in the sea. *Mar. Ecol. Prog. Ser.* 10, 257–263.
- Baines, S., and Pace, M. (1991). The production of dissolved organic matter by phytoplankton and its importance to bacteria: Patterns across marine and freshwater systems. *Limnol. Oceanogr.* 36, 1078–1090.
- Banase, K. (1995). Zooplankton: Pivotal role in the control of ocean production. *ICES J. Mar. Sci.* 52, 265–277.
- Behrenfeld, M. J., and Falkowski, P. G. (1997). Photosynthetic rates derived from satellite-based chlorophyll concentration. *Limnol. Oceanogr.* 42, 1–20.
- Bender, M., Grande, K., Johnson, K., Marra, J., Williams, P., Sieburth, J., et al. (1987). A comparison of four methods for determining planktonic community production. *Limnol. Oceanogr.* 32, 1085–1098.
- Biddanda, B., Ogdahl, M., and Cotner, J. (2001). Dominance of bacterial metabolism in oligotrophic relative to eutrophic waters. *Limnol. Oceanogr.* 46, 730–739.
- Binder, B. J., and DuRand, M. D. (2002). Diel cycles in surface waters of the equatorial Pacific. *Deep Sea Res II* 49, 2601–2617. doi:10.1016/S0967-0645(02)00050-4.
- Bjørnsen, P. K. (1988). Phytoplankton exudation of organic matter: Why do healthy cells do it? *Limnol. Oceanogr.* 33, 151–154.
- Campbell, L., Nolla, H. A., and Vaultot, D. (1994). The importance of *Prochlorococcus* to community structure in the central North Pacific Ocean. *Limnol. Oceanogr.* 39, 954–961.
- Carlson, C. A. (2002). “Production and removal processes,” in *Biogeochemistry of Marine Dissolved Organic Matter*, eds. D. Hansell and C. A. Carlson (Amsterdam: Academic), 91–151.
- Carlson, C. A., Ducklow, H. W., Hansell, D. A., and Smith, W. O. (1998). Organic carbon partitioning during spring phytoplankton blooms in the Ross Sea polynya and the Sargasso Sea. *Limnol. Oceanogr.* 43, 375–386.

- Carlson, C. A., Hansell, D. A., Peltzer, E. T., and Smith Jr., W. O. (2000). Stocks and dynamics of dissolved and particulate organic matter in the southern Ross Sea, Antarctica. *Deep Sea Res II* 47, 3201–3225. doi:10.1016/S0967-0645(00)00065-5.
- Carlson, C., Ducklow, H., and Michaels, A. (1994). Annual flux of dissolved organic carbon from the euphotic zone in the northwestern Sargasso Sea. *Nature* 371, 405–408.
- Chavez, F. P., Buck, K. R., Bidigare, R. R., Karl, D. M., Hebel, D., Latasa, M., et al. (1995). On the chlorophyll *a* retention properties of glass-fiber GF/F filters. *Limnol. Oceanogr.* 40, 428–433. doi:10.4319/lo.1995.40.2.0428.
- Cherrier, J., Valentine, S., Hamill, B., Jeffrey, W. H., and Marra, J. F. (2014). Light-mediated release of dissolved organic carbon by phytoplankton. *J. Marine Syst.* 147, 45-51. doi:10.1016/j.jmarsys.2014.02.008.
- Christaki, U., Courties, C., Karayanni, H., Giannakourou, A., Maravelias, C., Kormas, K. A., et al. (2002). Dynamic characteristics of *Prochlorococcus* and *Synechococcus* consumption by bacterivorous nanoflagellates. *Microb. Ecol.* 43, 341–352. doi:10.1007/s00248-002-2002-3.
- Church, M. J., Lomas, M. W., and Muller-Karger, F. (2013). Sea change: Charting the course for biogeochemical ocean time-series research in a new millennium. *Deep Sea Res II* 93, 2–15. doi:10.1016/j.dsr2.2013.01.035.
- Church, M. J., Mahaffey, C., Letelier, R. M., Lukas, R., Zehr, J. P., and Karl, D. M. (2009). Physical forcing of nitrogen fixation and diazotroph community structure in the North Pacific subtropical gyre. *Global Biogeochem. Cycles* 23, GB2020. doi:10.1029/2008GB003418.
- Conan, P., Sondergaard, M., Kragh, T., Thingstad, F., Pujo-Pay, M., Williams, P. J. le B., et al. (2007). Partitioning of organic production in marine plankton communities: The effects of inorganic nutrient ratios and community composition on new dissolved organic matter. *Limnol. Oceanogr.* 52, 753–765.
- Dore, J. E., and Karl, D. M. (1996). Nitrite distributions and dynamics at Station ALOHA. *Deep Sea Res II* 43, 385–402. doi:10.1016/0967-0645(95)00105-0.
- Dore, J., Letelier, R., Church, M., Lukas, R., and Karl, D. (2008). Summer phytoplankton blooms in the oligotrophic North Pacific Subtropical Gyre: Historical perspective and recent observations. *Prog. Oceanogr.* 76, 2–38. doi:10.1016/j.pocean.2007.10.002.
- Druffel, E., Williams, P., Bauer, J., and Erel, J. (1992). Cycling of dissolved and particulate organic matter in the open ocean. *J. Geophys. Res.* 97, 15639–15659.
- Emerson, S. (2014). Annual net community production and the biological carbon flux in the ocean. *Global Biogeochem. Cycles* 28, 2013GB004680. doi:10.1002/2013GB004680.

- Evans, C., Pearce, I., and Brussaard, C. P. D. (2009). Viral-mediated lysis of microbes and carbon release in the sub-Antarctic and Polar Frontal zones of the Australian Southern Ocean. *Environ. Microbiol.* 11, 2924–2934. doi:10.1111/j.1462-2920.2009.02050.x.
- Field, C. B., Behrenfeld, M. J., Randerson, J. T., and Falkowski, P. (1998). Primary production of the biosphere: Integrating terrestrial and oceanic components. *Science* 281, 237–240. doi:10.1126/science.281.5374.237.
- Fogg, G. E. (1966). The extracellular products of algae. *Oceanogr. Mar. Biol.* 4, 195–212.
- Garside, C. (1982). A chemiluminescent technique for the determination of nanomolar concentrations of nitrate and nitrite in seawater. *Mar. Chem.* 11, 159–167. doi:10.1016/0304-4203(82)90039-1.
- Hansell, D. A., Carlson, C. A., Repeta, D. J., and Schlitzer, R. (2009). Dissolved organic matter in the ocean: A controversy stimulates new insights. *Oceanography* 22, 202–211.
- Hedges, J. I. (1992). Global biogeochemical cycles: progress and problems. *Mar. Chem.* 39, 67–93. doi:10.1016/0304-4203(92)90096-S.
- Hellebust, J. A. (1965). Excretion of some organic compounds by marine phytoplankton. *Limnol. Oceanogr.* 10, 192–206.
- Huete-Ortega, M., Cermeño, P., Calvo-Díaz, A., and Marañón, E. (2012). Isometric size-scaling of metabolic rate and the size abundance distribution of phytoplankton. *P. Roy. Soc. Lond. B Biol. Sci.* 279:1815–1823. doi:10.1098/rspb.2011.2257.
- Hygum, B. H., Petersen, J. W., and Søndergaard, M. (1997). Dissolved organic carbon released by zooplankton grazing activity—a high-quality substrate pool for bacteria. *J. Plankton Res.* 19, 97–111. doi:10.1093/plankt/19.1.97.
- Kaiser, K., and Benner, R. (2009). Biochemical composition and size distribution of organic matter at the Pacific and Atlantic time-series stations. *Mar. Chem.* 113, 63–77. doi:10.1016/j.marchem.2008.12.004.
- Karl, D., Bidigare, R., and Letelier, R. (2001). Long-term changes in plankton community structure and productivity in the North Pacific Subtropical Gyre: The domain shift hypothesis. *Deep Sea Res II* 48, 1449–1470.
- Karl, D., Christian, J., Dore, J., Hebel, D., Letelier, R., Tupas, L., et al. (1996). Seasonal and interannual variability in primary production and particle flux at Station ALOHA. *Deep Sea Res II* 43, 539–568.
- Karl, D., Hebel, D., Björkman, K., and Letelier, R. (1998). The role of dissolved organic matter release in the productivity of the oligotrophic North Pacific Ocean. *Limnol. Oceanogr.* 43, 1270–1286.

- Karl, D. M., and Church, M. J. (2014). Microbial oceanography and the Hawaii Ocean Time-series programme. *Nat. Rev. Microbiol.* 12, 699–713. doi:10.1038/nrmicro3333.
- Karl, D. M., and Tien, G. (1992). MAGIC: A sensitive and precise method for measuring dissolved phosphorus in aquatic environments. *Limnol. Oceanogr.* 37, 105–116.
- Lampert, W. (1978). Release of dissolved organic carbon by grazing zooplankton. *Limnol. Oceanogr.* 23, 831–834.
- Lancelot, C. (1979). Gross excretion rates of natural marine phytoplankton and heterotrophic uptake of excreted products in the Southern North Sea, as determined by short-term kinetics. *Mar. Ecol. Prog. Ser.* 1, 179–186.
- Lancelot, C. (1983). Factors affecting phytoplankton extracellular release in the Southern Bight of the North Sea. *Mar. Ecol. Prog. Ser.* 12, 115–121.
- Landry, M., Al-Mutairi, H., Selph, K., Christensen, S., and Nunnery, S. (2001). Seasonal patterns of mesozooplankton abundance and biomass at Station ALOHA. *Deep Sea Res II* 48, 2037–2061. doi:10.1016/S0967-0645(00)00172-7.
- Legendre, L., and Rassoulzadegan, F. (1995). Plankton and nutrient dynamics in marine waters. *Ophelia* 41, 153–172. doi:10.1080/00785236.1995.10422042.
- Letelier, R., Dore, J., Winn, C., and Karl, D. (1996). Seasonal and interannual variations in photosynthetic carbon assimilation at Station ALOHA. *Deep Sea Res II* 43, 467–490.
- Letelier, R., Karl, D., Abbott, M., and Bidigare, R. (2004). Light driven seasonal patterns of chlorophyll and nitrate in the lower euphotic zone of the North Pacific Subtropical Gyre. *Limnol. Oceanogr.* 49, 508–519.
- Lignell, R. (1990). Excretion of organic carbon by phytoplankton: its relation to algal biomass, primary productivity and bacterial secondary production in the Baltic Sea. *Mar. Ecol. Prog. Ser.* 68, 85–99.
- Llope, M., Anadón, R., Sostres, J. Á., and Viesca, L. (2007). Nutrients dynamics in the southern Bay of Biscay (1993-2003): Winter supply, stoichiometry, long-term trends, and their effects on the phytoplankton community. *J. Geophys. Res.* 112, C07029. doi:10.1029/2006JC003573.
- López-Sandoval, D. C., Fernández, A., and Marañón, E. (2011). Dissolved and particulate primary production along a longitudinal gradient in the Mediterranean Sea. *Biogeosciences* 8, 815–825.
- Mague, T. H., Friberg, E., Hughes, D. J., and Morris, I. (1980). Extracellular release of carbon by marine phytoplankton; A physiological approach. *Limnol. Oceanogr.* 25, 262–279.

- Malinsky-Rushansky, N., and Legrand, C. (1996). Excretion of dissolved organic carbon by phytoplankton of different sizes and subsequent bacterial uptake. *Mar. Ecol. Prog. Ser.* 132, 249–255. doi:10.3354/meps132249.
- Marañón, E., Cermeño, P., Fernández, E., Rodríguez, J., and Zabala, L. (2004). Significance and mechanisms of photosynthetic production of dissolved organic carbon in a coastal eutrophic ecosystem. *Limnol. Oceanogr.* 49, 1652–1666.
- Marra, J. (2009). Net and gross productivity: Weighing in with  $^{14}\text{C}$ . *Aquat. Microb. Ecol.* 56, 123–131.
- Marra, J., and Barber, R. T. (2004). Phytoplankton and heterotrophic respiration in the surface layer of the ocean. *Geophys. Res. Lett.* 31, L09314. doi:10.1029/2004GL019664.
- Maske, H., and Garcia-Mendoza, E. (1994). Adsorption of dissolved organic matter to the inorganic filter substrate and its implications for  $^{14}\text{C}$  uptake measurements. *Appl. Environ. Microbiol.* 60, 3887–3889.
- Møller, E. F. (2005). Sloppy feeding in marine copepods: prey-size-dependent production of dissolved organic carbon. *J. Plankton Res.* 27, 27–35. doi:10.1093/plankt/fbh147.
- Møller, E., Thor, P., and Nielsen, T. (2003). Production of DOC by *Calanus finmarchicus*, *C. glacialis* and *C. hyperboreus* through sloppy feeding and leakage from fecal pellets. *Mar. Ecol. Prog. Ser.* 262, 185–191. doi:10.3354/meps262185.
- Morán, X. A. G., and Estrada, M. (2001). Short-term variability of photosynthetic parameters and particulate and dissolved primary production in the Alboran Sea (SW Mediterranean). *Mar. Ecol. Prog. Ser.* 212, 53–67. doi:10.3354/meps212053.
- Morán, X. A. G., Gasol, J. M., Arin, L., and Estrada, M. (1999). A comparison between glass fiber and membrane filters for the estimation of phytoplankton POC and DOC production. *Mar. Ecol. Prog. Ser.* 187, 31–41.
- Ottesen, E. A., Young, C. R., Eppley, J. M., Ryan, J. P., Chavez, F. P., Scholin, C. A., et al. (2013). Pattern and synchrony of gene expression among sympatric marine microbial populations. *Proc. Natl. Acad. Sci. U.S.A.* 110, E488–E497. doi:10.1073/pnas.1222099110.
- Ottesen, E. A., Young, C. R., Gifford, S. M., Eppley, J. M., Marin, R., Schuster, S. C., et al. (2014). Multispecies diel transcriptional oscillations in open ocean heterotrophic bacterial assemblages. *Science* 345, 207–212. doi:10.1126/science.1252476.
- Pei, S., and Laws, E. A. (2013). Does the  $^{14}\text{C}$  method estimate net photosynthesis? Implications from batch and continuous culture studies of marine phytoplankton. *Deep Sea Res I* 82, 1–9. doi:10.1016/j.dsr.2013.07.011.

- Peterson, B. J. (1980). Aquatic primary productivity and the  $^{14}\text{C}$ - $\text{CO}_2$  method: A history of the productivity problem. *Annu. Rev. Ecol. Syst.* 11, 359–385. doi:10.1146/annurev.es.11.110180.002043.
- Platt, T., Gallegos, C., and Harrison, W. (1980). Photoinhibition of photosynthesis in natural assemblages of marine phytoplankton. *J. Mar. Res.* 38, 687–701.
- Poretsky, R. S., Hewson, I., Sun, S., Allen, A. E., Zehr, J. P., and Moran, M. A. (2009). Comparative day/night metatranscriptomic analysis of microbial communities in the North Pacific subtropical gyre. *Environ. Microbiol.* 11, 1358–1375. doi:10.1111/j.1462-2920.2008.01863.x.
- Quay, P. D., Peacock, C., Björkman, K., and Karl, D. M. (2010). Measuring primary production rates in the ocean: Enigmatic results between incubation and non-incubation methods at Station ALOHA. *Global Biogeochem. Cycles* 24, 1–14. doi:10.1029/2009GB003665.
- R Development Core Team (2008). *R: A Language and Environment for Statistical Computing*. Vienna, Austria: R Foundation for Statistical Computing Available at: <http://www.R-project.org>.
- Ruf, T. (1999). The Lomb-Scargle periodogram in biological rhythm research: Analysis of incomplete and unequally spaced time-series. *Biol. Rhythm Res.* 30, 178–201. doi:10.1076/brhm.30.2.178.1422.
- Saba, G. K., Steinberg, D. K., and Bronk, D. A. (2011). The relative importance of sloppy feeding, excretion, and fecal pellet leaching in the release of dissolved carbon and nitrogen by *Acartia tonsa* copepods. *J. Exper. Mar. Biol. Ecol* 404, 47–56. doi:10.1016/j.jembe.2011.04.013.
- Scargle, J. D. (1982). Studies in astronomical time series analysis. II - Statistical aspects of spectral analysis of unevenly spaced data. *Astrophys. J.* 263, 835–853. doi:10.1086/160554.
- Schindler, D. W., Schmidt, R. V., and Reid, R. A. (1972). Acidification and bubbling as an alternative to filtration in determining phytoplankton production by the  $^{14}\text{C}$  method. *J. Fish. Res. Board. Can.* 29, 1627–1631. doi:10.1139/f72-250.
- Skoog, D. A., and Leary, J. J. (1992). *Principles of Instrumental Analysis*. Fort Worth, Texas: Saunders College Pub.
- Steemann Nielsen, E. (1952). The use of radio-active carbon ( $\text{C}^{14}$ ) for measuring organic production in the sea. *J. Conseil Int. Explor. Mer* 18, 117–140. doi:10.1093/icesjms/18.2.117.
- Strickland, J. D. H., and Parsons, T. R. (1972). *A Practical Handbook of Seawater Analysis*. Ottawa, Ontario: Fisheries Research Board of Canada.
- Suttle, C. A. (2005). Viruses in the sea. *Nature* 437, 356–361. doi:10.1038/nature04160.

- Teira, E., Pazo, M. J., Quevedo, M., Fuentes, M. V., Niell, F. X., and Fernandez, E. (2003). Rates of dissolved organic carbon production and bacterial activity in the eastern North Atlantic Subtropical Gyre during summer. *Mar. Ecol. Prog. Ser.* 249, 53–67.
- Teira, E., Pazo, M. J., Serret, P., and Fernandez, E. (2001). Dissolved organic carbon production by microbial populations in the Atlantic Ocean. *Limnol. Oceanogr.* 46, 1370–1377.
- Tsai, A.-Y., Chiang, K.-P., Chang, J., and Gong, G.-C. (2005). Seasonal diel variations of picoplankton and nanoplankton in a subtropical western Pacific coastal ecosystem. *Limnol. Oceanogr.* 50, 1221–1231. doi:10.4319/lo.2005.50.4.1221.
- Vaulot, D., Marie, D., Olson, R., and Chisholm, S. (1995). Growth of *Prochlorococcus*, a photosynthetic prokaryote, in the Equatorial Pacific Ocean. *Science* 268, 1480–1482.
- Wilhelm, S., and Suttle, C. (1999). Viruses and nutrient cycles in the sea - Viruses play critical roles in the structure and function of aquatic food webs. *Bioscience* 49, 781–788. doi:10.2307/1313569.
- Wilson, S. T., Barone, B., Ascani, F., Bidigare, R. R., Church, M. J., del Valle, D. A., et al. (2015). Short-term variability in euphotic zone biogeochemistry and primary productivity at Station ALOHA: A case study of summer 2012. *Global Biogeochem. Cycles*, 29. 2015GB005141. doi:10.1002/2015GB005141.
- Winn, C., Campbell, L., Christian, J., Letelier, R., Hebel, D., Dore, J., et al. (1995). Seasonal variability in the phytoplankton community of the North Pacific Subtropical gyre. *Global Biogeochem. Cycles* 9, 605–620.
- Zar, J. H. (1999). *Biostatistical Analysis*. New Jersey: Prentice Hall PTR.

**Table 2.1.** Seasonally averaged ( $\pm$  standard deviations) rates of productivity and irradiance for the two time periods of this study. Mean irradiance (PAR) at the sea surface and at the 75 meter depth horizon and vertically-binned (0-45 and 75-125 m) rates of  $^{14}\text{C}$ -GFF and  $^{14}\text{C}$ -PC from October 2004-October 2007, and from April 2010-October 2012. Also shown are vertically-binned  $^{14}\text{C}$ -DOC and %PER ( $^{14}\text{C}$ -DOC / ( $^{14}\text{C}$ -DOC +  $^{14}\text{C}$ -PC)) from April 2010-October 2012. Number of measurements (n) used to compute seasonal means shown in parentheses. Mean values denoted with the same letter are statistically indistinguishable. P-values are denoted with \* ( $p < 0.05$ ), \*\* ( $p < 0.005$ ), ● ( $p < 0.001$ ), and ●● ( $p < 0.0001$ ).

Season	October 2004-October 2007			April 2010-October 2012				
	PAR (mol quanta $\text{m}^{-2} \text{d}^{-1}$ )	$^{14}\text{C}$ -GFF ( $\mu\text{mol C L}^{-1}$ $\text{d}^{-1}$ )	$^{14}\text{C}$ -PC ( $\mu\text{mol C L}^{-1}$ $\text{d}^{-1}$ )	PAR (mol quanta $\text{m}^{-2} \text{d}^{-1}$ )	$^{14}\text{C}$ -GFF ( $\mu\text{mol C L}^{-1}$ $\text{d}^{-1}$ )	$^{14}\text{C}$ -PC ( $\mu\text{mol C L}^{-1}$ $\text{d}^{-1}$ )	$^{14}\text{C}$ -DOC ( $\mu\text{mol C L}^{-1}$ $\text{d}^{-1}$ )	%PER
Winter 0-45 m	21.0 $\pm$ 7.5 (n=7) B●●	0.45 $\pm$ 0.09 (n=18) B●	0.28 $\pm$ 0.05 (n=18) B●●	29.9 $\pm$ 3.6 (n=4) B*	0.58 $\pm$ 0.12 (n=15) A	0.37 $\pm$ 0.11 (n=15) A	0.11 $\pm$ 0.11 (n=11) A	23.78 $\pm$ 14.28 (n=11) A
Spring 0-45 m	47.8 $\pm$ 4.0 (n=7) A●●	0.52 $\pm$ 0.07 (n=21) AB	0.29 $\pm$ 0.06 (n=21) B●●	39.4 $\pm$ 10.1 (n=6) AB	0.51 $\pm$ 0.10 (n=18) A	0.30 $\pm$ 0.07 (n=18) A	0.06 $\pm$ 0.06 (n=21) A	11.94 $\pm$ 12.79 (n=19) A
Summer 0-45m	46.3 $\pm$ 6.9 (n=8) A●●	0.56 $\pm$ 0.14 (n=24) A●	0.38 $\pm$ 0.10 (n=24) A●●	43.4 $\pm$ 2.8 (n=8) A*	0.42 $\pm$ 0.08 (n=27) A	0.28 $\pm$ 0.04 (n=27) A	0.07 $\pm$ 0.04 (n=25) A	17.66 $\pm$ 10.3 (n=25) A
Fall 0-45 m	30.8 $\pm$ 5.7 (n=9) B●●	0.46 $\pm$ 0.10 (n=27) B●	0.27 $\pm$ 0.05 (n=27) B●●	29.3 $\pm$ 9.9 (n=5) B*	0.49 $\pm$ 0.09 (n=18) A	0.28 $\pm$ 0.06 (n=21) A	0.05 $\pm$ 0.04 (n=15) A	11.57 $\pm$ 9.77 (n=15) A
Winter 75-125 m	0.69 $\pm$ 0.25 (n=7) C●	0.13 $\pm$ 0.12 (n=18) B**	0.08 $\pm$ 0.08 (n=18) B*	1.04 $\pm$ 0.30 (n=3) A	0.22 $\pm$ 0.13 (n=15) A	0.13 $\pm$ 0.09 (n=15) A	0.03 $\pm$ 0.04 (n=12) A	18.98 $\pm$ 20.32 (n=11) A
Spring 75-125 m	1.83 $\pm$ 0.50 (n=7) A●	0.23 $\pm$ 0.12 (n=21) A**	0.14 $\pm$ 0.08 (n=21) A*	1.85 $\pm$ 0.62 (n=6) A	0.16 $\pm$ 0.13 (n=18) A	0.10 $\pm$ 0.08 (n=18) A	0.02 $\pm$ 0.05 (n=18) A	12.63 $\pm$ 20.54 (n=18) A
Summer 75-125 m	1.42 $\pm$ 0.66 (n=6) AB	0.18 $\pm$ 0.13 (n=24) AB	0.11 $\pm$ 0.08 (n=24) AB	1.95 $\pm$ 0.88 (n=8) A	0.11 $\pm$ 0.09 (n=27) A	0.08 $\pm$ 0.06 (n=27) A	0.04 $\pm$ 0.04 (n=24) A	18.43 $\pm$ 21.23 (n=23) A
Fall 75-125 m	1.11 $\pm$ 0.28 (n=9) BC	0.13 $\pm$ 0.11 (n=27) B**	0.08 $\pm$ 0.07 (n=27) B*	2.09 $\pm$ 1.44 (n=5) A	0.20 $\pm$ 0.15 (n=18) A	0.12 $\pm$ 0.10 (n=18) A	0.02 $\pm$ 0.05 (n=15) A	12.32 $\pm$ 23.65 (n=12) A

**Table 2.2.** Mean ( $\pm$  standard deviation; stdev) of  $^{14}\text{C}$ -DOC concentrations measured at the beginning (time zero;  $T_0$ ) and end of incubation period (time final;  $T_f$ ) at six euphotic zone depths evaluated in this study. The percent detectable indicates the proportion of the  $T_f$  samples that were greater than three times the standard deviation of the mean  $T_0$  (defined as the limit of detection). Incubation times for  $T_f$  measurements ranged from 11-13 hours (full photoperiod). Shown in parentheses are number of measurements (n) used to compute means.

Depth (m)	Mean $\pm$ stdev $^{14}\text{C}$ -DOC $T_0$ ( $\mu\text{mol C L}^{-1}$ )	Mean $\pm$ stdev $^{14}\text{C}$ -DOC $T_f$ ( $\mu\text{mol C L}^{-1}$ )	Mean $\pm$ stdev $T_f:T_0$	% detectable
5	0.07 $\pm$ 0.06 (n=25)	0.15 $\pm$ 0.06 (n=69)	2.87 $\pm$ 1.57	71%
25	0.08 $\pm$ 0.07 (n=24)	0.14 $\pm$ 0.06 (n=69)	2.54 $\pm$ 1.68	70%
45	0.06 $\pm$ 0.04 (n=25)	0.12 $\pm$ 0.06 (n=69)	2.30 $\pm$ 1.48	60%
75	0.09 $\pm$ 0.12 (n=23)	0.10 $\pm$ 0.07 (n=68)	1.73 $\pm$ 1.55	38%
100	0.08 $\pm$ 0.10 (n=23)	0.08 $\pm$ 0.05 (n=70)	1.26 $\pm$ 0.67	29%
125	0.09 $\pm$ 0.08 (n=23)	0.07 $\pm$ 0.06 (n=64)	1.06 $\pm$ 0.56	17%

**Table 2.3.** Descriptive characteristics of production-irradiance curve fitting results based on the Platt et al. (1980) model. Parameters derived for  $^{14}\text{C}$ -GFF and  $^{14}\text{C}$ -PC from data collected October 2004-October 2007 and April 2010-October 2012;  $^{14}\text{C}$ -DOC parameters from data collected April 2010-April 2013. Significance (p value) and coefficients of determination ( $r^2$ ) for regression analyses are shown, along with derived parameters and standard error (S.E.). Units for  $P_{\max}$ ,  $\alpha$ ,  $\beta$ , and  $E_k$  are  $\mu\text{mol C L}^{-1} \text{d}^{-1}$ ,  $\mu\text{mol C L}^{-1} \text{d}^{-1} (\text{mol quanta m}^{-2} \text{d}^{-1})^{-1}$ ,  $\mu\text{mol C L}^{-1} \text{d}^{-1} (\text{mol quanta m}^{-2} \text{d}^{-1})^{-1}$ , and  $\text{mol quanta m}^{-2} \text{d}^{-1}$ , respectively.

Rate	Curve fitting significance	$P_{\max}$	$P_{\max}$ S.E.	$\alpha$	$\alpha$ S.E.	$\beta$	$E_k$	$E_k$ S.E.
$^{14}\text{C}$ -GFF	$p < 0.0001$ , $r^2 = 0.82$	0.53 <sup>A</sup>	0.02	0.35 <sup>A,C</sup>	0.02	0.00 <sup>B</sup>	1.5	0.10
$^{14}\text{C}$ -PC	$p < 0.0001$ , $r^2 = 0.74$	0.31 <sup>A</sup>	0.01	0.21 <sup>A</sup>	0.02	0.00 <sup>B</sup>	1.5	0.12
$^{14}\text{C}$ -DOC	$p > 0.05$ , $r^2 = 0.12$	0.09 <sup>A</sup>	0.01	0.15 <sup>B</sup>	0.08	0.00 <sup>B</sup>	6.2	3.3

<sup>A</sup>  $p < 0.0001$

<sup>B</sup>  $p > 0.05$

<sup>C</sup>  $\alpha$  derived for  $^{14}\text{C}$ -GFF rates was above the 95% confidence interval of  $\alpha$  calculated for  $^{14}\text{C}$ -PC.

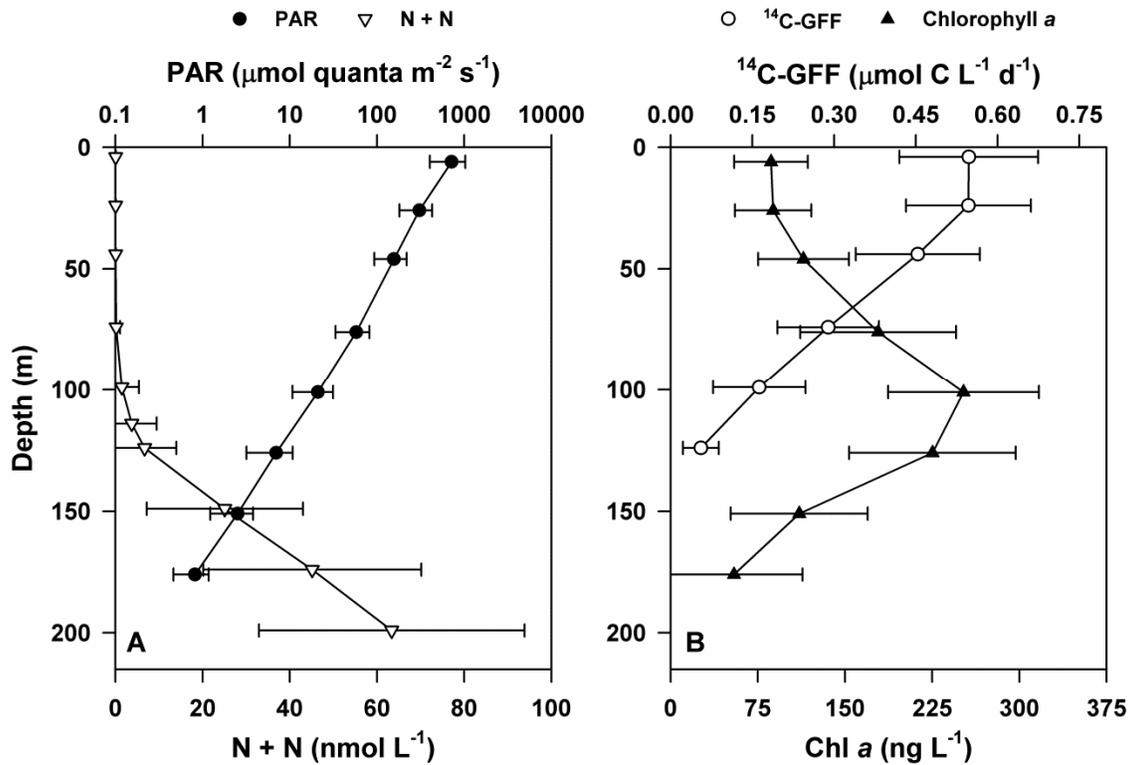


**Figure 2.1.** Depth profiles of mean upper ocean properties at Station ALOHA during the period of study (2004-2013). (A) Concentrations of nitrate + nitrite (N+N; open triangles) and flux of photosynthetically active radiation (PAR; closed circles). (B) Concentrations of chlorophyll *a* (Chl *a*; closed triangles) and rates of <sup>14</sup>C-GFF based primary production (open circles). Error bars are ± 1 standard deviation of the time-averaged means.

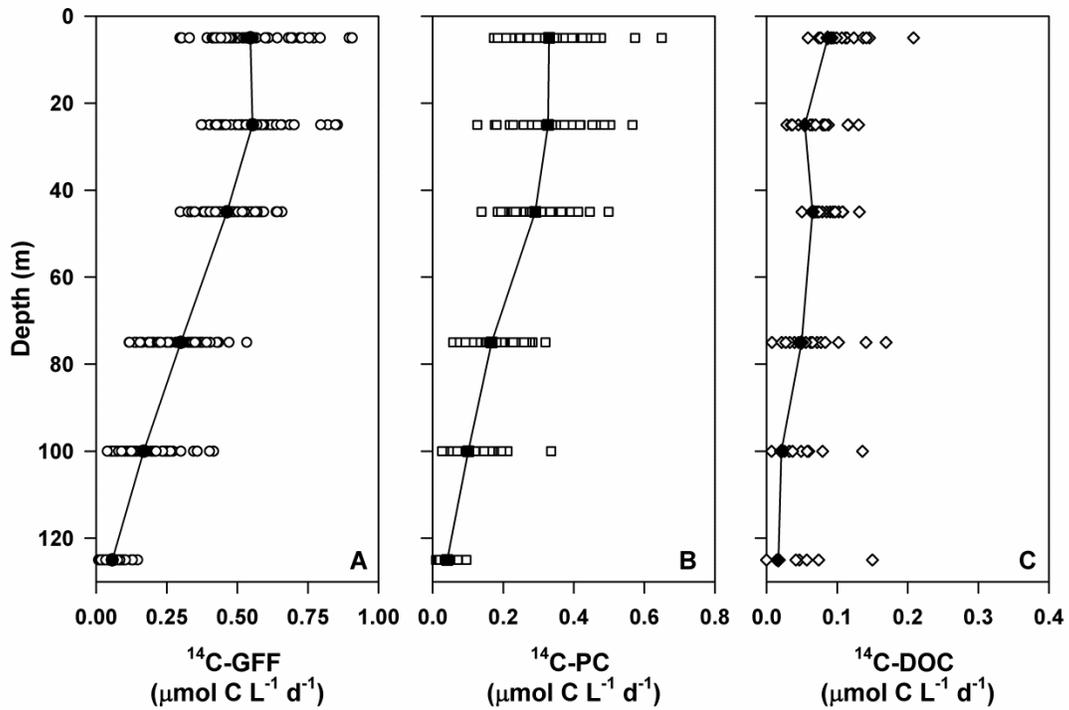


**Figure 2.2.** Vertical profiles of rates of  $^{14}\text{C}$ -based primary production filtered onto (A) glass fiber filters ( $^{14}\text{C}$ -GFF) and (B)  $0.2 \mu\text{m}$  polycarbonate membrane filters ( $^{14}\text{C}$ -PC). Also shown are (C) rates of  $^{14}\text{C}$ -DOC production.

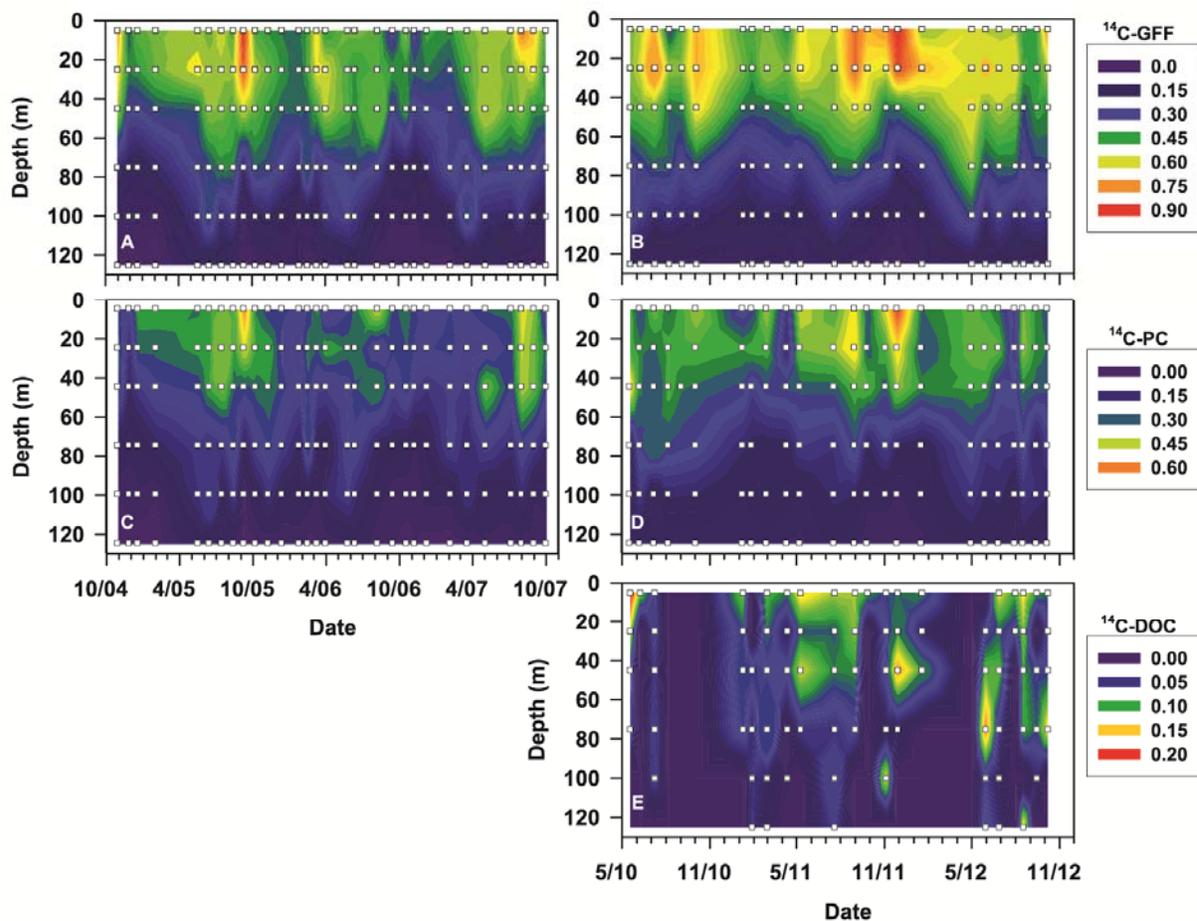


**Figure 2.3.** Contour plots depicting vertical distributions of rates of  $^{14}\text{C}$ - GFF (A,B),  $^{14}\text{C}$ -PC (C,D), and  $^{14}\text{C}$ -DOC (E), in  $\mu\text{mol C L}^{-1} \text{d}^{-1}$ , over the time periods (October 2004-October 2007 and April 2010-October 2012) evaluated for this study. White squares depict depths and dates where detectable rates were measured.

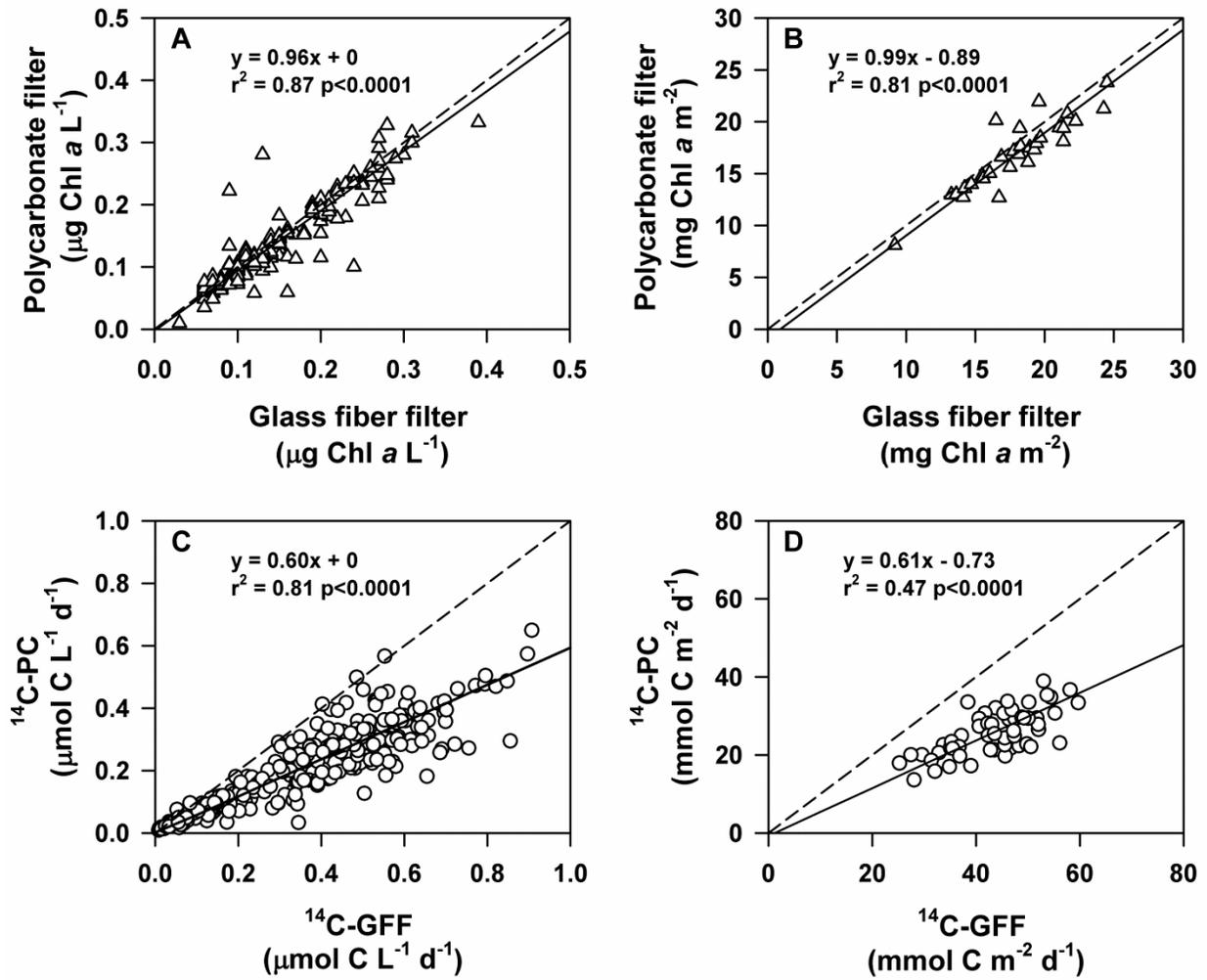


**Figure 2.4.** Comparison of measurements of chlorophyll *a* and  $^{14}\text{C}$ -primary production on either glass fiber or polycarbonate filters. Solid lines are Model II (geometric mean) linear regressions, while dashed lines depict the 1:1 ratio. Shown on each plot are given the regression equation, the  $r^2$  of the relationship, and the  $p$ -value for (A) volumetric measurements of chlorophyll *a*, (B) depth-integrated (0-125 m) chlorophyll *a*, (C) volumetric measurements of  $^{14}\text{C}$ -primary production, and (D) depth-integrated (0-125 m) measurements of  $^{14}\text{C}$ -primary production.

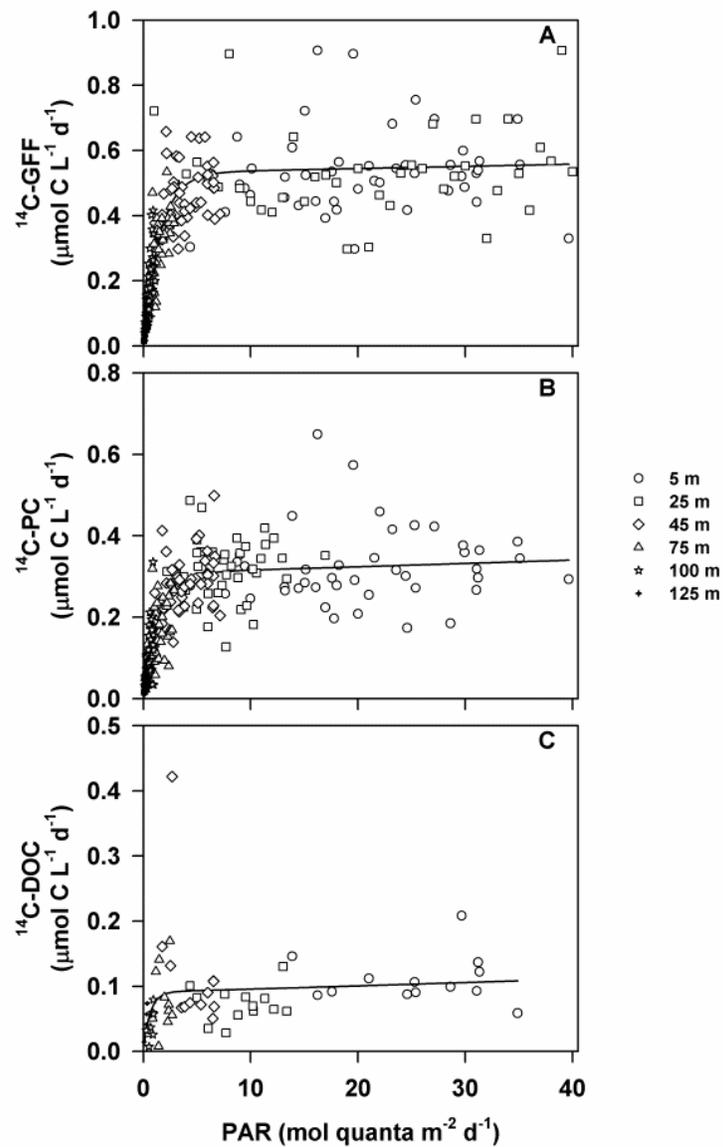


**Figure 2.5.** Relationships between downwelling photosynthetically active radiation (PAR) and rates of (A)  $^{14}\text{C}$ -GFF; (B)  $^{14}\text{C}$ -PC; and (C)  $^{14}\text{C}$ -DOC. Circles represent data points collected from 5 meters, squares from 25 meters, diamonds from 45 meters, triangles from 75 meters, stars 100 meters and crosses from 125 meters. Lines depict least-squares regression fits to the measured production rates and PAR using the Platt et al. (1980) formulation. Parameters describing the regression fits are provided in Table 2.2.

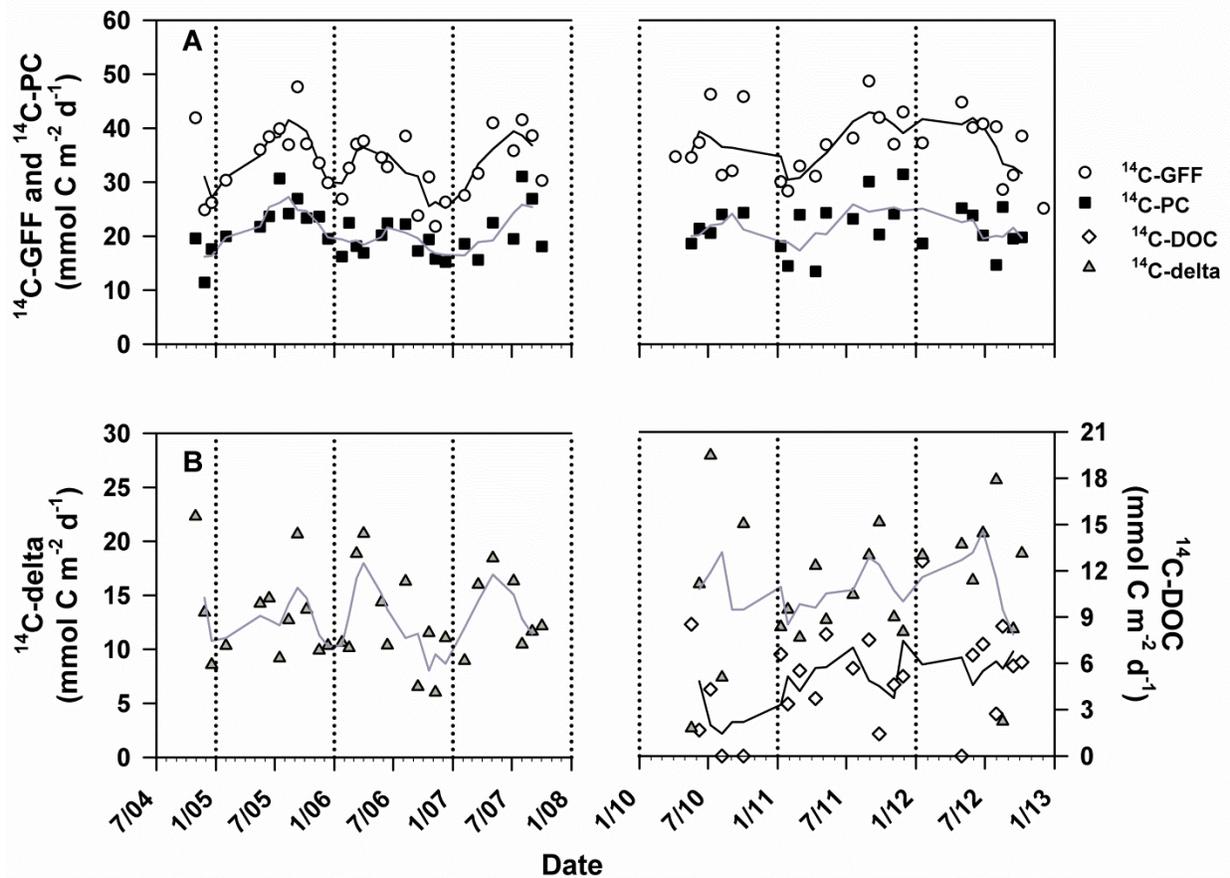


**Figure 2.6.** Time-series measurements of depth integrated (0-75 m) rates of (A)  $^{14}\text{C}$ -GFF (open circles) and  $^{14}\text{C}$ -PC production (closed squares). Also depicted are depth-integrated (0-75 m) rates of (B)  $^{14}\text{C}$ -delta production ( $^{14}\text{C}$ -GFF -  $^{14}\text{C}$ -PC; grey triangles) and  $^{14}\text{C}$ -DOC production (open diamonds). Lines are 3-point running means. Break in time-series indicate period where measurements were not conducted. Rates of  $^{14}\text{C}$ -DOC below detection were considered to be equal to zero.

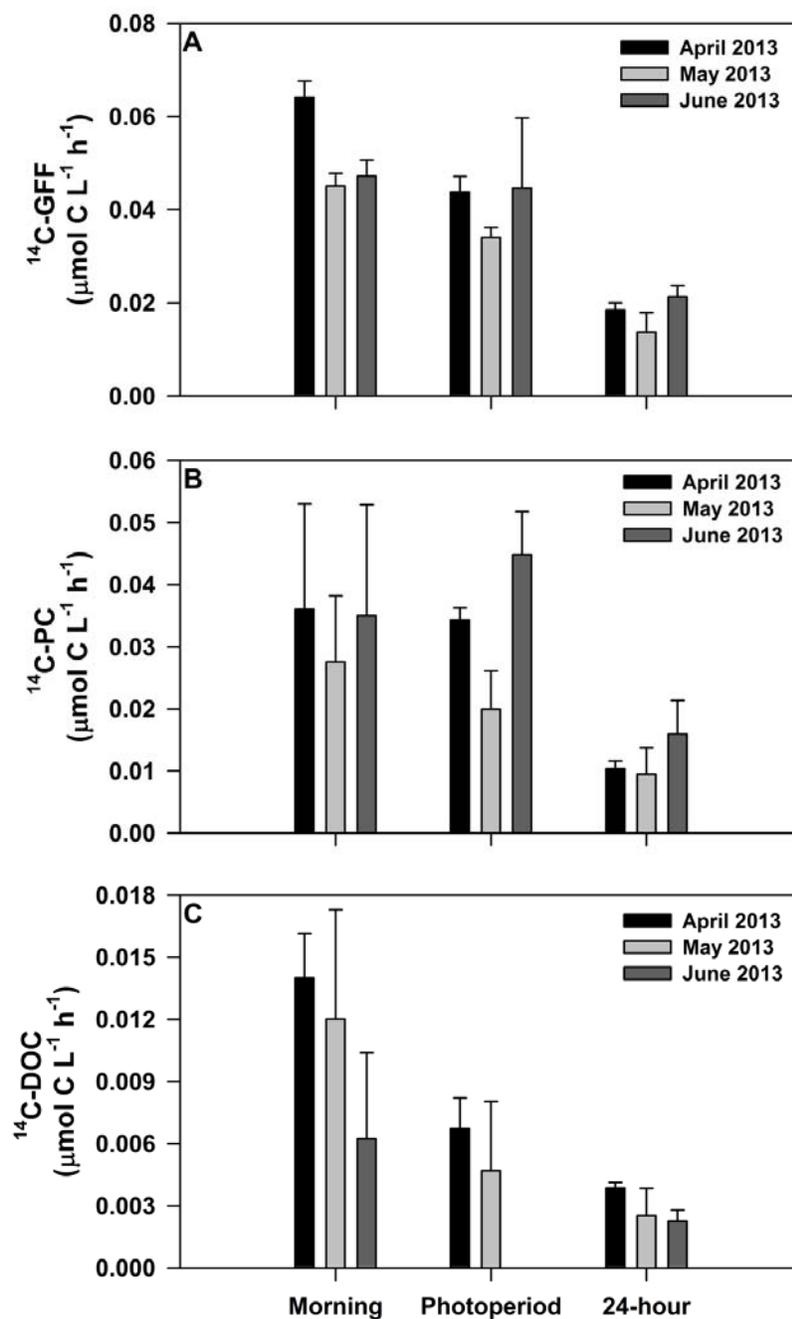


**Figure 2.7.** Results from experiments conducted in April, May, and June 2013 examining daytime and nighttime changes in hourly rates of carbon fixation. Depicted are average hourly rates of (A)  $^{14}\text{C-GFF}$ ; (B)  $^{14}\text{C-PC}$ ; and (C)  $^{14}\text{C-DOC}$ . All rates represent incubations initiated before dawn and terminated at different periods of the day (“morning” samples terminated at noon, “photoperiod” samples terminated at sunset, and “24-hour” samples terminated before dawn the following day).

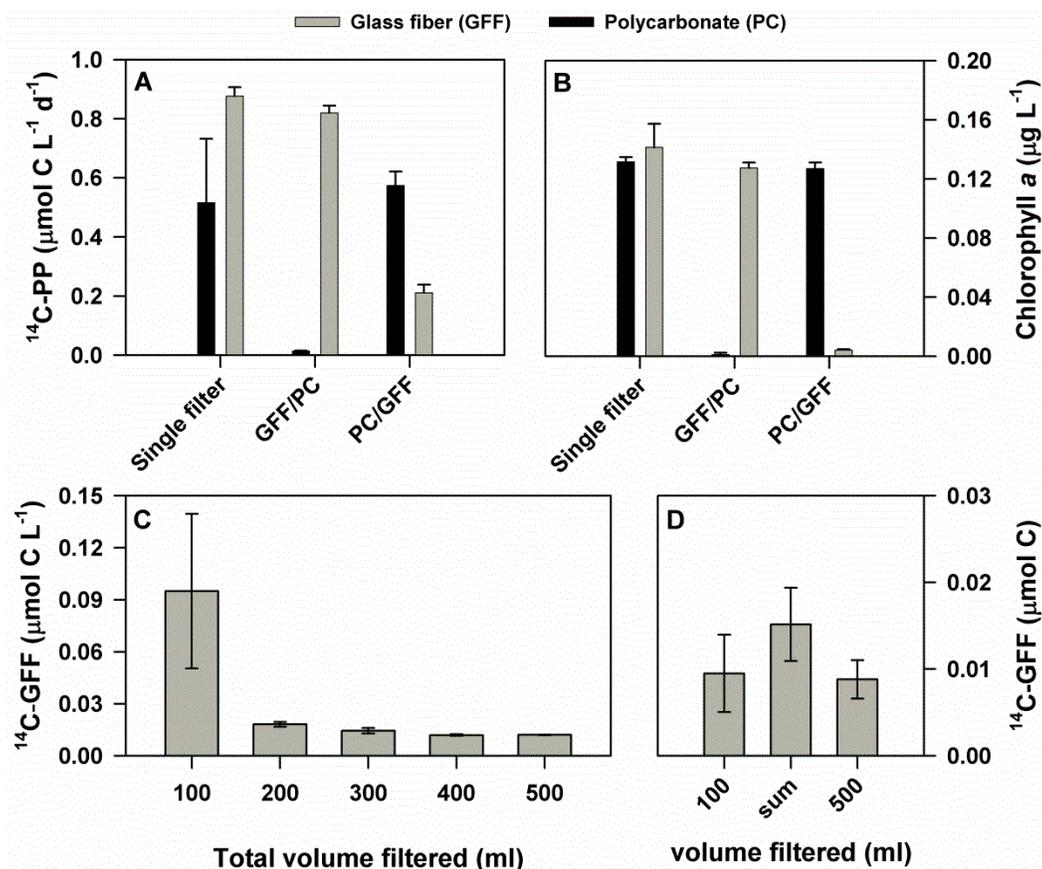


**Figure 2.S1.** Results from experiments comparing retention of  $^{14}\text{C}$  organic matter onto either glass fiber or polycarbonate membrane filters. (A)  $^{14}\text{C}$ -labeled primary production samples filtered either onto glass fiber filters alone, polycarbonate filters alone, glass fiber filters placed on top of polycarbonate filters (GFF/PC), or polycarbonate filters placed on top of glass fiber filters (PC/GFF); (B) chlorophyll *a* samples filtered across the same configuration of filters. (C) Sequential 100 ml re-filtrations of  $^{14}\text{C}$ -PC filtrate onto successive new glass fiber filters (in triplicate). (D) Comparison of average (from triplicates)  $^{14}\text{C}$ -DOC adsorbed to glass fiber filters from initial 100 ml filtration, sum of all five 100 ml re-filtrations (for a total volume of 500 ml, 100 ml per filter) onto five separate filters, and filtration of 500 ml onto single glass fiber filters.

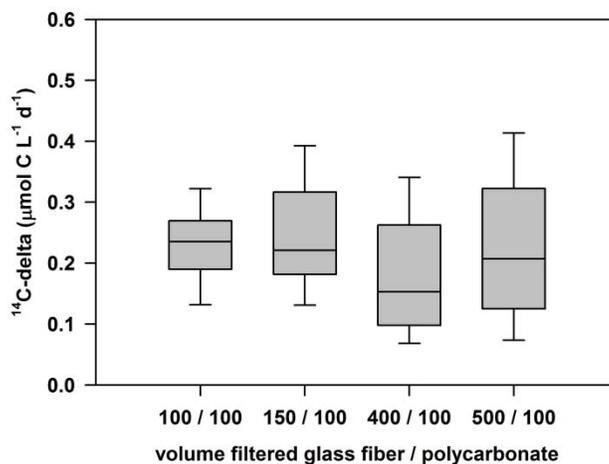


**Figure 2.S2.** Differences between  $^{14}\text{C}$ -activity on glass fiber and polycarbonate filters ( $^{14}\text{C}$ -delta =  $^{14}\text{C}$ -GFF -  $^{14}\text{C}$ -PC) where different volumes of seawater were filtered.  $^{14}\text{C}$ -delta derived from paired samples where 100 ml of seawater was filtered onto polycarbonate filters, while varying volumes (100, 150, 400, and 500 ml) of seawater were filtered onto glass fiber filters. Midline of box plots indicates median value, while the upper and lower borders of the box represent the 75<sup>th</sup> and 25<sup>th</sup> percentiles, respectively.

## CHAPTER 3 - Temporal variability in bacterial production in the North Pacific Subtropical Gyre

Donn A. Viviani, Matthew J. Church, additional coauthors likely

### Abstract

Bacterial growth and metabolism constitute major pathways for the flow of reduced carbon through marine ecosystems. In this study, we measured rates of  $^3\text{H}$ -leucine incorporation, a proxy for bacterial biomass production, at Station ALOHA ( $22^{\circ}45'\text{N}$ ,  $158^{\circ}\text{W}$ ) in the oligotrophic North Pacific Subtropical Gyre. We report vertically resolved measurements of upper ocean (0–125 m) rates of  $^3\text{H}$ -leucine incorporation conducted at daily to monthly time scales between 2011 and 2013. Rates of  $^3\text{H}$ -leucine incorporation were 6 to 20-fold greater in the upper euphotic zone (0–45 m) compared to the lower euphotic zone (75–125 m). In addition, throughout the euphotic zone (0–125 m), rates of  $^3\text{H}$ -leucine incorporation were stimulated (by 1.5 fold, on average) by sunlight relative to coincident measurements conducted in the dark. Together, the resulting daily rates of depth-integrated (0–125 m) bacterial production were equivalent to 2–9% of contemporaneous  $^{14}\text{C}$ -PP measurements. However, rates of  $^3\text{H}$ -leucine incorporation did not appear significantly related to contemporaneous rates of  $^{14}\text{C}$ -PP, with rates of  $^{14}\text{C}$ -PP typically elevated during the summer (May through August) when the flux of incident irradiance was greatest, while rates of  $^3\text{H}$ -leucine incorporation tended to peak in the fall (August through October) when seawater temperatures were warmest. Daily scale measurements of  $^3\text{H}$ -Leu and  $^{14}\text{C}$ -PP over a 62 day period in the summer of 2012 revealed that  $^3\text{H}\text{-Leu}_{\text{Light}}$  and  $^3\text{H}\text{-Leu}_{\text{Dark}}$

varied by 2.5-fold and 2-fold, respectively, while day to day variability in  $^{14}\text{C}$ -PP averaged 1.8-fold. Moreover, higher frequency sampling during the summer of 2012 revealed that rates of  $^3\text{H}$ -Leu<sub>Light</sub> and  $^3\text{H}$ -Leu<sub>Dark</sub> demonstrated different diel-scale patterns, with rates of  $^3\text{H}$ -Leu<sub>Light</sub> elevated at mid-day, while rates of  $^3\text{H}$ -Leu<sub>Dark</sub> increased 1.5-fold in the early evening. Together, these results suggest temporal uncoupling in photosynthetic production of organic matter and bacterial production over daily and monthly time scales, with rates of  $^{14}\text{C}$ -PP seasonally co-varying with changes in light, and bacterial growth lagging this response and increasing with seasonal warming of the upper ocean.

## Introduction

The ocean supports nearly half of global net primary productivity (PP), with much of that production occurring in the oligotrophic gyres of the open ocean (Behrenfeld & Falkowski 1997, Field et al. 1998). A significant fraction of this photosynthetically-fixed carbon supports the growth and metabolic activities of bacterioplankton (Ducklow & Carlson 1992, Duarte & Cebrian 1996, del Giorgio et al. 1997). Bacterial production (BP) of cell biomass is a central component of aquatic food webs (Pomeroy 1974, Azam et al. 1983), and BP rates are estimated to be equivalent to 10–15% of net primary productivity in open ocean ecosystems (Ducklow & Carlson 1992, Ducklow 1999), with bacterial metabolism (inclusive of biomass production and respiration) estimated to be equivalent to >70% of contemporaneous rates of primary production (Kirchman 2004, Church et al. 2008). Hence, estimates of the magnitude and variability of bacterial growth in the sea are critical to understanding ocean carbon cycling.

The spatiotemporal coupling between BP and PP provides insight into the relative dependence of bacterial growth on contemporaneous phytoplankton production and the strength of this coupling can be regulated by numerous processes, including availability of inorganic and organic nutrients and temperature (Billen et al. 1990, Shiah & Ducklow 1994, Carlson et al. 1996, Cotner & Biddanda 2002, Alonso-Sáez et al. 2008). To date, there are limited studies examining temporal variability in bacterial growth and metabolism in open ocean ecosystems. At the Bermuda Atlantic Time-series Study (BATS) in the Sargasso Sea, rates of BP demonstrate weak to moderate seasonality, generally increasing 2-3-fold during mid-summer and declining into fall and winter (Carlson et al. 1996, Steinberg et al. 2001). In contrast, rates of  $^{14}\text{C}$ -primary production ( $^{14}\text{C}$ -PP) demonstrate relatively strong seasonality, varying up to 5-fold over the year, peaking in early spring (Michaels et al. 1994, Steinberg et al. 2001). The seasonal-scale

decoupling of PP and BP in this ecosystem coincides with seasonal-scale changes in the coupling between production and removal of dissolved organic carbon (DOC), with concentrations of DOC increasing throughout the spring and summer (Carlson et al. 1994, Hansell & Carlson 1998). The difference in seasonal patterns between BP, PP, and net production of DOC appears driven by a combination of biological and physical processes, highlighting the importance of evaluating BP in the context of open ocean oceanographic and ecological dynamics.

Since 1988, the Hawaii Ocean Time-series (HOT) program has conducted near-monthly measurements of ocean biogeochemistry and physical hydrography at the open ocean field site Station ALOHA (22° 45'N, 158° 00'W) in the North Pacific Subtropical Gyre (NPSG). This ecosystem is characterized by a deep euphotic zone (defined here as the compensation depth, which at Station ALOHA has a median depth of ~150 m; Laws et al. 2014), persistently low concentrations of inorganic nutrients, and planktonic biomass dominated by picoplankton (< 2 µm). A major fraction of primary productivity in this ecosystem appears sustained by intensive recycling of nutrients through the metabolic activities of planktonic microorganisms (Karl 1999). HOT program measurements of <sup>14</sup>C-PP reveal significant seasonality, with rates increasing 2-3-fold in summer, coincident with increased insolation (Letelier et al. 2004, Karl et al. 2012, Church et al. 2013). Despite these seasonal-scale increases in <sup>14</sup>C-PP, rates of photosynthetic production of DOC (as measured by production of extracellular <sup>14</sup>C-DOC) do not demonstrate significant seasonality or correlate to rates of PP (Viviani et al. 2015). To date however, less is known about temporal variability in BP, or possible relationships between rates of BP and PP in this ecosystem. Previous work at ALOHA has demonstrated that sunlight stimulates rates of <sup>3</sup>H-leucine incorporation, a proxy for BP, an effect that appears largely driven by assimilation of <sup>3</sup>H-

leucine by the unicellular cyanobacterium *Prochlorococcus* (Church et al. 2004, 2006, Björkman et al. 2015).

In this study, we examine coupling between BP and PP on time scales ranging from hourly to near-monthly at Station ALOHA. Doing so allowed us to examine the strength of coupling between BP and PP over a range of time scales. Moreover, examining our results in the framework of the rich biogeochemical and physical context provided by the HOT program allowed us to better understand factors controlling BP in the NPSG.

## Methods

### **<sup>14</sup>C- primary production and <sup>3</sup>H-leucine incorporation measurements**

Samples were collected from 24 different cruises between January 2011 and April 2013 sampling at or in the vicinity of Station ALOHA. On each cruise, rates of <sup>3</sup>H-leucine (<sup>3</sup>H-Leu) incorporation into protein were measured as a proxy for BP (Kirchman et al. 1985, Simon & Azam 1989). In addition, rates of PP were measured on each cruise as the assimilation of <sup>14</sup>C-bicarbonate into plankton biomass (Steemann Nielsen 1952). Seawater samples for both of these measurements were collected from pre-dawn vertical hydrocasts at 6 discrete depths (5, 25, 45, 75, 100, 125 m) using polyvinyl chloride sampling bottles affixed to a rosette sampler equipped with a Sea-Bird 911+ conductivity, temperature, and depth (CTD) sensors (Karl & Lukas 1996). Measurements of <sup>14</sup>C-PP were conducted following HOT program protocols (Letelier et al. 1996). Briefly, seawater was subsampled under subdued light from the rosette sampling bottles into triplicate acid-cleaned 500 ml polycarbonate bottles. Samples were inoculated with <sup>14</sup>C-bicarbonate to a final activity of ~1.85 MBq, affixed to a free-drifting array, and incubated *in situ*

for the daily photoperiod. During the summer of 2012, rates of  $^{14}\text{C}$ -PP were measured daily as part of the Center for Microbial Oceanography: Research and Education (C-MORE) HOE-DYLAN cruises. For these daily scale measurements, seawater was collected at 25 m from a predawn CTD rosette cast; triplicate 500 ml polycarbonate bottles were filled from the CTD rosette bottles, inoculated with  $\sim 1.85$  MBq  $^{14}\text{C}$ -bicarbonate (MP Biomedicals), and placed for the duration of the photoperiod in a seawater-cooled, deckboard incubator, shaded with blue Plexiglass to  $\sim 30\%$  of surface irradiance, appropriate for simulating the mean light field at the 25 m depth horizon.

At the end of the photoperiod (photoperiods lasted between 11 and 13 hours), bottles were retrieved from the incubator or from the *in situ* array, and 250  $\mu\text{l}$  was subsampled from each sample bottle into a 20 ml glass scintillation vial containing 500  $\mu\text{l}$  of  $\beta$ -phenethylamine for subsequent determination of the total activity of  $^{14}\text{C}$  added to each sample. The remaining sample volume was gently vacuum filtered onto 25 mm diameter glass fiber filters (Whatman GF/F). Filters were collected and stored in glass 20 ml scintillation vials and frozen until analysis. At the shore-based laboratory, samples were thawed and 1 ml of 2 M hydrochloric acid was added to each vial containing a filter; filters were allowed to passively vent in a fume hood overnight. After venting, 10 ml of Ultima Gold liquid scintillation cocktail was added to each filter and to the total activity vials, and vials were placed in a liquid scintillation counter for determination of the resulting  $^{14}\text{C}$  activities. Samples were stored in the dark and recounted after a month (Karl et al. 1998); the values from the second counts were used to calculate rates of  $^{14}\text{C}$ -PP.

Seawater for measurements of  $^3\text{H}$ -Leu incorporation was collected from the same CTD hydrocasts and depths as coincident  $^{14}\text{C}$ -PP measurements. Polyethylene amber bottles (125 ml

capacity) were subsampled from the CTD rosette bottles, transferred to a shipboard radiation laboratory van, and used to fill duplicate acid-cleaned 12 ml polycarbonate centrifuge tubes (Nalgene Oak Ridge) from each depth. Each polycarbonate tube was inoculated with 20 nmol L<sup>-1</sup> (final concentration) 3,4,5-<sup>3</sup>H-leucine (Perkin Elmer; stock specific activities ranged from 108 to 144 Ci/mmol). An additional 1.5 ml was subsampled into 2 ml microcentrifuge tubes (Axygen; Pace et al. 2004) containing 100 µl of 100% (w/v) ice-cold trichloroacetic acid (TCA) to serve as a killed blank. The polycarbonate sample tubes were capped and incubated *in situ* over the photoperiod in both dark (through use of black cloth bags; hereafter <sup>3</sup>H-Leu<sub>Dark</sub>) and light (hereafter <sup>3</sup>H-Leu<sub>Light</sub>) on the same free-drifting array utilized for the <sup>14</sup>C-PP measurements. At the end of the photoperiod, triplicate 1.5 ml subsamples were removed from each tube and added to 2 ml microcentrifuge tubes (Axygen) containing 100 µl of 100% ice-cold TCA; these tubes were stored frozen until analysis. Samples were processed following a modified method of the microcentrifuge method (Smith & Azam 1992). Briefly, the microcentrifuge tubes were spun at ~23,900 g for 15 minutes at 4°C in a refrigerated microcentrifuge; supernatants were decanted, 1 ml ice-cold 5% TCA was added to each microcentrifuge tube and samples were spun for an additional 5 minutes at ~23,900 g at 4°C. Supernatants were decanted and 1 ml of 80% ethanol was added to each sample, and tubes were spun for an additional 5 minutes at ~23,900 g at 4°C. After decanting supernatants, samples were left uncapped for 12–16 hours in a fume hood to evaporate any residual ethanol from the microcentrifuge tubes. When samples had completely dried, 1 ml of Ultima Gold LLT scintillation cocktail was added to each tube, the tubes were vortexed, placed into 7 ml polyethylene scintillation vials (serving as a carrier vials), and counted on a liquid scintillation counter.

During the summer of 2012, rates of  $^3\text{H}$ -Leu were measured at near-daily time scales during a series of cruises to Station ALOHA as part of the C-MORE HOE-DYLAN sampling effort. For these measurements, seawater samples from 25 m were collected from a predawn CTD rosette cast; the seawater was transferred into 125 ml amber polyethylene bottles and triplicate 1.5 ml subsamples were added to 2 ml microcentrifuge tubes (Axygen) containing  $^3\text{H}$ -Leu (20 nmol L<sup>-1</sup> final concentration). Triplicate samples were incubated in the dark (inside a black cloth bag) and in the light for 6.5 to 10 hours in the same deckboard incubator used for  $^{14}\text{C}$ -PP measurements. Time zero (blank) samples were prepared as previously described. In addition, we performed higher frequency “diel” sampling over a 48-hour period (August 31 to September 1), in which 25 m samples were collected every four hours, and incubated in the deckboard incubator for between 2.5 and 6.7 hours. Measurements conducted during daylight hours included both dark and light incubations (as described previously), while nighttime incubations were only incubated in the dark. Measured rates of  $^3\text{H}$ -Leu incorporation from this diel sampling were fit in MATLAB (Mathworks) using a nonlinear least squares fit to a sinusoidal model (John et al. 2011) of the form:

$$^3\text{H}\text{-Leu incorporation} = e^{(A*\sin(2\pi*(t+ B)/24) + C)} \quad (1)$$

where A, B, and C are constants determined by the least squares fit, and t is local time on a 24-hour clock.

### **Time-course experiments to evaluate linearity of $^3\text{H}$ -leucine incorporation**

We conducted the measurements of  $^3\text{H}$ -Leu reported for the monthly HOT program cruises on the same free-drifting array used for measurements of  $^{14}\text{C}$ -PP, allowing incubation of samples under *in situ* temperature and light conditions. However, this procedure resulted in

relatively long incubation times (photoperiods ranging 11–13 hours), and thus had the potential to underestimate  $^3\text{H}$ -Leu incorporation rates due to increased likelihood of turnover of the  $^3\text{H}$ -labeled protein pool (Kirchman et al. 1986). To evaluate potential non-linearity in rates of  $^3\text{H}$ -Leu incorporation, we performed a series of time-course incubation experiments (April 2013, May 2013, June 2013, and April 2014). For these experiments, samples were incubated from ~3 to 15 hours to ascertain the period over which rates of  $^3\text{H}$ -Leu incorporation into TCA insoluble macromolecules remained linear. Near-surface (5 m and 25 m) seawater was subsampled into amber polyethylene bottles from the CTD rosette; 1.5 ml subsamples were aliquoted into 2 ml microcentrifuge tubes (Axygen) and inoculated with 20 nmol L<sup>-1</sup> (final concentration)  $^3\text{H}$ -Leu. Samples were incubated in a surface seawater-cooled incubator, in both the light and dark (as described previously), and triplicate 1.5 ml samples were sacrificed at regular intervals to evaluate the relationship between incubation time and  $^3\text{H}$  activity (disintegrations per minute). Least-squares regression analyses were used to fit candidate models, including both hyperbolic tangent and linear models, to the observations. The best model fit to the resulting time-course activity measurements was determined based on Akaike information criterion (AIC) scores (Burnham et al. 2010). In all cases, the best fit to the observations was given by the hyperbolic tangent model,

$$^3\text{H}\text{-Leu incorporation} = A * \tanh(B * (^3\text{H}\text{-Leu}_t) / A) \quad (2)$$

where A and B are constants determined by the least squares fit, and  $^3\text{H}\text{-Leu}_t$  is measured rate of  $^3\text{H}$ -Leu incorporation at time t. We used the resulting constants of this model to determine the slope of the linear component of the model and the maximum value, and solved for the time over which the measurements were linear. This provided an estimate of the duration of linear incorporation of  $^3\text{H}$ -leucine for these incubations (average of 10 hours). We then used the

measured rates of  $^3\text{H-Leu}_{\text{Dark}}$  and  $^3\text{H-Leu}_{\text{Light}}$  incorporation from the *in situ* incubations from each cruise, and correct for non-linearity deriving from incubation length:

$$^3\text{H-Leu} = ^3\text{H-Leu}_{\text{measured}} + [\text{time of incubation} - 10] * (^3\text{H-Leu}_{\text{measured}}/10) \quad (3)$$

where  $^3\text{H-Leu}_{\text{measured}}$  is the  $^3\text{H-Leu}$  incorporation measured in the incubation, time of incubation is the duration of each incubation, and 10 represents the length (in hours) of linear incorporation.

### **Contextual measurements of light, cell abundances, and nutrients**

The daily flux of incoming photosynthetically active radiation (PAR; 400 to 700 nm) was measured using a deckboard LI-COR LI-192 cosine collector. Vertical profiles of downwelling photosynthetically active radiation (PAR) were measured at noon using a Satlantic HyperPro radiometer; in addition, a ship-mounted radiometer (Satlantic) collected coincident measurements of incident PAR. These measurements were used to derive attenuation coefficients of PAR ( $K_{\text{PAR}}$ ) for each cruise. Derived  $K_{\text{PAR}}$  values and incident surface irradiance were used to calculate daily light fluxes at specific depth horizons. Sea surface temperature (SST) measurements were taken from the Woods Hole Oceanographic Institute (WHOI) Hawaii Ocean Time-series (WHOTS) mooring (<http://www.soest.hawaii.edu/whots/index.html>).

Non-pigmented picoplankton and *Prochlorococcus* cell abundances were enumerated by flow cytometry following standard HOT protocols (<http://hahana.soest.hawaii.edu/hot/methods/bact.html>). Briefly, samples for subsequent picoplankton abundance measurements were collected from the CTD rosette sampling bottles, subsampled into 2 ml Cryovials containing 30  $\mu\text{l}$  of 16% paraformaldehyde, flash-frozen in liquid nitrogen, and stored at  $-80^\circ\text{C}$  until shore-based analysis. On land, samples were thawed and counted on a Cytopeia Influx Mariner flow cytometer, utilizing a 488 nm solid-state laser,

and triggering on forward scatter. Cell counts and fluorescence were analyzed using FlowJo software (Tree Star, www.flowjo.com). Picoplankton populations were enumerated by double discrimination of flow cytometry-derived forward light scatter and relative fluorescence. Non-pigmented picoplankton were determined as the difference between total SYBR Green I (Molecular Probes) stained cells minus the abundances of *Prochlorococcus* derived from unstained samples. We used these abundances to calculate cell-specific rates of leucine incorporation. Recent work in the NPSG (Björkman et al., 2015) has found that *Prochlorococcus* is responsible for ~20% of  $^3\text{H}$ -Leu incorporation in the dark, similar to the *Prochlorococcus* contribution to total picoplanktonic bacterial abundances. Hence, we calculated cell-specific rates of  $^3\text{H}$ -Leu incorporation in the dark by dividing  $^3\text{H}$ -Leu<sub>Dark</sub> by the combined abundances of *Prochlorococcus* and non-pigmented picoplankton. Björkman et al. (2015) estimated *Prochlorococcus* accounted for ~60% of  $^3\text{H}$ -Leu<sub>Light</sub>, dominating  $^3\text{H}$ -Leu incorporation in the light on a per-cell basis. Thus, we computed cell-specific rates of incorporation for the light stimulated rates of  $^3\text{H}$ -Leu as the difference between  $^3\text{H}$ -Leu<sub>Light</sub> and  $^3\text{H}$ -Leu<sub>Dark</sub> ( $\Delta\text{Leu} = ^3\text{H}$ -Leu<sub>Light</sub> -  $^3\text{H}$ -Leu<sub>Dark</sub>) divided by the abundances of *Prochlorococcus* cells. Inorganic nutrient concentrations (nitrate + nitrite, N+N and soluble reactive phosphorus, SRP) were collected and analyzed using standard HOT program protocols (Karl et al. 2001).

### **Statistics and data analysis**

Seasons were defined based on the solstice to equinox (*i.e.* Spring from March 20 to June 20; Summer from June 21 to September 22, Fall from September 23 to December 20, and Winter from December 21 to March 19). Depth-integrated (0–125 m) rates and stocks were calculated using trapezoidal integration. Statistical analyses and curve fitting were performed using MATLAB (Mathworks) or in the R statistical environment (R Development Core Team 2008).

Data that did not meet the assumptions of normality were  $\log_{10}$  transformed before analysis. For statistical analysis of ratios, geometric mean and standard deviations were used (Zar 1999).

We computed daily rates of  $^3\text{H}$ -Leu incorporation as the sum of  $^3\text{H}$ -Leu<sub>Light</sub> rates multiplied by the duration of the photoperiod and  $^3\text{H}$ -Leu<sub>Dark</sub> rates multiplied by the length of the nighttime period. Conversion of leucine incorporation rates to carbon-based estimates of BP assumed 1.5 kg C per mole leucine incorporated (Simon & Azam 1989).

## Results

The current study sought to examine coupling between BP and PP at Station ALOHA in the persistently oligotrophic upper ocean (0–125 m) habitat of the NPSG. A total of 24 different cruises at or in the vicinity of Station ALOHA were sampled over an ~2-year period. Throughout the study, sea surface temperatures (SST) varied from 22.5 to 26.8 °C, reaching an annual maximum in September and October, and minimum during the late winter (February and March). The mixed layer fluctuated between 34 and 126 m, with deeper mixed layers in the winter, followed by rapid shoaling and stratification through the spring to early fall (Figure 3.1). Incident PAR fluctuated between 15.2 and 48.4 mol quanta  $\text{m}^{-2} \text{d}^{-1}$ , with lower fluxes in the winter, increasing steadily through the spring and summer months (Figure 3.1). Concentrations of inorganic nutrients (specifically N+N and SRP) were persistently low (averaging  $4 \pm 2$  and  $100 \pm 49$  nM, respectively) in the well-lit regions (< 45 m) of the upper ocean, with concentrations increasing sharply in those regions of the upper ocean where PAR fluxes were  $< 5$  mol quanta  $\text{m}^{-2} \text{d}^{-1}$ . Rates of  $^{14}\text{C}$ -PP measured during this study (2011–2013) demonstrated the expected depth-dependent patterns, with rates in the upper euphotic zone (0–45 m) ~3-fold greater than those in

the lower euphotic zone (75–125 m; Figure 3.1). Depth-integrated (0–125 m) rates of  $^{14}\text{C}$ -PP varied less than 2-fold, ranging between 2.7 and 4.6  $\text{mmol C m}^{-2} \text{h}^{-1}$ , with a major fraction (46–75%) of this production occurring in the upper 45 m of the water column (Table 3.1).

### **Time-course experiments to examine linearity in $^3\text{H}$ -leucine incorporation**

Time course experiments revealed that rates of  $^3\text{H}$ -leucine incorporation remained linear over ~10 hours (Figure 3.2). Extrapolation of the linear portion of the measured rates of  $^3\text{H}$ -Leu incorporation to the full length of incubation indicated that the *in situ* incubations may have underestimated both  $^3\text{H}$ -Leu<sub>Dark</sub> and  $^3\text{H}$ -Leu<sub>Light</sub> by 53–78%, depending on the length of the photoperiod. Hence, we corrected the *in situ* rates of both  $^3\text{H}$ -Leu<sub>Dark</sub> and  $^3\text{H}$ -Leu<sub>Light</sub> based on the time-course experiment results.

### **Monthly and seasonal scale variability in rates of $^3\text{H}$ -leucine incorporation**

Rates of both  $^3\text{H}$ -Leu<sub>Dark</sub> and  $^3\text{H}$ -Leu<sub>Light</sub> showed depth-dependent patterns (Figure 3.3), with rates significantly greater in the well-lit upper euphotic zone (<45 m) compared to the lower euphotic zone (75–125 m; Figure 3.3; t-test;  $p < 0.001$ ). Rates of both  $^3\text{H}$ -Leu<sub>Dark</sub> and  $^3\text{H}$ -Leu<sub>Light</sub> in the upper euphotic zone (<45 m) ranged 2.5 to 13.2  $\text{pmol Leu L}^{-1} \text{h}^{-1}$  and 3.4 to 22.9  $\text{pmol Leu L}^{-1} \text{h}^{-1}$ , respectively. In the lower euphotic zone (75–125 m) rates of  $^3\text{H}$ -Leu<sub>Dark</sub> and  $^3\text{H}$ -Leu<sub>Light</sub> ranged 0.5 to 9.1  $\text{pmol Leu L}^{-1} \text{h}^{-1}$  and 0.7 to 13.5  $\text{pmol Leu L}^{-1} \text{h}^{-1}$ , respectively (Figure 3.3). Throughout the euphotic zone (0–125 m), the ratio of  $^3\text{H}$ -Leu<sub>Light</sub> to  $^3\text{H}$ -Leu<sub>Dark</sub> (L:D ratio) averaged 1.5, and demonstrated no significant depth-dependent differences (Figure 3.3; t-test,  $p > 0.05$ ).  $\Delta\text{Leu}$ , the difference between  $^3\text{H}$ -Leu<sub>Light</sub> and  $^3\text{H}$ -Leu<sub>Dark</sub> ( $\Delta\text{Leu} = ^3\text{H}\text{-Leu}_{\text{Light}} - ^3\text{H}\text{-Leu}_{\text{Dark}}$ ) averaged  $4.2 \pm 3.0 \text{ pmol Leu L}^{-1} \text{h}^{-1}$  in the upper euphotic zone (0–45 m), and  $2.2 \pm 2.5 \text{ pmol Leu L}^{-1} \text{h}^{-1}$  in the lower euphotic zone (75–125 m).

Rates of depth-integrated (0–125 m)  $^3\text{H-Leu}_{\text{Dark}}$  varied ~4-fold (ranging 0.3 to 1.1  $\mu\text{mol Leu m}^{-2} \text{ h}^{-1}$ ), averaging  $0.7 \pm 0.2 \mu\text{mol Leu m}^{-2} \text{ h}^{-1}$ , while  $^3\text{H-Leu}_{\text{Light}}$  rates varied 5-fold (ranging 0.4 to 1.7  $\mu\text{mol Leu m}^{-2} \text{ h}^{-1}$ ), averaging  $1.1 \pm 0.3 \mu\text{mol Leu m}^{-2} \text{ h}^{-1}$  (Figure 3.4, Table 3.1). The L:D ratio derived from the depth-integrated rates averaged 1.6, and ranged 1.0 to 2.5. Beginning in the late summer and fall of 2012, rates of  $^3\text{H-Leu}_{\text{Light}}$  decreased nearly 2-fold relative to rates measured in 2011 (Figure 3.4); this coincided with a period of anomalous physical and biogeochemical conditions previously described at Station ALOHA (Wilson et al. 2015); during the summer of 2012, rates of  $^{14}\text{C-PP}$  were relatively low compared to the HOT program climatology. In contrast, during the winter of 2011–2012, rates of  $^{14}\text{C-PP}$  remained relatively elevated compared to the long-term HOT program  $^{14}\text{C-PP}$  climatology (Figure 3.4). For example, rates of  $^{14}\text{C-PP}$  measured in the upper euphotic zone (0–45 m) in November 2011 were above the 95% upper confidence intervals derived from HOT program measurements for the month of November. The summer 2012 decline in  $^3\text{H-Leu}_{\text{Light}}$  was not observed in  $^3\text{H-Leu}_{\text{Dark}}$  such that the resulting L:D ratios of the depth integrated (0–125 m) rates from early 2011 through July 2012 averaged 1.8, while L:D ratios after July 2012 averaged 1.2. Despite this decrease in  $^3\text{H-Leu}_{\text{Light}}$ ,  $^3\text{H-Leu}_{\text{Dark}}$  and  $^3\text{H-Leu}_{\text{Light}}$  rates were significantly correlated throughout the study period (Pearson's linear correlation coefficient;  $r = 0.67$ ;  $p < 0.001$ ; Table 3.2). Moreover, temporal variability in rates of  $^{14}\text{C-PP}$ ,  $^3\text{H-Leu}_{\text{Dark}}$ , and  $^3\text{H-Leu}_{\text{Light}}$  in the well-lit region of the euphotic zone had a large influence on the resulting depth-integrated (0–125 m) rates. For example, variation in measured volumetric rates of  $^{14}\text{C-PP}$ ,  $^3\text{H-Leu}_{\text{Dark}}$ , and  $^3\text{H-Leu}_{\text{Light}}$  at 25 m depth explained 68%, 79%, and 65% of the variability in the depth-integrated rates (0–125 m), respectively. These relationships were determined based on Model II linear regression analyses (Ordinary Least Squares; Legendre 2014) of the 25 m volumetric rates (in units of  $\mu\text{mol}$

C L<sup>-1</sup> h<sup>-1</sup>) and 0–125 m depth-integrated <sup>14</sup>C-PP rates (in units of mmol C m<sup>-2</sup> h<sup>-1</sup>) across the full HOT time-series ( $y = 47.02x + 1.36$ ;  $r^2 = 0.68$ ;  $p < 0.001$ ), and between 25 m volumetric rates (in units of pmol Leu L<sup>-1</sup> h<sup>-1</sup>) and 0–125 m depth-integrated <sup>3</sup>H-Leu rates (in rates of nmol Leu m<sup>-2</sup> h<sup>-1</sup>) measured during this study in the dark ( $y = 63.36x + 199.19$ ;  $r^2 = 0.79$ ;  $p < 0.001$ ) and in the light ( $y = 62.71x + 337.56$ ;  $r^2 = 0.65$ ;  $p < 0.001$ ).

### Daily and diel scale variability

During the summer of 2012, rates of <sup>3</sup>H-Leu incorporation and <sup>14</sup>C-PP were measured from the well-lit upper ocean (25 m) at near-daily time scales over a 62-day period (July to September) to assess potential coupling among these processes in the upper ocean. During this period, rates of <sup>3</sup>H-Leu<sub>Dark</sub> and <sup>3</sup>H-Leu<sub>Light</sub> varied 2- and 2.5-fold, respectively, with rates in the light and dark ranging between 5.9 and 13 pmol Leu L<sup>-1</sup> h<sup>-1</sup> and 7.7 and 20 pmol Leu L<sup>-1</sup> h<sup>-1</sup> (compared to ~5- and ~6-fold variation in 25 m monthly scale rates, respectively; Figure 3.5). Rates of both <sup>3</sup>H-Leu<sub>Dark</sub> and <sup>3</sup>H-Leu<sub>Light</sub> increased during the first half of this near-daily time-series, with rates in the latter half of August ~40% higher than rates measured in July. Following this increase, rates declined, with rates in September less than 80% of rates measured in August (Figure 3.5). During this summer period, rates of <sup>14</sup>C-PP at 25 m varied 1.8-fold, ranging between 32 and 58 nmol C L<sup>-1</sup> hr<sup>-1</sup> (compared to ~3-fold variability over 25 m monthly scale measurements; Figure 3.6); however, rates of <sup>3</sup>H-Leu<sub>Dark</sub> and <sup>3</sup>H-Leu<sub>Light</sub> were not significantly related to daily scale variations in rates of <sup>14</sup>C-PP (Model II reduced major axis regression;  $p > 0.05$ ; Table 3.2).

We utilized the empirical relationships between rates of <sup>14</sup>C-PP and <sup>3</sup>H-Leu incorporation measured at 25 m and the 0–125 m depth-integrated rates to estimate depth-integrated rates of

$^{14}\text{C-PP}$ ,  $^3\text{H-Leu}_{\text{Dark}}$ , and  $^3\text{H-Leu}_{\text{Light}}$  during the near-daily scale sampling of 2012 where productivity measurements were restricted to 25 m. The derived depth-integrated rates of  $^{14}\text{C-PP}$  ranged between 2.9 and 4.1  $\text{mmol C m}^{-2} \text{ h}^{-1}$  (Figure 3.4) and averaged  $3.5 \pm 0.3 \text{ mmol C m}^{-2} \text{ h}^{-1}$ . The depth-integrated rates of  $^3\text{H-Leu}_{\text{Dark}}$  computed by this approach ranged from 0.6 to 1.0  $\mu\text{mol Leu m}^{-2} \text{ h}^{-1}$ , averaging  $0.8 \pm 0.1 \mu\text{mol Leu m}^{-2} \text{ h}^{-1}$ , while rates of  $^3\text{H-Leu}_{\text{Light}}$  varied between 0.8 and 1.6  $\text{Leu m}^{-2} \text{ h}^{-1}$ , averaging  $1.2 \pm 0.2 \mu\text{mol Leu m}^{-2} \text{ h}^{-1}$  (Figure 3.4).

In addition to the near daily scale rate measurements, we also examined diel variability in  $^3\text{H-Leu}$  incorporation over a two-day period (August 31 to September 1) during the summer of 2012 (Figure 3.7). Rates of  $^3\text{H-Leu}$  varied ~1.5- and 1.7-fold during this diel sampling period, in the dark and light respectively, with rates of  $^3\text{H-Leu}$  incorporation in both dark and light following a quasi-sinusoidal pattern. Rates of  $^3\text{H-Leu}_{\text{Dark}}$  were greatest shortly before sunset or in the early evening, while rates of  $^3\text{H-Leu}_{\text{Light}}$  were elevated in the midmorning and early afternoon when incident PAR peaked (Figure 3.7).

### **Proportion of BP to $^{14}\text{C-PP}$ and cell-specific rates of production**

Computed daily rates of BP ranged between 0.9 to 4.3  $\text{mmol C m}^{-2} \text{ d}^{-1}$ , equivalent to 2–9% (averaging 6%) of the measured rates of  $^{14}\text{C-PP}$ , respectively (Figure 3.8). Normalizing the upper ocean (0–45 m) depth-integrated rates of  $^3\text{H-Leu}_{\text{Dark}}$  to the combined inventories of non-pigmented picoplankton and *Prochlorococcus* resulted in cell-specific rates of incorporation averaging  $0.012 \pm 0.020 \text{ amol Leu cell}^{-1} \text{ h}^{-1}$  (Table 3.1). In the lower euphotic zone (75–125 m), on average, cell-specific rates of incorporation in the dark were  $0.006 \pm 0.003 \text{ amol Leu cell}^{-1} \text{ h}^{-1}$ , or approximately half (47%) the rates measured in the upper ocean. In the upper euphotic zone, cell specific incorporation in the light, based on the  $\Delta\text{Leu}$  ( $^3\text{H-Leu}_{\text{Light}} - ^3\text{H-Leu}_{\text{Dark}}$ ) rates

normalized to *Prochlorococcus* cell inventories, averaged  $0.023 \pm 0.017$  amol Leu cell<sup>-1</sup> h<sup>-1</sup>, with rates in the lower euphotic zone averaging  $0.014 \pm 0.012$  amol Leu cell<sup>-1</sup> h<sup>-1</sup>. No significant seasonal differences were observed in cell-specific incorporation rates derived from either dark or light incubations. Cell-specific incorporation rates during the daily scale sampling from the summer of 2012 in dark and light varied 2- to 7-fold, ranging 0.009 to 0.020 amol Leu cell<sup>-1</sup> h<sup>-1</sup> in the dark and 0.011 to 0.073 amol Leu cell<sup>-1</sup> h<sup>-1</sup> for the  $\Delta$ Leu rates.

### **Statistical relationships between <sup>3</sup>H-Leu, <sup>14</sup>C-PP, temperature, and PAR**

We utilized linear regression and correlation analyses to identify possible interactions between time-varying changes in measured rates of <sup>14</sup>C-PP, <sup>3</sup>H-Leu<sub>Dark</sub>, and <sup>3</sup>H-Leu<sub>Light</sub> and fluctuations in PAR, temperature, and picoplankton abundances. These analyses revealed no significant relationships in volumetric rates of <sup>3</sup>H-Leu<sub>Dark</sub> and <sup>14</sup>C-PP at any of the depths where coincident measurements were conducted (Model II reduced major axis regression;  $p > 0.05$ ). At 25 m, variations in temperature alone explained 41% and 27% of the variability in rates of <sup>3</sup>H-Leu<sub>Dark</sub> and <sup>3</sup>H-Leu<sub>Light</sub>, respectively (Model II reduced major axis regression;  $r^2 = 0.41$  and 0.27;  $p < 0.001$  and  $p < 0.001$ , respectively; Table 3.2), with variations in PAR significantly correlated with rates of <sup>3</sup>H-Leu<sub>Dark</sub> and <sup>3</sup>H-Leu<sub>Light</sub>, respectively (Pearson's linear correlation;  $r = 0.46$  and 0.31;  $p < 0.001$  and  $p < 0.05$ ; Table 3.2). Abundances of *Prochlorococcus* showed no significant relationships with rates of <sup>3</sup>H-Leu<sub>Light</sub> or  $\Delta$ Leu (Pearson's linear correlation;  $p > 0.05$ ); however, the combined abundances of *Prochlorococcus* and non-pigmented bacteria were significantly correlated with rates of <sup>3</sup>H-Leu<sub>Dark</sub> (Pearson's linear correlation;  $r = 0.34$ ;  $p < 0.01$ ; Table 3.2). Rates of  $\Delta$ Leu were significantly related to PP (Pearson's linear correlation;  $r = 0.40$ ;  $p < 0.005$ ; Table 3.2). In the lower euphotic zone (100 m depth horizon), variability in temperature, PAR, or rates of <sup>14</sup>C-PP did not explain variation in rates of <sup>3</sup>H-Leu<sub>Dark</sub> and <sup>3</sup>H-

Leu<sub>Light</sub> ( $p > 0.05$ ; Table 3.2), and  $^{14}\text{C}$ -PP demonstrated no significant relationship to  $\Delta\text{Leu}$ . The combined abundances of *Prochlorococcus* and non-pigmented bacteria were correlated to variability in rates of  $^3\text{H}$ -Leu<sub>Dark</sub> (Pearson's linear correlation;  $r = 0.55$ ;  $p < 0.05$ ; Table 3.2), while abundances of *Prochlorococcus* were not significantly related to rates of  $^3\text{H}$ -Leu<sub>Light</sub> (Pearson's linear correlation;  $p > 0.05$ ; Table 3.2). We also utilized stepwise multiple linear regression analyses to evaluate possible interactive relationships between rates of  $^3\text{H}$ -Leu incorporation rates and  $^{14}\text{C}$ -PP, surface PAR, and mixed layer temperature. Results from these analyses revealed that in the upper euphotic zone there was a significant interactive influence of temperature and  $^{14}\text{C}$ -PP on rates of  $^3\text{H}$ -Leu<sub>Dark</sub> (Stepwise Multiple Linear Regression for 5 m and 25 m values;  $r^2 = 0.88$  and  $0.59$ ;  $p < 0.001$  and  $p < 0.005$ , respectively), but no significant interactions were observed for rates of  $^3\text{H}$ -Leu<sub>Light</sub> (data not shown).

## **Discussion**

Bacterial metabolism plays a central role in ocean carbon cycling (Cho & Azam 1988, Duarte & Agusti 1998); however, despite decades of research examining the contribution of bacteria to ocean productivity, to date there are relatively few studies examining temporal variability in bacterial growth across multiple scales in the open sea. In the current study, we examined time-variability in rates of  $^3\text{H}$ -Leu incorporation, a proxy for bacterial biomass production, over time scales ranging from diel to seasonal, in the persistently oligotrophic waters of the central North Pacific Ocean. By evaluating temporal variability associated with rates of BP we sought to better understand the coupling between contemporaneous rates of PP and BP in this habitat, and to gain insight into factors controlling bacterial growth in this ecosystem.

Overall, we observed that depth-integrated (0–125 m) rates of  $^3\text{H}\text{-Leu}_{\text{Dark}}$  and  $^3\text{H}\text{-Leu}_{\text{Light}}$  varied 4- and 5-fold, respectively, over monthly to seasonal time scales, with peak rates occurring in the late summer and early fall when upper ocean temperatures were maximal. In contrast, rates of  $^{14}\text{C}\text{-PP}$  fluctuated by less than 2-fold over these same time scales. Moreover, while rates of  $^{14}\text{C}\text{-PP}$  were generally elevated in the early to mid-summer when incident PAR was maximal, peak rates of BP lagged  $^{14}\text{C}\text{-PP}$  by 1 to 2 months. Analyses of the resulting measurements suggest that while seasonal scale fluctuations in temperature may be an important control on the magnitude of material flow into bacterial biomass in this ecosystem, there is also an interactive effect of primary production, potentially representing the importance of resource availability as a control on BP (e.g. Pomeroy & Wiebe 2001, Lopez-Urrutia & Moran 2007). This suggests that while temperature may influence the potential maximum and minimum metabolic rates of the bacterial community, the availability and quality of DOM would determine how much carbon is partitioned into biomass.

By conducting parallel  $^3\text{H}\text{-Leu}$  incubations in both the dark and light, we examined how vertical and time-varying changes in irradiance influenced rates of bacterial protein production. Consistent with previous reports (Church et al. 2004, 2006), we found that upper ocean (<125 m) rates of  $^3\text{H}\text{-Leu}_{\text{Light}}$  were consistently greater than  $^3\text{H}\text{-Leu}_{\text{Dark}}$  by 1.5-fold, on average, a finding consistent with incorporation of  $^3\text{H}\text{-Leu}$  by *Prochlorococcus* (Zubkov et al. 2004, Zubkov & Tarran 2005, Michelou et al. 2007, Björkman et al. 2015). Despite large changes in the vertical flux of light through the upper ocean, we observed no consistent depth-dependent patterns to the photostimulation of  $^3\text{H}\text{-Leu}$  incorporation. In a recent study, Björkman et al. (2015) quantified rates of  $^3\text{H}\text{-Leu}$  incorporation by both *Prochlorococcus* and non-pigmented picoplankton at Station ALOHA based on flow cytometric sorting of radiolabeled cells. These authors report that

~60% of the  $^3\text{H}$ -Leu incorporation occurring in the light was attributable to *Prochlorococcus*, with rates of  $^3\text{H}$ -Leu incorporation by these cyanobacteria 7-fold greater (on average) in the light than in the dark. In contrast, *Prochlorococcus* contributed ~20% of the total  $^3\text{H}$ -Leu incorporation in the dark, slightly less than the proportional contribution of these cells to total picoplankton abundances (in the current study *Prochlorococcus* accounted for 26% of the total picoplankton cell inventories). Such results complicate interpretation of  $^3\text{H}$ -Leu incorporation as a measure of heterotrophic BP and highlight the potential complexity of organic matter cycling by the upper ocean bacterial assemblage in this habitat.

The extent to which *Prochlorococcus* relies on organic matter to supplement autotrophic production remains unclear; however, *Prochlorococcus* is responsible for a large fraction of daily net primary productivity in the NPSG (Liu et al. 1997) and demonstrates relatively high per cell rates of  $^3\text{H}$ -Leu incorporation (Björkman et al. 2015). In the current study, rates of  $^3\text{H}$ -Leu<sub>Light</sub> were notably lower in the summer and fall of 2012 relative to the previous year, while rates of  $^3\text{H}$ -Leu<sub>Dark</sub> were generally similar. The resulting  $^3\text{H}$ -Leu L:D ratio decreased by ~25% between these years; these changes coincided with a period during which *Prochlorococcus* cell abundances and rates of primary productivity were anomalously low for this region (Wilson et al. 2015). Together these findings suggest variability in the biomass and growth of *Prochlorococcus* exerts substantial control over upper ocean carbon cycling in this ecosystem. Assuming *Prochlorococcus* assimilation of  $^3\text{H}$ -Leu was responsible for the majority of the observed light stimulation of rates of BP, we normalized the difference between  $^3\text{H}$ -Leu<sub>Light</sub> and  $^3\text{H}$ -Leu<sub>Dark</sub> ( $\Delta\text{Leu}$ ) to *Prochlorococcus* cell abundances. We also made the assumption that the *Prochlorococcus* contribution to  $^3\text{H}$ -Leu<sub>Dark</sub> rates scaled proportionally with the fractional contribution of *Prochlorococcus* to picoplankton abundances; consequently we normalized the

$^3\text{H-Leu}_{\text{Dark}}$  rates to the combined abundances of non-pigmented picoplankton and *Prochlorococcus*. The resulting cell-specific rates of  $^3\text{H-Leu}_{\text{Dark}}$  demonstrated no apparent seasonal variability.

During the near-monthly sampling, cell-specific rates of  $^3\text{H-Leu}_{\text{Dark}}$  at 25 m varied 5-fold, while the cell-specific rates of  $\Delta\text{Leu}$  varied by 67-fold. The lack of relationship between *Prochlorococcus* cell abundance and  $\Delta\text{Leu}$ , together with the resulting large variability in cell-specific rates of  $\Delta\text{Leu}$  production, suggest variability in the rates of  $^3\text{H-Leu}_{\text{Light}}$  reflect variations in *Prochlorococcus* physiology rather than temporal changes in *Prochlorococcus* biomass. In contrast, the observed relationship between rates of  $^3\text{H-Leu}_{\text{Dark}}$  and the summed abundances of non-pigmented picoplankton and *Prochlorococcus*, together with the overall lower temporal variability in the cell-normalized rates, suggests that time-varying changes in the biomass of non-pigmented picoplankton and *Prochlorococcus* contribute to much of the temporal variability in  $^3\text{H-Leu}_{\text{Dark}}$  incorporation rates. The resulting cell-normalized rates of both  $^3\text{H-Leu}_{\text{Dark}}$  and  $\Delta\text{Leu}$  were relatively low (Kirchman & Hoch 1988, Turley & Stutt 2000), but consistent with the conclusion that, on average, marine bacteria grow relatively slowly ( $\sim 0.05$  to  $0.1 \text{ d}^{-1}$ ; Kirchman 2016).

We derived daily rates of bacterial production as the sum of the  $^3\text{H-Leu}_{\text{Light}}$  and  $^3\text{H-Leu}_{\text{Dark}}$  hourly rates multiplied by the respective daylight and nighttime periods for each cruise. This assumes the  $^3\text{H-Leu}_{\text{Dark}}$  rates approximate nighttime rates of BP; our sampling of rates of  $^3\text{H-Leu}$  over diel scales (Figure 3.7) suggests rates of  $^3\text{H-Leu}_{\text{Dark}}$  increase  $\sim 25\%$  in the early evening, so the daily rates of BP derived by this approach are likely to be underestimates. The resulting carbon-based rates of daily BP averaged  $2.6 \pm 0.7 \text{ mmol C m}^{-2} \text{ d}^{-1}$ , equivalent to 3–9% of contemporaneous  $^{14}\text{C-PP}$ . This ratio is similar to the BP:PP ratios of 5% reported by Ducklow

et al. (2012) and ratios reported at BATS during the winter (1–6%; Steinberg et al. 2001) or over the full year (2–15%; Carlson et al. 1996), but are somewhat low in comparison to the 10–30% reported in other regions of the open sea (Cole et al. 1988, del Giorgio et al. 1997, Ducklow 1999, Anderson & Ducklow 2001, Hoppe et al. 2002). Such results imply a relatively low fraction of contemporaneous primary production fuels BP in the NPSG ecosystem. A recent study reported rates of euphotic zone microbial community respiration (R) measured in the dark at Station ALOHA that averaged  $41.2 \pm 8.7 \text{ mmol C m}^{-2} \text{ d}^{-1}$  (based on depth-integrated (0–125 m) rates estimated for 0.2–0.8  $\mu\text{m}$  size fractionated plankton; Martínez-García & Karl 2015). Combining these data with our measurements of bacterial production suggests bacterial carbon demand ( $\text{BCD} = \text{BP} + \text{R}$ ) at Station ALOHA averages  $\sim 44 \pm 8.7 \text{ mmol C m}^{-2} \text{ d}^{-1}$ , equivalent to nearly all ( $99\% \pm 27\%$ ) of the contemporaneous  $^{14}\text{C}$ -PP. Notably, various studies at Station ALOHA indicate that rates of gross primary production may be 1.5 to 2.5-fold greater than estimates derived from  $^{14}\text{C}$ -PP (Juranek & Quay 2005, Quay et al. 2010). Combining the derived daily rates of BP with estimates of R from Martínez-García and Karl (2015) helps constrain bacterial growth efficiencies ( $\text{BGE} = \text{BP} / \text{BCD}$ ), which average  $6\% \pm 2\%$ . In general, BGEs for marine bacteria have been reported to range between approximately 10–40% (Carlson & Ducklow 1996, del Giorgio et al. 1997, del Giorgio & Cole 1998, Carlson et al. 1999), with BGE often lower in oligotrophic relative to more eutrophic marine ecosystems (Carlson & Ducklow 1996, del Giorgio & Cole 1998), including at BATS where the average BGE is 14% (Carlson & Ducklow 1996). Hence, although our measurements suggest that a relatively low fraction of contemporaneous primary production supports BP, the apparently low BGE at Station ALOHA suggests the daily flux of carbon supporting bacterial metabolism is a major pathway for primary production and is comparable to other open ocean ecosystems.

During the summer of 2012 we examined higher frequency (at diel and daily scales) fluctuations in rates of  $^3\text{H}$ -Leu incorporation. Over diel scales, rates of  $^3\text{H}$ -Leu<sub>Dark</sub> and  $^3\text{H}$ -Leu<sub>Light</sub> oscillated by 1.5- and 1.7-fold, respectively, while day-to-day changes in these rates varied ~2- and ~2.5-fold, respectively. Our diel scale measurements indicated that rates of  $^3\text{H}$ -Leu<sub>Dark</sub> were greatest at or near dusk, consistent with observations from the tropical Atlantic (Mary et al. 2008). However, research in the North Sea (Winter et al. 2004) and Southern California Bight (Fuhrman et al. 1985) found rates of bacterial production were higher during daytime, while Riemann & Søndergaard (1984) found no consistent diel pattern in bacterial production in freshwater and coastal samples. In contrast, the peak in rates of  $^3\text{H}$ -Leu<sub>Light</sub> near noon supports the notion that photostimulation of  $^3\text{H}$ -Leu was likely controlled by variations in *Prochlorococcus* growth. Together, these results appear consistent with recent results suggesting that phytoplankton and heterotrophic bacteria may exhibit synchronous activity, with *Prochlorococcus* transcriptional maxima of photosystem genes followed on the order of hours by a succession of transcript maxima in oxidative phosphorylation genes by heterotrophic bacteria (Ottesen et al. 2014, Aylward et al. 2015).

In the current study, rates of  $^3\text{H}$ -Leu (either in the light or dark) were not significantly related to monthly to daily scale variations in rates of  $^{14}\text{C}$ -PP. However, we observed strong relationships between temperature and  $^3\text{H}$ -Leu incorporation (both light and dark) for the well-lit regions of the euphotic zone (<45 m). These relationships were not observed below the mixed layer, where temperature no longer exhibits a significant seasonal pattern. In well-lit regions of the euphotic zone, temporal fluctuations in PAR also appeared significantly related to rates of  $^3\text{H}$ -Leu incorporation, although changes in PAR explained less of the variability in  $^3\text{H}$ -Leu incorporation than temperature. Additionally, within the well-lit upper waters of the euphotic

zone, primary production and temperature demonstrated significant interactive effects on  $^3\text{H}$ -Leu<sub>Dark</sub>, highlighting what may be an important dynamic between resource availability and temperature as controls on bacterial metabolism in this ecosystem.

Over two years of near-monthly observations in this persistently oligotrophic habitat, BP and PP appeared temporally decoupled over a range of time scales, although PP in combination with temperature affects rates of  $^3\text{H}$ -Leu<sub>Dark</sub>. While variability in  $^{14}\text{C}$ -PP was similar between daily and monthly scales (varying by ~2- and ~3-fold, respectively), variability in rates of  $^3\text{H}$ -Leu incorporation decreased from monthly to daily to diel scales (5-, 2-, and 1.5-fold, in the dark and 6-, 3-, and 2-fold in the light). The consistent stimulation of leucine incorporation by sunlight and the greater variability in per cell rates of light stimulated leucine incorporation highlight the importance of *Prochlorococcus* growth on carbon cycling in this ecosystem. Moreover, such results also suggest that temporally variable rates of photoheterotrophic production by *Prochlorococcus* are superimposed over a less variable heterotrophic metabolism that appears partly controlled by variations in temperature and resource availability.

## Literature cited

- Alonso-Sáez L, Vázquez-Domínguez E, Cardelús C, Pinhassi J, Sala MM, Lekunberri I, Balagué V, Vila-Costa M, Unrein F, Massana R, Simó R, Gasol JM (2008) Factors controlling the year-round variability in carbon flux through bacteria in a coastal marine system. *Ecosystems* 11:397–409
- Anderson T, Ducklow H (2001) Microbial loop carbon cycling in ocean environments studied using a simple steady-state model. *Aquat Microb Ecol* 26:37–49
- Aylward FO, Eppley JM, Smith JM, Chavez FP, Scholin CA, DeLong EF (2015) Microbial community transcriptional networks are conserved in three domains at ocean basin scales. *Proc Natl Acad Sci* 112:5443–5448
- Azam F, Fenchel T, Field J, Gray J, Meyer-Reil L, Thingstad F (1983) The ecological role of water-column microbes in the sea. *Mar Ecol Prog Ser* 10:257–263
- Behrenfeld MJ, Falkowski PG (1997) Photosynthetic rates derived from satellite-based chlorophyll concentration. *Limnol Oceanogr* 42:1–20
- Billen G, Servais P, Becquevort S (1990) Dynamics of bacterioplankton in oligotrophic and eutrophic aquatic environments: bottom-up or top-down control? *Hydrobiologia* 207:37–42
- Björkman KB, Church MJ, Doggett K, Karl DM (2015) Differential assimilation of inorganic carbon and leucine by *Prochlorococcus* in the oligotrophic North Pacific Subtropical Gyre. *Front Microbiol* 6:1401
- Burnham KP, Anderson DR, Huyvaert KP (2010) AIC model selection and multimodel inference in behavioral ecology: some background, observations, and comparisons. *Behav Ecol Sociobiol* 65:23–35
- Carlson CA, Bates NR, Ducklow HW, Hansell DA (1999) Estimation of bacterial respiration and growth efficiency in the Ross Sea, Antarctica. *Aquat Microb Ecol* 19:229–244
- Carlson CA, Ducklow HW (1996) Growth of bacterioplankton and consumption of dissolved organic carbon in the Sargasso Sea. *Aquat Microb Ecol* 10:69–85
- Carlson C, Ducklow H, Michaels A (1994) Annual flux of dissolved organic carbon from the euphotic zone in the northwestern Sargasso Sea. *Nature* 371:405–408
- Carlson CA, Ducklow HW, Sleeter TD (1996) Stocks and dynamics of bacterioplankton in the northwestern Sargasso Sea. *Deep Sea Res II* 43:491–515
- Cho BC, Azam F (1988) Major role of bacteria in biogeochemical fluxes in the ocean's interior. *Nature* 332:441–443

- Church M, Björkman K, Karl D, Saito M, Zehr J (2008) Regional distributions of nitrogen-fixing bacteria in the Pacific Ocean. *Limnol Oceanogr* 53:63–77
- Church M, Ducklow H, Karl D (2004) Light dependence of [<sup>3</sup>H]Leucine incorporation in the oligotrophic North Pacific ocean. *Appl Environ Microbiol* 70:4079–4087
- Church M, Ducklow H, Letelier R, Karl D (2006) Temporal and vertical dynamics in picoplankton photoheterotrophic production in the subtropical North Pacific Ocean. *Aquat Microb Ecol* 45:41–53
- Church MJ, Lomas MW, Muller-Karger F (2013) Sea change: Charting the course for biogeochemical ocean time-series research in a new millennium. *Deep Sea Res II* 93:2–15
- Cole J, Findlay S, Pace M (1988) Bacterial production in fresh and saltwater ecosystems - a cross-system overview. *Mar Ecol Prog Ser* 43:1–10
- Cotner JB, Biddanda BA (2002) Small players, large role: microbial influence on biogeochemical processes in pelagic aquatic ecosystems. *Ecosystems* 5:105–121
- del Giorgio P, Cole J (1998) Bacterial growth efficiency in natural aquatic systems. *Ann Rev Mar Sci* 29:503–541
- del Giorgio P, Cole J, Cimleris A (1997) Respiration rates in bacteria exceed phytoplankton production in unproductive aquatic systems. *Nature* 385:148–151
- Duarte C, Agusti S (1998) The CO<sub>2</sub> balance of unproductive aquatic ecosystems. *Science* 281:234–236
- Duarte C, Cebrian J (1996) The fate of marine autotrophic production. *Limnol Oceanogr* 41:1758–1766
- Ducklow H (1999) The bacterial component of the oceanic euphotic zone. *FEMS Microbiol Ecol* 30:1–10
- Ducklow H, Carlson C (1992) Oceanic bacterial production. In: *Advances in Microbial Ecology*. Springer, USA, p 113–181
- Ducklow HW, Schofield OME, Vernet M, Stammerjohn SE, Erickson M (2012) Multiscale control of bacterial production by phytoplankton dynamics and sea ice along the western Antarctic Peninsula : a regional and decadal investigation. *J Marine Syst* 98:26–39
- Field CB, Behrenfeld MJ, Randerson JT, Falkowski P (1998) Primary production of the biosphere: Integrating terrestrial and oceanic components. *Science* 281:237–240

- Fuhrman JA, Eppley RW, Hagström Å, Azam F (1985) Diel variations in bacterioplankton, phytoplankton, and related parameters in the Southern California Bight. *Mar Ecol Prog Ser* 27:9–20
- Hansell D, Carlson C (1998) Net community production of dissolved organic carbon. *Global Biogeochem Cycles* 12:443–453
- Hoppe H-G, Gocke K, Koppe R, Begler C (2002) Bacterial growth and primary production along a north–south transect of the Atlantic Ocean. *Nature* 416:168–171
- John DE, López-Díaz JM, Cabrera A, Santiago NA, Corredor JE, Bronk DA, Paul JH (2011) A day in the life in the dynamic marine environment: how nutrients shape diel patterns of phytoplankton photosynthesis and carbon fixation gene expression in the Mississippi and Orinoco River plumes. *Hydrobiologia* 679:155–173
- Juranek L, Quay P (2005) In vitro and in situ gross primary and net community production in the North Pacific Subtropical Gyre using labeled and natural abundance isotopes of dissolved O<sub>2</sub>. *Global Biogeochem Cycles* 19
- Karl D (1999) A sea of change: Biogeochemical variability in the North Pacific Subtropical Gyre. *Ecosystems* 2:181–214
- Karl DM, Björkman KM, Dore JE, Fujieki L, Hebel DV, Houlihan T, Letelier RM, Tupas LM (2001) Ecological nitrogen-to-phosphorus stoichiometry at station ALOHA. *Deep Sea Res II* 48:1529–1566
- Karl DM, Church MJ, Dore JE, Letelier RM, Mahaffey C (2012) Predictable and efficient carbon sequestration in the North Pacific Ocean supported by symbiotic nitrogen fixation. *Proc Natl Acad Sci USA* 109:1842–1849
- Karl D, Hebel D, Björkman K, Letelier R (1998) The role of dissolved organic matter release in the productivity of the oligotrophic North Pacific Ocean. *Limnol Oceanogr* 43:1270–1286
- Karl D, Lukas R (1996) The Hawaii Ocean Time-series (HOT) program: Background, rationale and field implementation. *Deep Sea Res II* 43:129–156
- Kirchman DL (2004) A primer on dissolved organic material and heterotrophic prokaryotes in the oceans. In: Follows M, Oguz T (eds) *The Ocean Carbon Cycle and Climate*. Springer Netherlands, p 31–63
- Kirchman DL (2016) Growth rates of microbes in the oceans. *Ann Rev Mar Sci* 8:285–309
- Kirchman DL, Hoch MP (1988) Bacterial production in the Delaware Bay estuary estimated from thymidine and leucine incorporation rates. *Mar Ecol Prog Ser* 45:169–178

- Kirchman D, K'nees E, Hodson R (1985) Leucine incorporation and its potential as a measure of protein synthesis by bacteria in natural aquatic systems. *Appl Environ Microbiol* 49:599–607
- Kirchman D, Newell S, Hodson R (1986) Incorporation versus biosynthesis of leucine - implications for measuring rates of protein-synthesis and biomass production by bacteria. *Mar Ecol Prog Ser* 32:47–59
- Laws EA, Letelier RM, Karl DM (2014) Estimating the compensation irradiance in the ocean: The importance of accounting for non-photosynthetic uptake of inorganic carbon. *Deep Sea Res I* 93:35–40
- Legendre P (2014) lmodel2: Model II Regression. R package version 1.7-2. <http://CRAN.R-project.org/package=lmodel2>
- Letelier R, Dore J, Winn C, Karl D (1996) Seasonal and interannual variations in photosynthetic carbon assimilation at Station ALOHA. *Deep Sea Res II* 43:467–490
- Letelier R, Karl D, Abbott M, Bidigare R (2004) Light driven seasonal patterns of chlorophyll and nitrate in the lower euphotic zone of the North Pacific Subtropical Gyre. *Limnol Oceanogr* 49:508–519
- Liu H, Nolla H, Campbell L (1997) *Prochlorococcus* growth rate and contribution to primary production in the equatorial and subtropical North Pacific Ocean. *Aquat Microb Ecol* 12:39–47
- Lopez-Urrutia A, Moran X (2007) Resource limitation of bacterial production distorts the temperature dependence of oceanic carbon cycling. *Ecology* 88:817–822
- Martínez-García S, Karl DM (2015) Microbial respiration in the euphotic zone at Station ALOHA. *Limnol Oceanogr* 60:1039–1050
- Mary I, Garczarek L, Tarran GA, Kolowrat C, Terry MJ, Scanlan DJ, Burkill PH, Zubkov MV (2008) Diel rhythmicity in amino acid uptake by *Prochlorococcus*. *Environ Microbiol* 10:2124–2131
- Michaels A, Bates N, Buesseler K, Carlson C, Knap A (1994) Carbon-cycle imbalances in the Sargasso Sea. *Nature* 372:537–540
- Michelou VK, Cottrell MT, Kirchman DL (2007) Light-stimulated bacterial production and amino acid assimilation by cyanobacteria and other microbes in the North Atlantic Ocean. *Appl Environ Microbiol* 73:5539–5546
- Ottesen EA, Young CR, Gifford SM, Eppley JM, Marin R, Schuster SC, Scholin CA, DeLong EF (2014) Multispecies diel transcriptional oscillations in open ocean heterotrophic bacterial assemblages. *Science* 345:207–212

- Pace ML, Giorgio P del, Fischer D, Condon R, Malcom H (2004) Estimates of bacterial production using the leucine incorporation method are influenced by differences in protein retention of microcentrifuge tubes. *Limnol Oceanogr Methods* 2:55–61
- Pomeroy LR (1974) The ocean's food web, a changing paradigm. *BioScience* 24:499–504
- Pomeroy LR, Wiebe WJ (2001) Temperature and substrates as interactive limiting factors for marine heterotrophic bacteria. *Aquat Microb Ecol* 23:187–204
- Quay PD, Peacock C, Björkman K, Karl DM (2010) Measuring primary production rates in the ocean: Enigmatic results between incubation and non-incubation methods at Station ALOHA. *Global Biogeochem Cycles* 24:1–14
- R Development Core Team (2008) *R: A Language and Environment for Statistical Computing*. R Foundation for Statistical Computing, Vienna, Austria. <http://www.R-project.org>.
- Riemann B, Søndergaard M (1984) Measurements of diel rates of bacterial secondary production in aquatic environments. *Appl Environ Microbiol* 47:632–638
- Shiah F, Ducklow H (1994) Temperature regulation of heterotrophic bacterioplankton abundance, production, and specific growth-rate in Chesapeake Bay. *Limnol Oceanogr* 39:1243–1258
- Simon M, Azam F (1989) Protein content and protein synthesis rates of planktonic marine bacteria. *Mar Ecol Prog Ser* 51:201–213
- Smith DC, Azam F (1992) A simple, economical method for measuring bacterial protein synthesis rates in seawater using  $^3\text{H}$ -leucine. *Mar Microb Food Webs* 6:107–114
- Steemann Nielsen E (1952) The use of radio-active carbon ( $\text{C}^{14}$ ) for measuring organic production in the sea. *J Conseil Int Explor Mer* 18:117–140
- Steinberg DK, Carlson CA, Bates NR, Johnson RJ, Michaels AF, Knap AH (2001) Overview of the US JGOFS Bermuda Atlantic Time-series Study (BATS): a decade-scale look at ocean biology and biogeochemistry. *Deep Sea Res II* 48:1405–1447
- Turley CM, Stutt ED (2000) Depth-related cell-specific bacterial leucine incorporation rates on particles and its biogeochemical significance in the Northwest Mediterranean. *Limnol Oceanogr* 45:419–425
- Viviani DA, Karl DM, Church MJ (2015) Variability in photosynthetic production of dissolved and particulate organic carbon in the North Pacific Subtropical Gyre. *Front Mar Sci* 2:73

- Wilson ST, Barone B, Ascani F, Bidigare RR, Church MJ, Valle DA del, Dyhrman ST, Ferrón S, Fitzsimmons JN, Juranek LW, Kolber ZS, Letelier RM, Martínez-García S, Nicholson DP, Richards KJ, Rii YM, Rouco M, Viviani DA, White AE, Zehr JP, Karl DM (2015) Short-term variability in euphotic zone biogeochemistry and primary productivity at Station ALOHA: A case study of summer 2012. *Global Biogeochem Cycles* 29:2015GB005141
- Winter C, Herndl GJ, Weinbauer MG (2004) Diel cycles in viral infection of bacterioplankton in the North Sea. *Aquat Microb Ecol* 35:207–216
- Zar JH (1999) *Biostatistical Analysis*. Prentice Hall PTR, New Jersey
- Zubkov MV, Tarran GA (2005) Amino acid uptake of *Prochlorococcus* spp. in surface waters across the South Atlantic Subtropical Front. *Aquat Microb Ecol* 40:241–249
- Zubkov MV, Tarran GA, Fuchs BM (2004) Depth related amino acid uptake by *Prochlorococcus* cyanobacteria in the Southern Atlantic tropical gyre. *FEMS Microbiol Ecol* 50:153–161

**Table 3.1.** Depth-integrated stocks and rate measurements during this time-series study, including mean  $\pm$  standard deviation (SD) and ranges for rates of  $^3\text{H-Leu}_{\text{Dark}}$  and  $^3\text{H-Leu}_{\text{Light}}$  ( $\text{nmol Leu m}^{-2} \text{ h}^{-1}$ ), abundances of *Prochlorococcus* (*Prochloro*) and non-pigmented picoplankton (non-pig), and derived mean leucine incorporation rates per cell in both dark and light. Cell-specific rates in dark calculated by dividing  $^3\text{H-Leu}_{\text{Dark}}$  by total abundances of *Prochlorococcus* and non-pigmented picoplankton, while cell-specific rates in the light were calculated by dividing  $\Delta\text{Leu}$  (the difference between  $^3\text{H-Leu}_{\text{Dark}}$  and  $^3\text{H-Leu}_{\text{Light}}$ ), and are given in units of  $\text{amol Leu cell}^{-1} \text{ h}^{-1}$ . Also shown are rates of  $^{14}\text{C-PP}$  ( $\text{mmol C m}^{-2} \text{ h}^{-1}$ ), as well as BP as a percent of  $^{14}\text{C-PP}$ .

mean $\pm$ SD  range	$^3\text{H-Leu}_{\text{Dark}}$ ( $\text{nmol Leu m}^{-2} \text{ h}^{-1}$ )	$^3\text{H-Leu}_{\text{Light}}$ ( $\text{nmol Leu m}^{-2} \text{ h}^{-1}$ )	<i>Prochloro</i> ( $\text{cells} \cdot 10^{11} \text{ m}^{-2}$ )	non-pig ( $\text{cells} \cdot 10^{11} \text{ m}^{-2}$ )	Cell-specific $\text{Leu}_{\text{Dark}}$ ( $\text{amol Leu cell}^{-1} \text{ h}^{-1}$ )	Cell-specific $\Delta\text{Leu}_{\text{Light}}$ ( $\text{amol Leu cell}^{-1} \text{ h}^{-1}$ )	$^{14}\text{C-PP}$ ( $\text{mmol C m}^{-2} \text{ h}^{-1}$ )	BP/ $^{14}\text{C-PP}$ (%)
0–45 m	322.2 $\pm$ 104.1	516.3 $\pm$ 183.0	86.1 $\pm$ 15.7	214.4 $\pm$ 25.7	0.011 $\pm$ 0.003	0.023 $\pm$ 0.017	2.0 $\pm$ 0.4	5 $\pm$ 2
	128.1–557.0	176.3–898.9	65.0–110.9	179.2–281.8	0.004–0.017	0.001–0.059	1.2–3.2	2–8
75–125 m	161.9 $\pm$ 57.0	267.6 $\pm$ 120.4	73.6 $\pm$ 18.9	206.7 $\pm$ 21.1	0.006 $\pm$ 0.002	0.014 $\pm$ 0.012	0.7 $\pm$ 0.2	8 $\pm$ 4
	91.6–283.0	80.9–513.4	37.8–110.0	170.9–235.2	0.003–0.011	0.000–0.038	0.3–1.2	3–19
0–125 m	662.5 $\pm$ 182.8	1073.5 $\pm$ 346.8	221.6 $\pm$ 32.7	562.4 $\pm$ 45.5	0.009 $\pm$ 0.003	0.019 $\pm$ 0.014	3.6 $\pm$ 0.6	6 $\pm$ 2
	280.3–1074.1	343.8–1695.9	174.7–275.6	477.9–669.6	0.003–0.015	0.001–0.046	2.7–4.6	2–9

**Table 3.2.** Results of Model II reduced major axis regression (RMA) and Pearson's linear correlation coefficients (PC) analyses evaluating temporal coupling among rates of  $^3\text{H-Leu}_{\text{Light}}$ ,  $^3\text{H-Leu}_{\text{Dark}}$ , and  $^{14}\text{C-PP}$  and variation in temperature, PAR, and abundances of *Prochlorococcus* (*Prochloro*) and non-pigmented bacteria (non-pigs). Daily comparisons refer to measurements made during summer 2012. NS = not significant at  $p < 0.05$ .

Relationship	Depth range	Regression equation	r- or $r^2$ - value	p-value	Number of samples
Temperature to $^3\text{H-Leu}_{\text{Dark}}$ (RMA)	25 m	$y=2.23x-48.21$	$r^2 = 0.41$	<0.001	60
Temperature to $^3\text{H-Leu}_{\text{Light}}$ (RMA)	25 m	$y=3.76x-82.41$	$r^2 = 0.27$	<0.001	60
PAR to $^3\text{H-Leu}_{\text{Dark}}$ (PC)	25 m		$r = 0.46$	<0.001	50
PAR to $^3\text{H-Leu}_{\text{Light}}$ (PC)	25 m		$r = 0.31$	0.027	50
$\log_{10}$ PP to $\log_{10}$ $^3\text{H-Leu}_{\text{Dark}}$ (RMA)	25 m	NS	NS	NS	65
$\log_{10}$ PP to $\log_{10}$ $^3\text{H-Leu}_{\text{Light}}$ (RMA)	25 m	NS	NS	NS	65
PP to $\Delta\text{Leu}$ (PC)	25 m		$r = 0.40$	<0.005	65
[ <i>Prochloro</i> ] to $^3\text{H-Leu}_{\text{Light}}$ (PC)	25 m		NS	NS	61
[ <i>Prochloro</i> + non-pigs] to $^3\text{H-Leu}_{\text{Dark}}$ (PC)	25 m		$r = 0.34$	<0.01	61
$\log_{10}$ PP to $\log_{10}$ $^3\text{H-Leu}_{\text{Dark}}$ (RMA)	daily 25 m	NS	NS	NS	43
$\log_{10}$ PP to $\log_{10}$ $^3\text{H-Leu}_{\text{Light}}$ (RMA)	daily 25 m	NS	NS	NS	43
Temperature to $^3\text{H-Leu}_{\text{Dark}}$ (RMA)	100 m	NS	NS	NS	22
Temperature to $^3\text{H-Leu}_{\text{Light}}$ (RMA)	100 m	NS	NS	NS	22
PAR to $^3\text{H-Leu}_{\text{Dark}}$ (PC)	100 m		NS	NS	15
PAR to $^3\text{H-Leu}_{\text{Light}}$ (PC)	100 m		NS	NS	15
$\log_{10}$ PP to $\log_{10}$ $^3\text{H-Leu}_{\text{Dark}}$ (RMA)	100 m	NS	NS	NS	22
$\log_{10}$ PP to $\log_{10}$ $^3\text{H-Leu}_{\text{Light}}$ (RMA)	100 m	NS	NS	NS	22

Relationship	Depth range	Regression equation	r- or r <sup>2</sup> -value	p-value	Number of samples
PP to $\Delta$ Leu (PC)	100 m		NS	NS	22
[ <i>Prochloro</i> ] to <sup>3</sup> H-Leu <sub>Light</sub> (PC)	100 m		NS	NS	20
[ <i>Prochloro</i> + non-pigs] to <sup>3</sup> H-Leu <sub>Dark</sub> (PC)	100 m		r = 0.55	0.011	20
integrated <sup>3</sup> H-Leu <sub>Light</sub> to <sup>3</sup> H-Leu <sub>Dark</sub> (PC)	0–125m integrated		r = 0.67	0.001	22
SST to integrated <sup>3</sup> H-Leu <sub>Dark</sub> (RMA)	0–125m integrated	y=194.41x-4108.1	r <sup>2</sup> = 0.24	0.022	22
SST to integrated <sup>3</sup> H-Leu <sub>Light</sub> (RMA)	0–125m integrated	y=368.92x - 7979.5	r <sup>2</sup> = 0.22	0.027	22
Surface PAR to integrated <sup>3</sup> H-Leu <sub>Dark</sub> (PC)	0–125m integrated		NS	NS	18
Surface PAR to integrated <sup>3</sup> H-Leu <sub>Light</sub> (PC)	0–125m integrated		NS	NS	18
log <sub>10</sub> PP to log <sub>10</sub> <sup>3</sup> H-Leu <sub>Dark</sub> (RMA)	0–125m integrated	NS	NS	NS	22
log <sub>10</sub> PP to log <sub>10</sub> <sup>3</sup> H-Leu <sub>Light</sub> (RMA)	0–125m integrated	NS	NS	NS	22

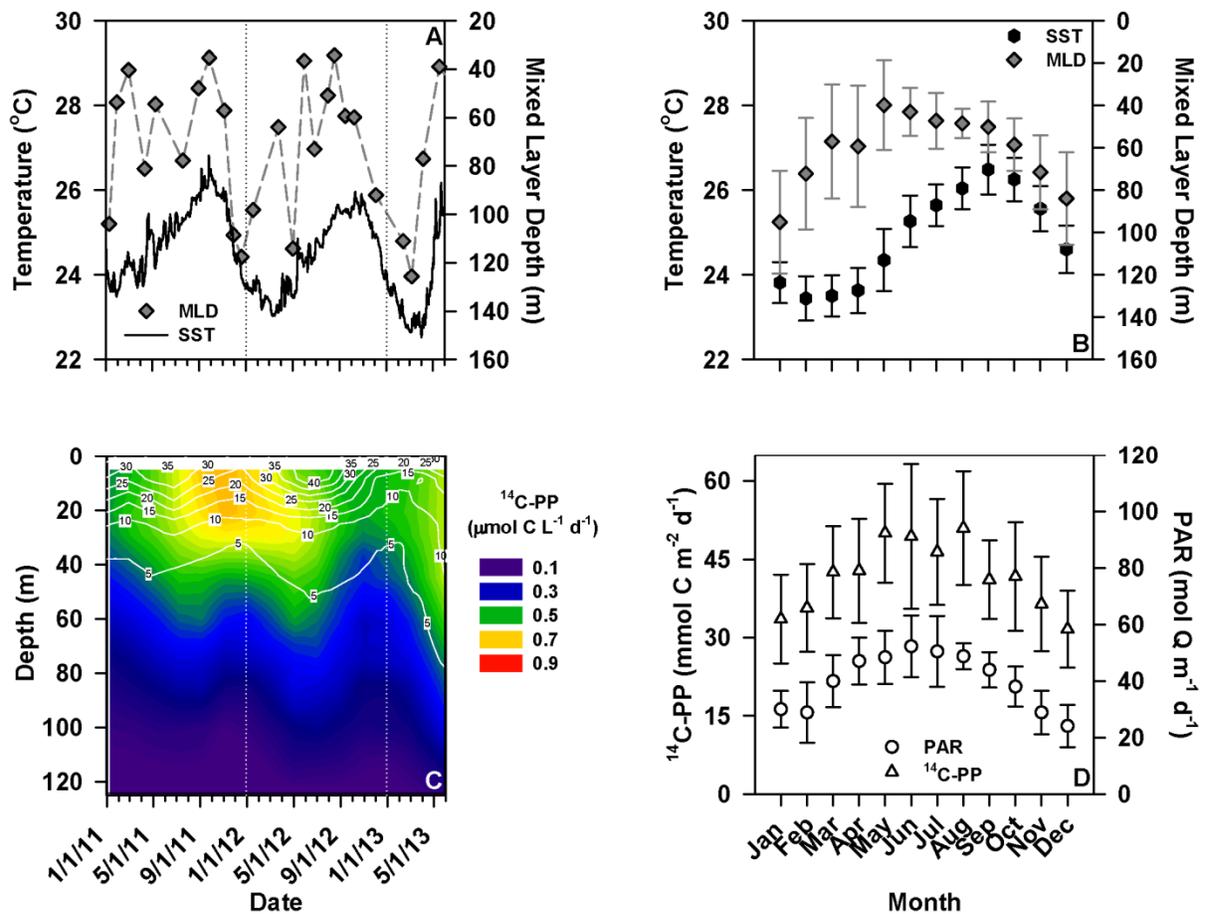


Figure 3.1. Measurements of mixed layer depth (MLD) from HOT cruises and sea surface temperature (SST) from the WHOI Hawaii Ocean Time-series WHOTS mooring during this study (panel A). Also shown are mean monthly MLD and SST from HOT program climatology (1988–2014; panel B) at Station ALOHA (error bars depict standard deviation of the mean properties). Rates of <sup>14</sup>C-PP measured during this study (color contours; panel C) overlain by downwelling photosynthetically active radiation (PAR; in units of mol quanta m<sup>-2</sup> d<sup>-1</sup>; white contours). The climatology of monthly-binned depth-integrated (0–125 m) rates of <sup>14</sup>C-PP and surface PAR at Station ALOHA (panel D); error bars are standard deviation of time-averaged mean.

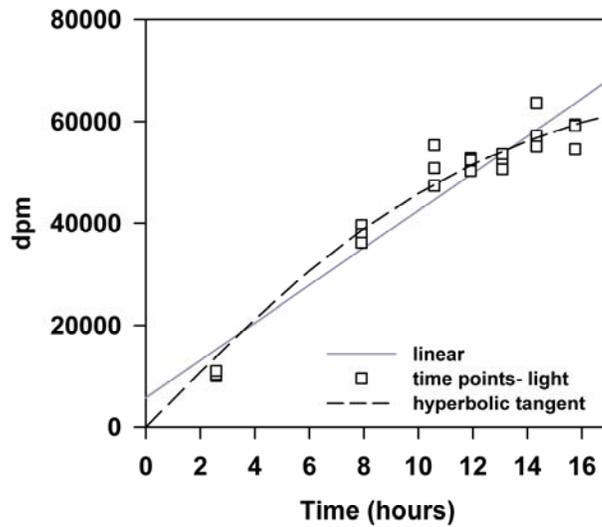


Figure 3.2. Representative time-course experiment depicting incorporation of  $^3\text{H}$ -leucine (as disintegrations per minute; dpm) as a function of time measured in the light. Also shown are the linear regression model fit (solid grey line) and the hyperbolic tangent fit (dashed black line).

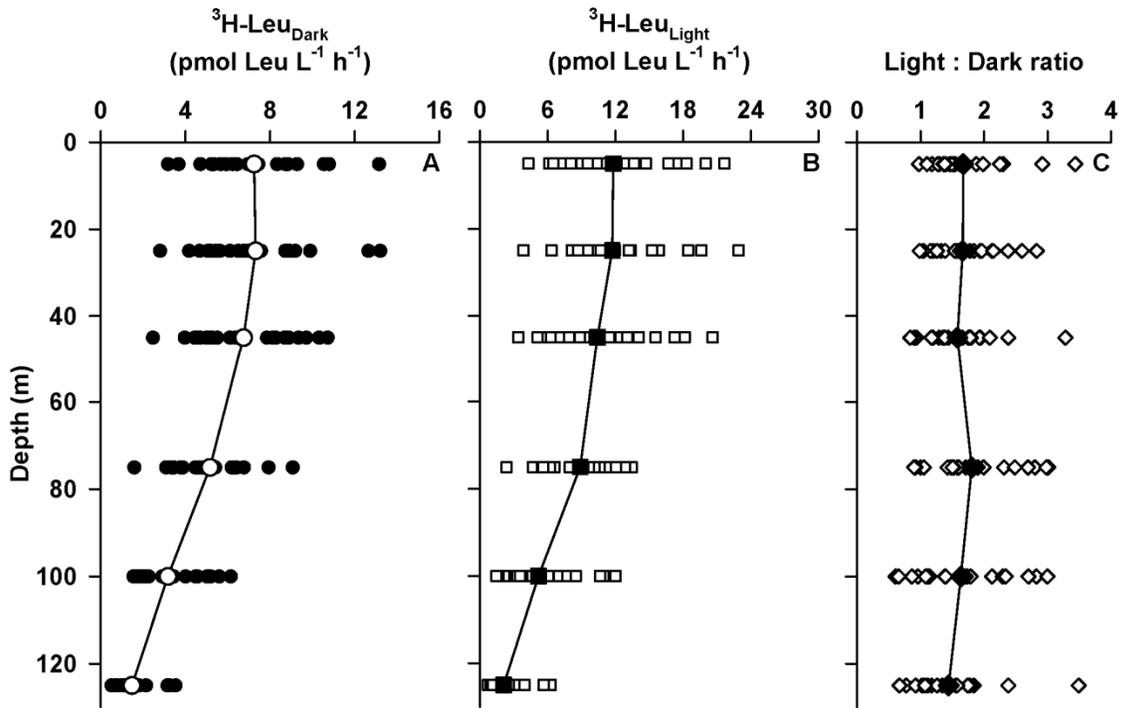


Figure 3.3. Depth profiles of  $^3\text{H-Leu}_{\text{Dark}}$  (panel A),  $^3\text{H-Leu}_{\text{Light}}$  (panel B), and the ratio of  $^3\text{H-Leu}_{\text{Light}} : ^3\text{H-Leu}_{\text{Dark}}$  (L:D ratio; panel C). Individual measurements are given as filled circles ( $^3\text{H-Leu}_{\text{Dark}}$ ), open squares ( $^3\text{H-Leu}_{\text{Light}}$ ), and open diamonds (L:D ratio). Larger symbols connected by lines represent time-averaged mean values.

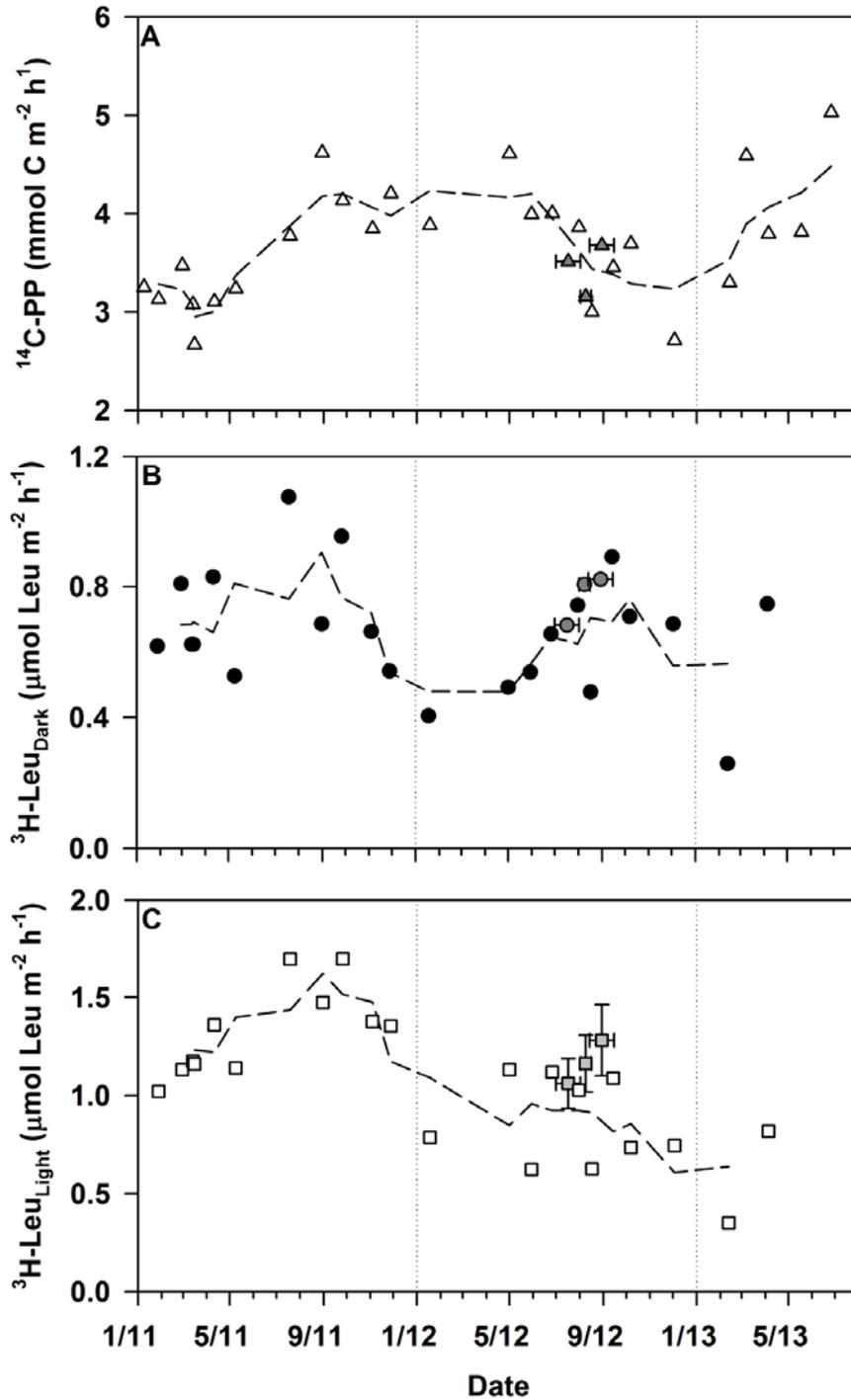


Figure 3.4. Time-series measurements of depth-integrated (0–125 m) rates of  $^{14}\text{C-PP}$  (panel A),  $^3\text{H-Leu}_{\text{Dark}}$  (panel B), and  $^3\text{H-Leu}_{\text{Light}}$  (panel C). Dashed line depicts 3-point running mean of each time-series. Grey symbols are monthly means of the derived depth-integrated rates during the HOE-DYLAN cruises in summer 2012 (vertical error bars represent the standard deviation of derived rates during this period, horizontal error bars depict the range of days over which the rates were averaged).

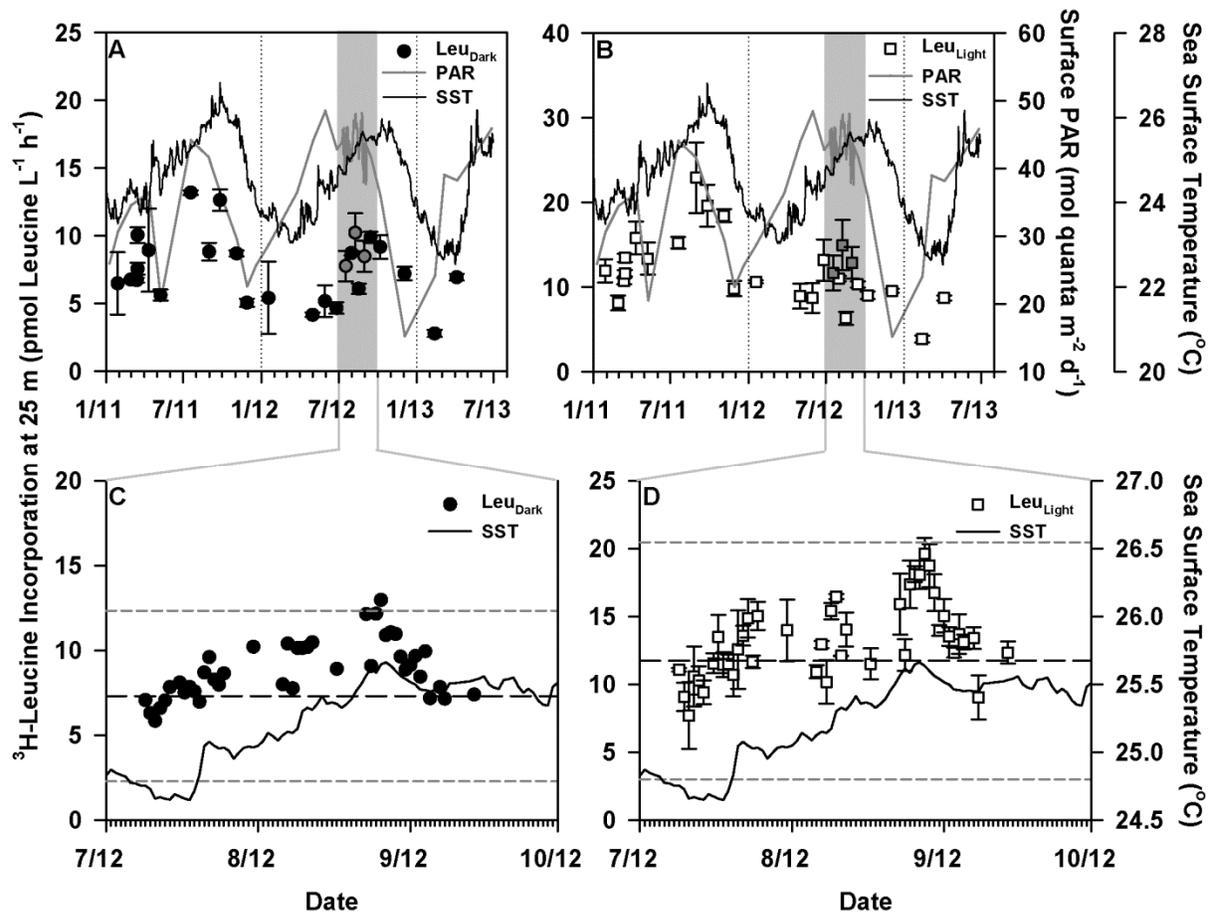


Figure 3.5. Time-series of rates of  $^3\text{H-Leu}_{\text{Dark}}$  (panel A),  $^3\text{H-Leu}_{\text{Light}}$  (panel B) measured at 25 m (error bars represent standard deviation of triplicate measurements). Black line represents sea surface temperature (SST) and grey line depicts incident PAR. Lower panels are daily-scale measurements of  $^3\text{H-Leu}_{\text{Dark}}$  (panel C) and  $^3\text{H-Leu}_{\text{Light}}$  (panel D) during the summer of 2012. Solid black line represents SST, dashed black line represents time-averaged rates at 25 m depth for the entire period of this study, and dashed grey lines represent upper and lower 95% confidence intervals.

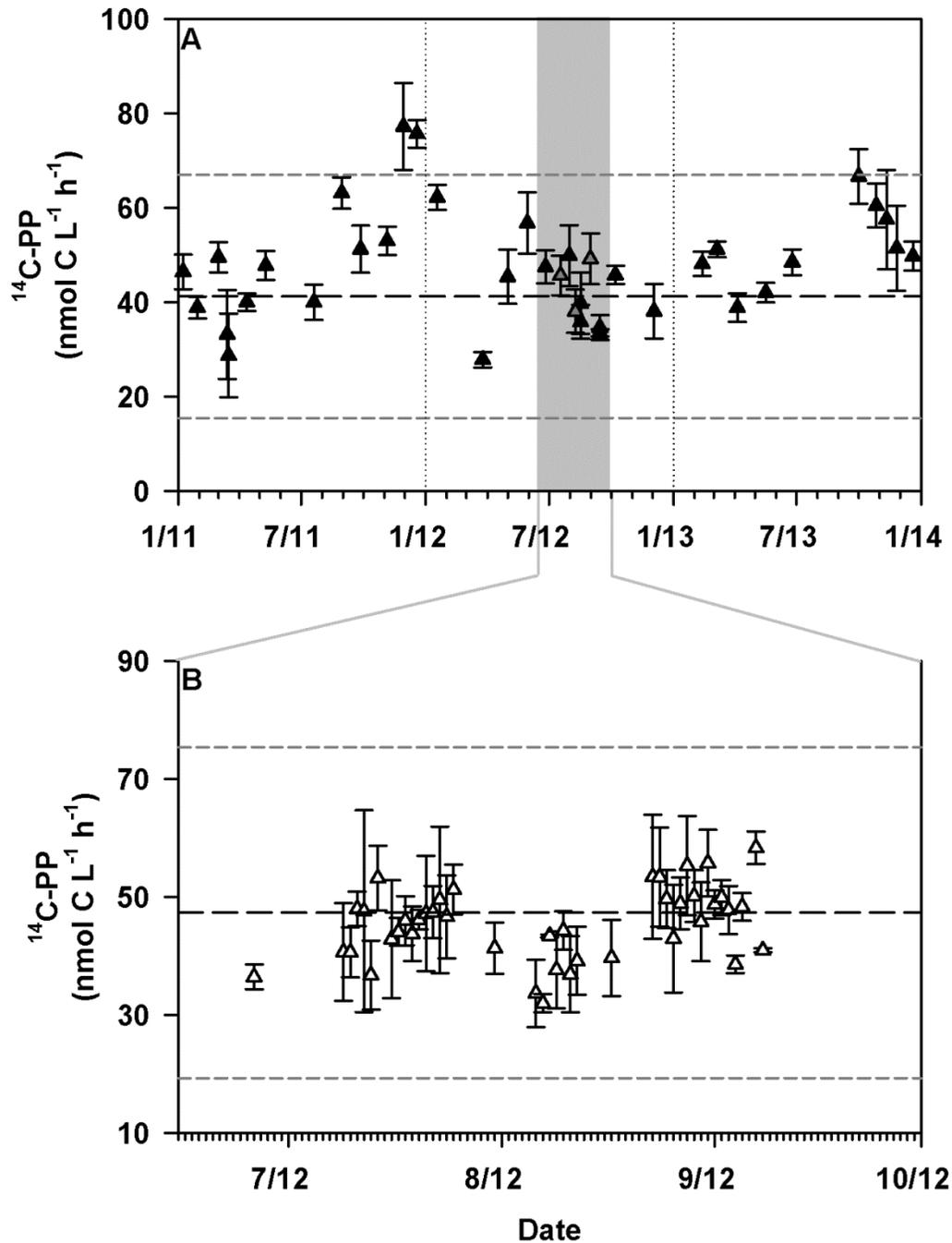


Figure 3.6. Time-series of  $^{14}\text{C-PP}$  measured at 25 m during this study (panel A); dashed black line depicts the mean time-averaged rate of  $^{14}\text{C-PP}$  measured by the HOT program for this depth; dashed grey lines represent 95% confidence intervals for these measurements. Also shown are rates of  $^{14}\text{C-PP}$  at 25 m measured during summer 2012 (panel B). The mean HOT program derived rate of  $^{14}\text{C-PP}$  (1988–2014) for July, August, and September is shown as a black dashed line, with the associated 95% confidence intervals shown as grey dashed lines.

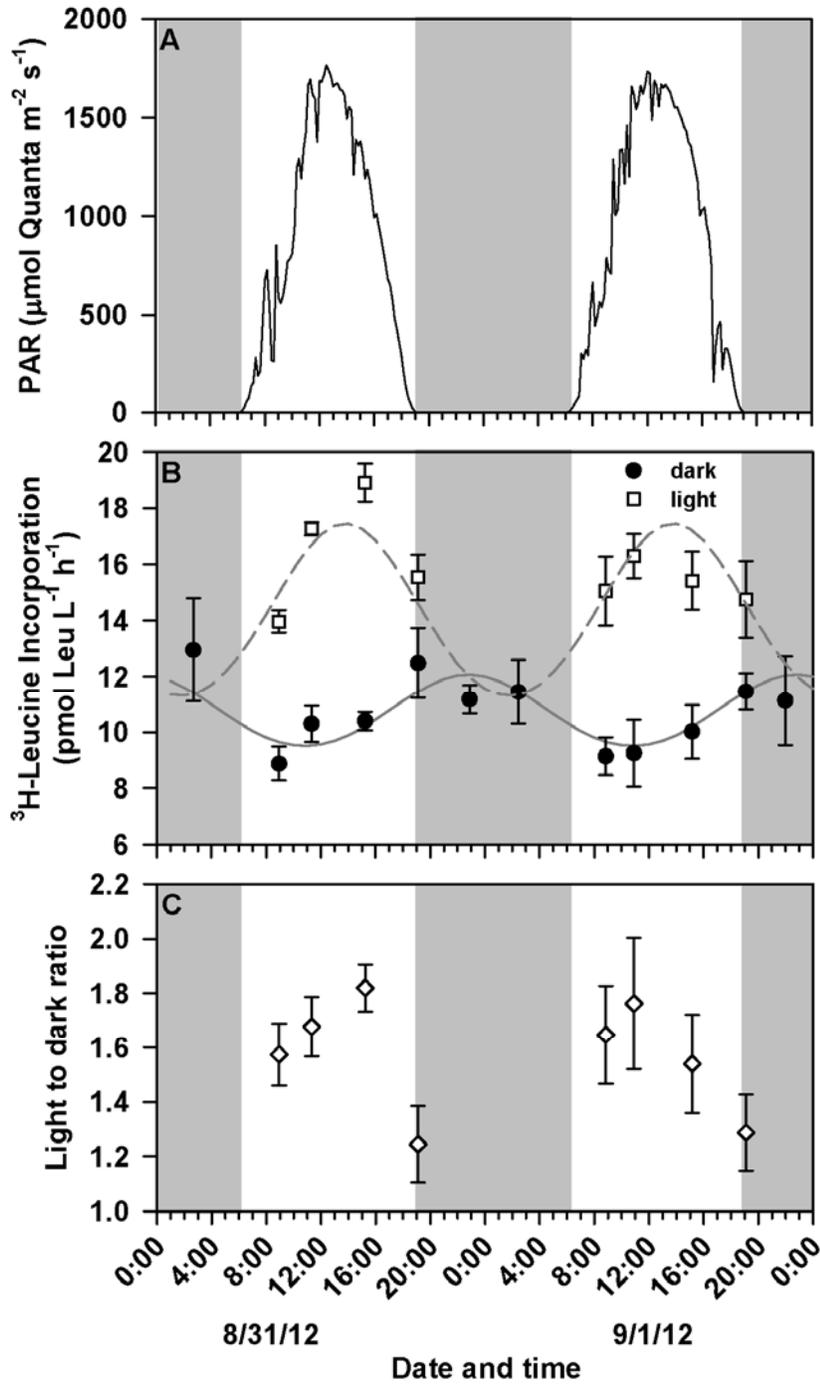


Figure 3.7. Diel variability in rates of  $^3\text{H}$ -Leu incorporation (both light and dark) measured at 25 m during the summer of 2012. Grey bars represent night periods. Daily variation in incident PAR (panel A),  $^3\text{H}$ -Leu<sub>Light</sub> and  $^3\text{H}$ -Leu<sub>Dark</sub> (panel B), and ratio of  $^3\text{H}$ -Leu<sub>Light</sub> :  $^3\text{H}$ -Leu<sub>Dark</sub> (panel C). Error bars represent standard deviations of triplicate measurements at each time point. Grey line depicts sinusoidal model fit ( $r^2 = 0.64$ ) from John et al. (2011).

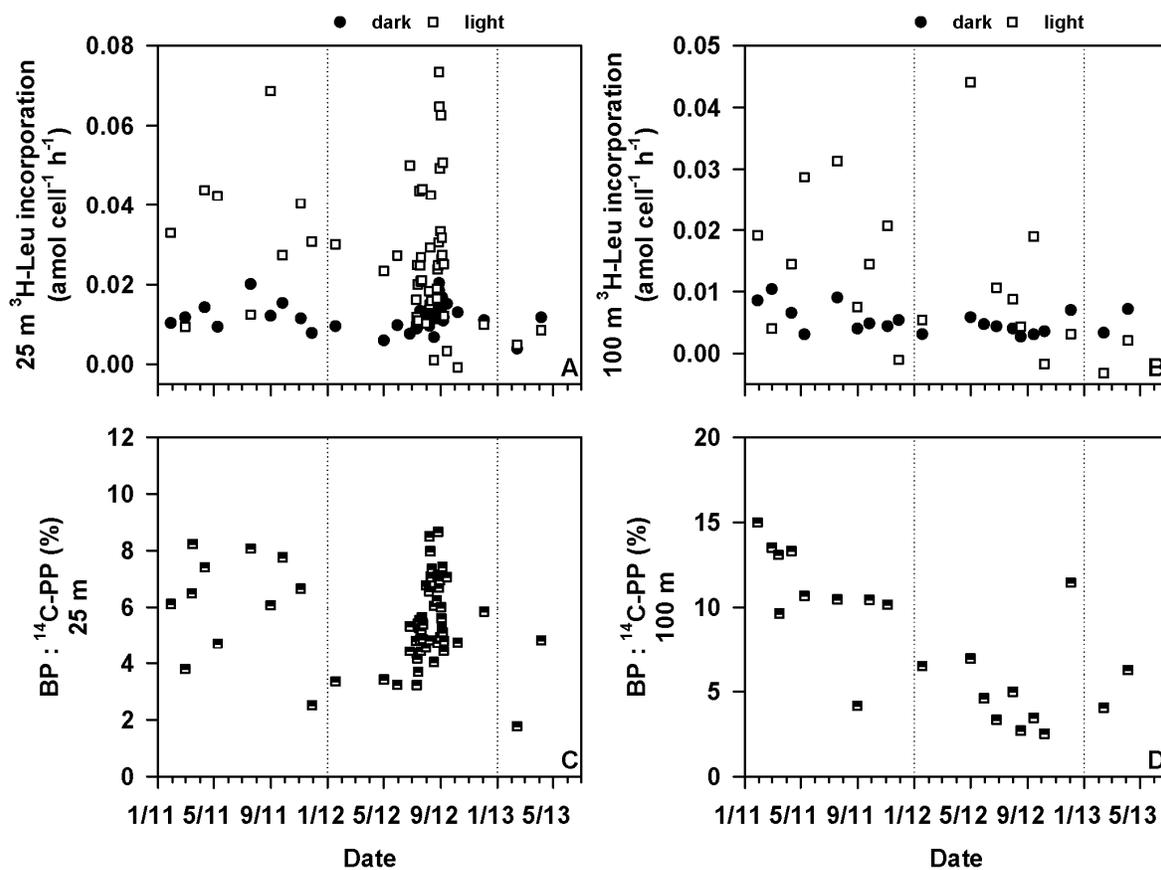


Figure 3.8. Time-series of cell specific rates of  $^3\text{H-Leu}_{\text{Dark}}$  and  $\Delta\text{Leu}$  incorporation at 25 m (panel A) and at 100 m (panel B). Also shown are the ratios of BP to PP at 25 m (panel C) and at 100 m (panel D).

## CHAPTER 4 - The influence of abrupt increases in seawater $p\text{CO}_2$ on rates of microbial production in the subtropical North Pacific Ocean

Donn A. Viviani, Daniela Böttjer, Matthew J. Church, additional coauthors likely

### Abstract

We examined short-term (24 to 96 hours) effects of abrupt increases in the partial pressure of carbon dioxide ( $p\text{CO}_2$ ) on rates of primary and bacterial production in the near-surface ocean waters at Station ALOHA in the North Pacific Subtropical Gyre (NPSG). In the majority of experiments (8 out of 10 in total) we observed no response in rates of primary production as measured by the assimilation of  $^{14}\text{C}$ -bicarbonate ( $^{14}\text{C}$ -PP) under elevated  $p\text{CO}_2$  (1100 ppm) compared to the ambient  $p\text{CO}_2$  (< 390 ppm) conditions. In 2 of the 10 experiments, rates of  $^{14}\text{C}$ -PP decreased significantly in the elevated  $p\text{CO}_2$  treatments relative to the ambient controls. Similarly, in the majority of experiments (6 of 7) where bacterial production was measured from the incorporation of  $^3\text{H}$ -leucine ( $^3\text{H}$ -Leu) into biomass, elevated  $p\text{CO}_2$  had no significant effect on rates of  $^3\text{H}$ -Leu incorporation. In one experiment, rates of  $^3\text{H}$ -Leu incorporation measured in the dark increased significantly in the elevated  $p\text{CO}_2$  treatments relative to the controls. We also examined possible short-term (~12 hour), depth-dependent responses in rates of  $^{14}\text{C}$ -PP and rates of  $^3\text{H}$ -Leu to abrupt increases in  $p\text{CO}_2$  (to 750 ppm). In 4 of the 5 depth-resolved perturbation experiments,  $^{14}\text{C}$ -PP rates demonstrated no consistently significant response to elevated  $p\text{CO}_2$ ; however, on one occasion (August 2010) rates of  $^{14}\text{C}$ -PP in the > 2  $\mu\text{m}$  plankton size fraction increased ~33% in the dimly-lit waters of the lower euphotic zone (75–125 m) in the elevated

$p\text{CO}_2$  treatments relative to the unperturbed controls. In 2 of 5 experiments rates of  $^3\text{H}$ -Leu incorporation in the dark (0–125 m) were slightly lower (~10% to ~15%) in the elevated  $p\text{CO}_2$  treatments than in the ambient controls. In contrast, rates of  $^3\text{H}$ -Leu incorporation measured in the light were slightly greater (10% to 30%) in the ambient controls compared to elevated  $p\text{CO}_2$  treatments in all 5 experiments. Overall we find that abrupt changes in  $p\text{CO}_2$  had little effect on rates of primary and bacterial production in this persistently oligotrophic ecosystem.

## Introduction

Human socioeconomic activities, specifically fossil fuel combustion, cement production, and changes in land use, have resulted in progressive increases in atmospheric and oceanic CO<sub>2</sub> inventories (IPCC 2014). The ocean is a globally important net sink for CO<sub>2</sub>, and as such, has absorbed a significant fraction of anthropogenic carbon (Sabine et al. 2004). Increases in atmospheric carbon dioxide have raised the *p*CO<sub>2</sub> in seawater, with concomitant decreases in seawater pH (Wolf-Gladrow et al. 1999, Zeebe et al. 2008, Doney et al. 2009, Dore et al. 2009), and progressive declines in the saturation state of calcite and aragonite (Orr et al. 2005, Doney et al. 2009).

Examinations into the effects of changes in seawater carbonate chemistry on productivity in the oligotrophic ocean ecosystems that dominate the Earth are relatively scarce. While an appropriate null hypothesis could be that ocean acidification may lead to no significant changes in marine microbial contributions to biogeochemical cycling (Joint et al. 2011), testing such a hypothesis will demand rigorous experimental evidence. Previous results and observations suggest that, either as individual species or microbial assemblages, marine microbial physiology may be affected by increases in *p*CO<sub>2</sub> (Riebesell et al. 2000, Tortell et al. 2002, 2008, Grossart et al. 2006, Fu et al. 2007, Hutchins et al. 2007, Beman et al. 2010, Liu et al. 2010), although the reported sign and magnitude of these effects has varied (Liu et al. 2010). An important question is whether these changes in microbial physiology are large enough to alter ocean biogeochemical cycles.

To date, there is relatively little known about the capacity for phytoplankton to adapt or acclimate to changes in the seawater carbonate system. Changes in seawater carbonate chemistry

are likely to have complex influences on ocean biology. Most contemporary lineages of phytoplankton evolved during periods in Earth's history when atmospheric and oceanic CO<sub>2</sub> inventories were considerably greater than observed today (Raven 1997, Tortell 2000). Indeed, for many organisms RUBISCO, the enzyme that catalyzes the initial steps of carbon fixation, is less than half saturated at present day *p*CO<sub>2</sub> (Giordano et al. 2005), as a consequence many algae, including cyanobacteria, have efficient mechanisms for concentrating CO<sub>2</sub> (Badger 2003). Experiments examining the effect of elevated *p*CO<sub>2</sub> on natural phytoplankton communities have shown enigmatic results; in several studies, rates of productivity have increased under elevated *p*CO<sub>2</sub> (Hein & Sand-Jensen 1997, Tortell et al. 2008, Liu et al. 2010), although in other cases, no significant changes in rates of productivity have been observed (Lomas et al. 2012, Böttjer et al. 2014). There is also compelling evidence that for some groups of phytoplankton, specifically calcifying microorganisms, declines in carbonate ion concentrations that accompany decreases in seawater pH can be detrimental to growth (Riebesell et al. 2000, Langer et al. 2006), although this appears quite species specific (Hendriks et al. 2010).

There have been a number of laboratory-based *p*CO<sub>2</sub> manipulation studies that have examined the response of specific organisms to changes in seawater carbonate chemistry, where growth conditions are controlled and organisms are generally examined in isolation. Fewer studies have looked at natural planktonic community scale dynamics, particularly in the oligotrophic open ocean, and as a result, potential changes in microbial growth due to changes in the seawater carbonate system have not been investigated in the context of the feedbacks and controls that normally exist in open ocean communities. Recent experiments conducted in coastal waters found that elevated *p*CO<sub>2</sub> shifted the partitioning of carbon fixed during primary production from the particulate to the dissolved phase (Kim et al. 2011) and increased bacterial

growth (Grossart et al. 2006). These intriguing results highlight the need to perform experimental manipulations examining the effects of increased  $p\text{CO}_2$  on plankton growth in the open ocean, where a major fraction of global productivity occurs.

It has also been suggested that increasing seawater  $p\text{CO}_2$  can affect heterotrophic bacterial growth, either directly via changes to metabolic rates, for example alteration of enzymatic activities (Yamada & Suzumura 2010, Piontek et al. 2010, Endres et al. 2014) or indirectly (*i.e.* changes in organic matter production or substrate lability; Grossart et al. 2006, Piontek et al. 2013). Even small changes in bacterial consumption rates of organic matter could have a large influence on carbon cycling. Likewise, the importance of the microbial loop to nutrient recycling and maintaining gross primary production in oligotrophic waters suggests that changes in rates of heterotrophic metabolism rates could alter the magnitude and pathways of carbon cycling.

In this study, we conducted abrupt perturbations to the seawater carbonate system to artificially alter seawater  $p\text{CO}_2$  to conditions projected for the surface ocean within the next 50 to 100 years (IPCC 2014). During these experiments, we examined how such abrupt changes in  $p\text{CO}_2$  influenced rates of primary and bacterial production in a series of short-term incubation experiments. We conducted experiments in the near-surface ocean (5 m) as well as depth-resolved experiments extending into the lower euphotic zone (as deep as 125 m). All of the experiments were conducted using open ocean waters of the North Pacific Subtropical Gyre (NPSG), one of the largest biomes on the planet, and hence an ecosystem that is a major contributor to global cycles of bioelements.

## Methods

### Experimental design

All seawater carbonate system manipulation experiments were performed on either HOT cruises to Station ALOHA (22° 45' N 158° W), the field site of the Hawaii Ocean Time-series (HOT) program, between June 2010 and September 2012 or during two process cruises conducted in the vicinity of Station ALOHA in August 2010 and March 2011. Sampling was conducted aboard the R/V *Ka'imikai-O-Kanaloa* and R/V *Kilo Moana*. For these experiments, seawater was collected before midnight using polyvinyl chloride sampling bottles attached to a conductivity-temperature-density (CTD) rosette. Two types of carbonate system manipulation experiments were performed. The first kind of experiments (hereafter “bubbling”) were performed as described in Böttjer et al. (2014). Briefly, near-surface ocean seawater was subsampled from CTD rosette bottles under minimal light into acid-washed 20 L polycarbonate carboys fitted with sterile caps with ports for introducing and venting gases. After filling, carboys were placed into shaded (~50% surface irradiance) surface seawater-cooled incubators. The targeted  $p\text{CO}_2$  was attained by gentle bubbling ( $<3 \text{ L min}^{-1}$ ) of each carboy with either air (controls, ~390 ppm  $p\text{CO}_2$ ) or a mixture of air and  $\text{CO}_2$  (treatments, ~750 or ~1100 ppm  $p\text{CO}_2$ ), for 6-8 hours. Mixing and delivery of air or air and  $\text{CO}_2$  was regulated by use of mass flow controllers. During the initial bubbling, subsamples were collected regularly for measurements of seawater pH (see below for methods), and using HOT program measurements of total alkalinity (TA), the pH measurements (total scale) were used to estimate seawater  $p\text{CO}_2$  using the seacarb package (Gattuso et al. 2015) in the R statistical environment (R Development Core Team 2008) and relying on default settings for the carbonate dissociation constants (Uppström 1974, Perez & Fraga 1987, Dickson 1990, Lueker et al. 2000). Once the target  $p\text{CO}_2$  was achieved, the rate of

bubbling was reduced to less than  $1.5 \text{ L min}^{-1}$  for the duration of the experiment. Subsequent sampling was conducted before dawn at each time point from the carboys for measurements of TA, dissolved inorganic carbon (DIC),  $^{14}\text{C}$ -based primary productivity ( $^{14}\text{C}$ -PP), and rates of  $^3\text{H}$ -leucine ( $^3\text{H}$ -Leu) incorporation (as a proxy for bacterial production).

Additional experiments were conducted to evaluate depth-dependent responses in  $^{14}\text{C}$ -PP and  $^3\text{H}$ -Leu to perturbation of the seawater carbonate system. For these experiments, the carbonate system was manipulated and samples were incubated *in situ* to simulate the vertical gradients in light and temperature representative of the depths from which samples were collected. Rates of  $^{14}\text{C}$ -PP and  $^3\text{H}$ -Leu were measured from samples incubated at either ambient or elevated ( $\sim 750$  ppm) seawater  $p\text{CO}_2$ . For these experiments, water was collected before dawn from six euphotic zone depths (5, 25, 45, 75, 100, and 125 m) and subsampled from the CTD rosette bottles under minimal light into acid-washed 20 L polycarbonate carboys. These carboys were either left untreated (controls) or amended with trace metal grade hydrochloric acid and sodium bicarbonate to increase  $p\text{CO}_2$  to  $\sim 750$  ppm (elevated  $p\text{CO}_2$  treatments) while minimizing potential changes to TA. Once the carboys had been amended, seawater from each depth was subsampled into triplicate acid-cleaned 500 ml polycarbonate bottles and acid-cleaned 40 ml polycarbonate centrifuge tubes for subsequent measurements of  $^{14}\text{C}$ -PP and  $^3\text{H}$ -Leu incorporation, respectively. These bottles and tubes were affixed to a free-drifting array and incubated *in situ* at the depths of sample collection for the duration of the photoperiod (dawn to dusk).

### **Total alkalinity, dissolved inorganic carbon, and pH**

Seawater samples for determination of carbon system components (TA, DIC, and pH) were collected and analyzed following HOT program protocols (Winn et al. 1998, Dore et al. 2009). DIC and TA samples were collected from carboys into precombusted, 300 ml borosilicate bottles. Care was taken to avoid introducing bubbles into the sample during filling, and bottles were allowed to overflow three times during filling. Once filled, each sample was immediately fixed with 100  $\mu$ l of a saturated solution of mercuric chloride ( $\text{HgCl}_2$ ); bottles were capped with a grease seal, and stored in the dark for later analysis. DIC measurements were determined coulometrically using a Versatile INstrument for the Determination of Total inorganic carbon and Titration Alkalinity 3S (VINDTA) system (Dickson et al. 2007). TA was determined using an automated, closed-cell potentiometric titration. The precision and accuracy of these measurements were validated by comparison to a certified seawater  $\text{CO}_2$  reference sample (Dickson et al. 2007), with accuracies of approximately 3  $\mu\text{mol L}^{-1}$  for TA and 1  $\mu\text{mol L}^{-1}$  for DIC. Seawater pH (measured at 25  $^\circ\text{C}$ ) was analyzed using spectrophotometric detection of m-cresol purple with a precision of 0.001 (Clayton & Byrne 1993, Dore et al. 2009).

### **Measurements of $^{14}\text{C}$ -primary production**

Measurements were taken at each sampling time point during the bubbling experiments for determination of rates of  $^{14}\text{C}$ -bicarbonate assimilation into plankton biomass ( $^{14}\text{C}$ -PP). At each pre-dawn sampling, water was subsampled from the carboys into acid cleaned 500 ml polycarbonate bottles, and each bottle was spiked with  $\sim 1.85$  MBq  $^{14}\text{C}$ -bicarbonate. The total radioactivity added to each sample bottle was determined post-incubation by subsampling 250  $\mu$ l aliquots of seawater into scintillation vials containing 500  $\mu$ l of  $\beta$ -phenylethylamine. Bottles were placed in shaded ( $\sim 50\%$  irradiance) surface seawater-cooled incubators for the duration of the photoperiod. After sunset, 100 ml from each sample bottle was filtered at low vacuum ( $< 50$

mm Hg) onto 25 mm diameter, 0.2  $\mu\text{m}$  porosity polycarbonate membrane filters. The filters were then stored frozen in 20 ml scintillation vials until analysis at the shore based laboratory. At the shore-based laboratory, filters were acidified by the addition of 1 ml of 2 N hydrochloric acid, and allowed to passively vent for at least 24 hours in a fume hood to remove all inorganic  $^{14}\text{C}$ . Ten milliliters of Ultima Gold LLT liquid scintillation cocktail was added to all vials (acidified filters as well as vials for determining total radioactivity) and resulting radioactivity was determined on a Perkin Elmer 2600 liquid scintillation counter.

Measurements of  $^{14}\text{C}$ -PP from the *in situ* array experiments were conducted similarly, except that the samples were incubated at the respective collection depths on a free-drifting array for the duration of the photoperiod, and the incubations were terminated via sequential size fractionated filtration onto 10  $\mu\text{m}$ , 2  $\mu\text{m}$ , and 0.2  $\mu\text{m}$  filters. Briefly, at the end of the photoperiod incubation, 400 ml from each sample bottle was initially vacuum filtered onto 25 mm diameter, 10  $\mu\text{m}$  pore size polycarbonate filters; these filtrates were then filtered onto 25 mm diameter, 2  $\mu\text{m}$  pore size polycarbonate filters; 100 ml of the  $<2$   $\mu\text{m}$  filtrate was then filtered onto 25 mm diameter, 0.2  $\mu\text{m}$  pore size polycarbonate filters. Filters were treated as previously described for subsequent determination of  $^{14}\text{C}$  activity.

### **$^3\text{H}$ -leucine incorporation measurements**

We measured  $^3\text{H}$ -Leu incorporation into plankton protein as a proxy measurement for bacterial production (Kirchman et al. 1985, Simon & Azam 1989). Rates of  $^3\text{H}$ -Leu incorporation were measured following incubations conducted in both the light ( $^3\text{H}$ -Leu<sub>Light</sub>) and in the dark (through use of black cloth bags;  $^3\text{H}$ -Leu<sub>Dark</sub>). From the bubbling experiments, polyethylene amber bottles (125 ml) were subsampled from each carboy in the pre-dawn hours;

six 1.5 ml aliquots were then subsampled from each bottle into 2 ml microcentrifuge tubes (Axygen) containing 20 nmol L<sup>-1</sup> <sup>3</sup>H-leucine (final concentration). In addition, 1.5 ml of seawater was subsampled into a 2 ml microcentrifuge tube containing 20 nmol L<sup>-1</sup> <sup>3</sup>H-leucine (final concentration) and 100 µl of 100% (w/v) trichloroacetic acid (TCA); these samples served as time zero “blanks”. Samples were incubated for 2 to 12 hours in the same surface seawater-cooled incubator described previously. To terminate incubations, 100 µl of 100% TCA was added to each microcentrifuge tube and tubes were frozen (-20 °C) for later processing.

For those experiments incubated *in situ* on the free-drifting array, water was subsampled from each of the control and *p*CO<sub>2</sub>-elevated carboys into 40 ml polycarbonate centrifuge tubes and each tube was inoculated with <sup>3</sup>H-leucine to a final concentration of 20 nmol L<sup>-1</sup>. Time zero blanks were immediately subsampled from each tube; for these samples, 1.5 ml of seawater was aliquoted into 2 ml microcentrifuge tubes containing 100 µl of 100% TCA. The 40 ml tubes were then affixed to the same free drifting array utilized for the <sup>14</sup>C-bicarbonate assimilation measurements and samples were incubated under ambient light and in the dark (by placing the tubes in a darkened cloth bag). The array was then deployed for the duration of the photoperiod. After sunset, the array was recovered, and triplicate 1.5 ml subsamples were removed from each of the polycarbonate tubes and aliquoted into 2 ml microcentrifuge tubes containing 100 µl of 100% TCA. The microcentrifuge tubes were frozen (-20 °C) for later processing.

In the shore-based laboratory, microcentrifuge tubes were processed following a modified version of the (Smith & Azam 1992) methodology. Briefly, tubes were thawed, vortexed, and spun for 15 minutes in a refrigerated microcentrifuge at ~23,900 g at 4°C. Supernatants were decanted, 1 ml ice-cold 5% TCA was added to each microcentrifuge tube, and the samples were spun for 5 minutes at ~23,900 g. Supernatants were decanted, and 1 ml of 80%

ethanol was added to each sample and the tubes were spun for an additional 5 minutes at ~23,900 g. Supernatants were decanted and samples were uncapped and left in a fume hood overnight to evaporate residual ethanol. The following day, 1 ml of Ultima Gold LLT scintillation cocktail was added to the dried sample pellet, the tubes were vortexed, placed into 7 ml polyethylene scintillation vials (to serve as carrier vials), and samples were counted on a liquid scintillation counter (Perkin-Elmer TriCarb 2910TR) to assess rates of  $^3\text{H}$  incorporation.

### **Statistics and data analysis**

Statistical analyses were performed using Matlab (Mathworks). Data that did not meet the assumptions of normality were  $\log_{10}$  transformed prior to subsequent analyses.

### **Results**

We conducted a total of 10 shipboard  $p\text{CO}_2$  manipulation experiments where seawater  $p\text{CO}_2$  was altered by bubbling with  $\text{CO}_2$ -air gas mixtures. We measured rates of  $^{14}\text{C}$ -PP in all 10 experiments, and in 8 of these experiments, rates of  $^3\text{H}$ -Leu were also measured. An additional 5 experiments were conducted to evaluate depth-dependent response in rates of  $^{14}\text{C}$ -PP and  $^3\text{H}$ -Leu incorporation to elevated  $p\text{CO}_2$ . For these depth-resolved experiments, seawater  $p\text{CO}_2$  was manipulated through the addition of acid (HCl), minimizing perturbations in TA through additions of bicarbonate. The experiments were conducted across a range of initial conditions, including experiments conducted in all four seasons (Table 4.1). Both bubbling and *in situ* array experiments (with two exceptions) took place on cruises to Station ALOHA between 2010 and 2012; two *in situ* array experiments (August 26, 2015 and August 28, 2015) were initiated at sampling sites to the northwest of Station ALOHA (termed S1,  $24^\circ 45' \text{ N } 160^\circ 45' \text{ W}$  and S2,

25° 35' N 160° 32' W) where concentrations of chlorophyll *a* in the near-surface waters were elevated relative to Station ALOHA (Table 4.1, Figure 4.1).

Seawater for the bubbling experiments was collected from the near-surface ocean (5 m); for all experiments, concentrations of nitrate+nitrite (N+N) and soluble reactive phosphorus (SRP) were consistently below 10 nmol L<sup>-1</sup> and 150 nmol L<sup>-1</sup>, respectively, consistent with HOT program measurements of these nutrients. Rates of particulate <sup>14</sup>C-PP at the beginning of the experiments ranged between 0.17 to 0.93 μmol C L<sup>-1</sup> d<sup>-1</sup>, with the higher rates measured at those stations to the northwest of ALOHA where chlorophyll concentrations were elevated. Seawater *p*CO<sub>2</sub> in the near-surface waters when experiments were conducted ranged between 351 μatm to 418 μatm, consistent with HOT program observations at Station ALOHA (Dore et al. 2009, Böttjer et al. 2014), while sea surface temperatures ranged between ~23 and 27 °C (Figure 4.2).

Samples for DIC and TA were collected from each carboy to evaluate the stability of the carbonate system during bubbling. On average, TA varied less than 0.5% relative to the initial values (Figure 4.3), while DIC varied less than 0.6% relative to the beginning of the experiments. As a result, the derived *p*CO<sub>2</sub> of the treatment carboys remained within 7% of the targeted *p*CO<sub>2</sub> (1100 uatm) throughout the bubbling period (Figure 4.3), with the *p*CO<sub>2</sub> of the controls (<390 μatm) varying <7% (on average).

### **The response in rates of <sup>14</sup>C-PP and <sup>3</sup>H-Leu to elevated seawater *p*CO<sub>2</sub>**

In the majority of experiments (8 of 10 bubbling experiments) rates of <sup>14</sup>C-PP in the elevated *p*CO<sub>2</sub> treatments were not significantly different than the controls (two-way ANOVA; *p*>0.05; where *p*CO<sub>2</sub> and time were tested as factors controlling rates of <sup>14</sup>C-PP; Table 4.2). In 2 of the bubbling experiments (April 2011 and September 2012), rates of <sup>14</sup>C-PP in the controls

were significantly greater than rates measured in the enhanced  $p\text{CO}_2$  treatments (two-way ANOVA,  $p < 0.05$ ; where  $p\text{CO}_2$  and time were tested as factors controlling rates of  $^{14}\text{C}$ -PP). There were no significant interactions between  $p\text{CO}_2$  and time for any of the experiments (two-way ANOVA;  $p > 0.05$ ; where  $p\text{CO}_2$  and time were tested as factors controlling rates of  $^{14}\text{C}$ -PP). The median value of the percent differences between treatment and control ( $((\text{treatment} - \text{control}) / \text{control})$ ) across all time points was -6% (ranging between -70% and 123%; Figure 4.4), with the treatments differing from the controls during 20% of the sampling occasions.

We also examined possible responses in rates of  $^3\text{H}$ -Leu incorporation during the seawater carbonate system manipulation experiments (Table 4.2). In total, rates of  $^3\text{H}$ -Leu<sub>Dark</sub> were determined in 7 of the bubbling experiments (Table 4.2). Rates of  $^3\text{H}$ -Leu<sub>Dark</sub> were measured in all 7 of these experiments, with coincident measurements of  $^3\text{H}$ -Leu<sub>Light</sub> in 6 of the 7 experiments. Initial (i.e. at the first time point of the experiment) rates of  $^3\text{H}$ -Leu<sub>Dark</sub> in control samples ranged from 8 to 54 pmol Leu L<sup>-1</sup> h<sup>-1</sup>, with elevated rates measured in January 2011, March 2011, and September 2012, and the lowest rates measured in experiments conducted in 2010. Rates of  $^3\text{H}$ -Leu<sub>Dark</sub> at subsequent time points in the controls ranged between 6 and 67 pmol Leu L<sup>-1</sup> h<sup>-1</sup>. In the enhanced  $p\text{CO}_2$  treatments, rates of  $^3\text{H}$ -Leu<sub>Dark</sub> were similar to the controls, with initial rates ranging between 7 and 41 pmol Leu L<sup>-1</sup> h<sup>-1</sup>, and measurements at subsequent time points ranging from 4 to 98 pmol Leu L<sup>-1</sup> h<sup>-1</sup>. Rates of  $^3\text{H}$ -Leu<sub>Light</sub> in the controls ranged between 9 and 61 pmol Leu L<sup>-1</sup> h<sup>-1</sup> at the beginning of the experiments, and between 21 to 84 pmol Leu L<sup>-1</sup> h<sup>-1</sup> at subsequent time points. In the enhanced  $p\text{CO}_2$  treatments, initial rates of  $^3\text{H}$ -Leu<sub>Light</sub> ranged from 15 to 65 pmol Leu L<sup>-1</sup> h<sup>-1</sup>, and from 17 to 99 pmol Leu L<sup>-1</sup> h<sup>-1</sup> at subsequent time points. In 5 out of the 7 experiments where rates were measured,  $^3\text{H}$ -Leu<sub>Dark</sub> rates increased significantly over time in both the controls and treatments (two-way ANOVA,

$p < 0.05$ ;  $p\text{CO}_2$  and time tested as factors influencing rates of  $^3\text{H}\text{-Leu}_{\text{Dark}}$ ; Table 4.2). Similarly, in 4 of the 6 experiments in which  $^3\text{H}\text{-Leu}_{\text{Light}}$  was measured, rates increased significantly over the duration of the experiment in both the controls and treatments (two-way ANOVA,  $p < 0.05$ ;  $p\text{CO}_2$  and time were tested as factors controlling  $^3\text{H}\text{-Leu}_{\text{Light}}$ ). However, in the majority of experiments (6 out of 7 and all 6 for  $^3\text{H}\text{-Leu}_{\text{Dark}}$  and  $^3\text{H}\text{-Leu}_{\text{Light}}$ , respectively), there were no significant differences in the enhanced  $p\text{CO}_2$  treatments relative to the controls (two-way ANOVA,  $p > 0.05$ ;  $p\text{CO}_2$  and time were tested as factors controlling  $^3\text{H}\text{-Leu}$  incorporation; Table 4.2; Figure 4.4). There were also no significant interactions between  $p\text{CO}_2$  and time for any of the experiments (two-way ANOVA;  $p > 0.05$ ; where  $p\text{CO}_2$  and time were tested as factors controlling rates of  $^{14}\text{C}\text{-PP}$ ). In one experiment (August 2010) rates of  $^3\text{H}\text{-Leu}_{\text{Dark}}$  in the  $p\text{CO}_2$  treatment (in the 750 ppm treatment) were significantly greater than the controls (two-way ANOVA,  $p < 0.05$ ;  $p\text{CO}_2$  and time were tested as factors controlling  $^3\text{H}\text{-Leu}_{\text{Dark}}$ ; Table 4.2). The median values of the percent differences ( $[\text{CO}_2 \text{ treatment} - \text{ambient control}]/\text{control}$ ) in rates of  $^3\text{H}\text{-Leu}_{\text{Dark}}$  and  $^3\text{H}\text{-Leu}_{\text{Light}}$  across all time points were 3% and -1%, respectively (Figure 4.4). The resulting percent differences were significantly different in less than 20% of experimental time points (14% and 17% for  $^3\text{H}\text{-Leu}_{\text{Dark}}$  and  $^3\text{H}\text{-Leu}_{\text{Light}}$ , respectively).

### **Depth-dependent responses in $^{14}\text{C}\text{-PP}$ and $^3\text{H}\text{-Leu}$ to carbonate perturbations**

In addition to conducting  $p\text{CO}_2$  perturbation experiments where near-surface ocean water was bubbled continuously for 24–96 hours, we also conducted 5 experiments where we examined short-term (~12 hours) depth-dependent responses in rates of  $^{14}\text{C}\text{-PP}$  and  $^3\text{H}\text{-Leu}$  to perturbations in seawater  $p\text{CO}_2$ . For these experiments, seawater from 6 discrete depths in the upper ocean was perturbed through the addition of acid (and bicarbonate, to maintain constant alkalinity) and incubated *in situ* from dawn to dusk on a free-drifting array. Three of the five

experiments (August 21, 2010; March 14 and 16, 2011) took place at or in the close vicinity of Station ALOHA, with the remaining 2 experiments conducted in waters northwest of ALOHA where concentrations of chlorophyll *a* were greater than observed at Station ALOHA (Figure 4.1). For these experiments, the target seawater  $p\text{CO}_2$  for the treatments was 750 ppm. For samples in the upper euphotic zone (<45 m), the  $p\text{CO}_2$  derived from measurements of DIC and TA was within ~20% of the target  $p\text{CO}_2$ , while in the lower euphotic zone (>75 m) the derived  $p\text{CO}_2$  values were uniformly greater (by 2–52%) than the target  $p\text{CO}_2$  (Figure 4.5), largely because of depth-dependent increases in  $p\text{CO}_2$ .

Rates of  $^{14}\text{C}$ -PP were size fractionated (>10  $\mu\text{m}$ , 2 to 10  $\mu\text{m}$ , and 0.2 to 2  $\mu\text{m}$ ) from all six depths from both the controls and  $p\text{CO}_2$ -perturbed treatments (Table 4.3; Figure 4.6). Overall, rates of  $^{14}\text{C}$ -PP in all of the size fractions were greatest at the two stations (S1 and S2) sampled in August 2010 where chlorophyll *a* concentrations in the near-surface waters were elevated relative to Station ALOHA. Rates of  $^{14}\text{C}$ -PP in the >10  $\mu\text{m}$  size fraction at these two stations ranged from 0.04 to 0.54  $\mu\text{mol C L}^{-1} \text{d}^{-1}$ , approximately an order of magnitude greater than rates observed at ALOHA (Figure 4.6), however there were few significant differences in rates between the controls and the  $p\text{CO}_2$  perturbed treatments (Figure 4.7). In 1 of 5 experiments,  $^{14}\text{C}$ -PP rates in the  $p\text{CO}_2$ -elevated treatments were greater than in the controls for both the 10  $\mu\text{m}$  and 2  $\mu\text{m}$  size fractions at 25 m in the August Station ALOHA array, (t-Test;  $p < 0.005$  and  $p < 0.05$ , respectively). In contrast, in three experiments, at least one depth,  $^{14}\text{C}$ -PP rates in the controls that were greater than the  $p\text{CO}_2$ -elevated treatments (100m at ALOHA in August, 45 and 75 m at S2 for the 0.2  $\mu\text{m}$  size fraction, as well as 5 m at S1 for the 10  $\mu\text{m}$  size fraction; t-Test;  $p < 0.05$ ). The resulting depth-integrated (0–45 m) rates of  $^{14}\text{C}$ -PP in the >10  $\mu\text{m}$  size fraction ranged between 0.9 and 17.7  $\text{mmol C m}^{-2} \text{d}^{-1}$ , with average rates at S1 and S2 ~11-fold

greater than at ALOHA (Table 4.3). Similarly, rates measured at S1 and S2 were elevated in the 2  $\mu\text{m}$  and 0.2  $\mu\text{m}$  size fractions, with depth-integrated (0–45 m) rates at these stations ranging from 3.1 to 6.8 and 8.8 to 13.2  $\text{mmol C m}^{-2} \text{d}^{-1}$ , respectively (Table 4.3) compared to 1.6 to 3.2  $\text{mmol C m}^{-2} \text{d}^{-1}$  and 3.8 to 6.0  $\text{mmol C m}^{-2} \text{d}^{-1}$ , respectively at Station ALOHA. There was no consistent difference between control and  $p\text{CO}_2$ -elevated depth-integrated rates of  $^{14}\text{C}$ -PP in the upper euphotic zone (0–45 m; Table 3; t-Test;  $p>0.05$ ). In the lower euphotic zone (75–125 m), rates of  $^{14}\text{C}$ -PP in the two larger size fractions at Station ALOHA were 2- to 5- fold lower than the upper euphotic zone, with rates in the 0.2  $\mu\text{m}$  size fraction in the lower euphotic zone as much as 2.5-fold lower than the upper ocean (Table 4.3). In 4 of the 5 depth-resolved experiments, there were no consistent differences in rates of  $^{14}\text{C}$ -PP between control and  $p\text{CO}_2$  elevated treatments in the lower euphotic zone. In one of the experiments (August 2010) conducted at Station ALOHA, rates of  $^{14}\text{C}$ -PP in the lower euphotic zone (75–125 m) were significantly greater in the  $>10 \mu\text{m}$  and 2-10  $\mu\text{m}$  size fractions in the  $p\text{CO}_2$  perturbed treatments relative to the controls (t-Test;  $p>0.05$ ; Table 4.3).

Similar to rates of  $^{14}\text{C}$ -PP, in the upper euphotic zone (0–45 m)  $^3\text{H}$ -Leu<sub>Dark</sub> and  $^3\text{H}$ -Leu<sub>Light</sub> incorporation rates were greater at the two stations (S1 and S2) sampled in the chlorophyll *a* enriched waters (one-way ANOVA, respectively;  $p<0.001$  for both; Figure 8). The resulting depth-integrated euphotic zone (0–125 m) rates of  $^3\text{H}$ -Leu<sub>Dark</sub> were significantly greater in controls than in enhanced  $p\text{CO}_2$  treatments in 2 of the 5 depth-resolved experiments (t-Test;  $p<0.05$ ; Table 4.4). Euphotic zone (0–125 m) rates of  $^3\text{H}$ -Leu<sub>Light</sub> were significantly greater in controls than enhanced  $p\text{CO}_2$  treatments in all 5 of these depth-resolved experiments (t-Test;  $p<0.05$ ; Table 4.4). In the upper euphotic zone (0–45 m), rates of  $^3\text{H}$ -Leu<sub>Dark</sub> and  $^3\text{H}$ -Leu<sub>Light</sub> were significantly lower in the  $p\text{CO}_2$  treatments than in the controls in 2 of 5, and 4 of 5

experiments, respectively (t-Test;  $p < 0.05$ ; Table 4.4). In 4 of the 5 experiments, rates of  $^3\text{H}$ -Leu<sub>Light</sub> in the lower euphotic zone (75–125 m) were lower in the  $p\text{CO}_2$  treatments than the controls (t-Test;  $p < 0.05$ ; Table 4.4).

## Discussion

The objective of this study was to examine whether abrupt changes to the ocean carbonate system would influence short-term primary production and bacterial growth among contemporary microbial communities in the NPSG. Our goal was to examine the sensitivity of contemporary microbial communities to changes in the seawater carbonate system. The experiments conducted as part of this study were not designed to examine adaptations to progressive changes in  $p\text{CO}_2$  at the gene, species, or community level. Rather, through abrupt alteration of the seawater carbonate system, we sought to examine short-term impacts of elevated  $p\text{CO}_2$  on contemporary rates of production in the persistently oligotrophic waters of the NPSG. Two types of experiments were conducted: 1) Manipulation of the near-surface (5 m) seawater carbonate system by gentle bubbling with air or a mixture of air and  $\text{CO}_2$  and subsequent daily measurements of  $^{14}\text{C}$ -PP and  $^3\text{H}$ -Leu incorporation over 24 to 96 hour incubation periods; and 2) Perturbation of the seawater carbonate system through the addition of acid (and bicarbonate to keep TA unchanged) at different depths and examining the subsequent responses in rates of  $^{14}\text{C}$ -PP and  $^3\text{H}$ -Leu during *in situ* incubations lasting over the course of a photoperiod (~12 hours).

In the majority of the bubbling experiments (8 out of 10), we detected no significant changes in rates of  $^{14}\text{C}$ -PP in response to elevated  $p\text{CO}_2$ . In 2 of the 10 experiments, rates of  $^{14}\text{C}$ -PP were significantly lower in elevated  $p\text{CO}_2$  treatments relative to the controls across the full

experiment. We also sought to examine the effect of elevated  $p\text{CO}_2$  on bacterial production of biomass through measurements of  $^3\text{H}$ -Leu incorporation into protein (Kirchman et al. 1985). We observed no consistent effect of enhanced  $p\text{CO}_2$  on rates of  $^3\text{H}$ -Leu<sub>Light</sub>; likewise in most of experiments (6 out of 7) there was no significant effect of enhanced  $p\text{CO}_2$  on rates of  $^3\text{H}$ -Leu<sub>Dark</sub>. During one experiment (at 750 ppm) however, rates of  $^3\text{H}$ -Leu<sub>Dark</sub> were significantly greater in the  $p\text{CO}_2$  enhanced treatments relative to the controls, over the full experiment. There were individual time points during experiments where the percent difference in rates of  $^{14}\text{C}$ -PP,  $^3\text{H}$ -Leu<sub>Dark</sub>, and  $^3\text{H}$ -Leu<sub>Dark</sub> between control and enhanced  $p\text{CO}_2$  treatments were significantly different from 0, but in general there was no consistent pattern in the response. The overall lack of a consistent effect of enhanced  $p\text{CO}_2$  on either  $^{14}\text{C}$ -PP or  $^3\text{H}$ -Leu incorporation suggests that the contemporary microbial assemblages in this region of the NPSG appear relatively resilient to rapid increases in seawater  $p\text{CO}_2$ . Our observations that  $^{14}\text{C}$ -PP appeared generally invariant to increases in  $p\text{CO}_2$  are consistent with results from other studies conducted in oligotrophic ocean ecosystems (Lomas et al. 2012, Böttjer et al. 2014). Several studies have reported small to moderate increases in rates of  $^{14}\text{C}$ -PP (Riebesell et al. 2000, Egge et al. 2009) and bacterial biomass production (Endres et al. 2014) under elevated  $p\text{CO}_2$  in experiments conducted in relatively eutrophic coastal marine systems. In general we observed no measurable response in rates of  $^{14}\text{C}$ -PP to enhanced  $p\text{CO}_2$  in surface waters of the NPSG, and on the relatively rare instances that measurable responses occurred, the elevated  $p\text{CO}_2$  treatments decreased rates of  $^{14}\text{C}$ -PP.

In contrast to the bubbling experiments conducted in the near-surface waters, results from one of the depth-resolved experiments suggested that rates of  $^{14}\text{C}$ -PP by larger phytoplankton (>2  $\mu\text{m}$ ), growing in the lower euphotic zone, may at times be sensitive to changes in  $p\text{CO}_2$ . In

particular, rates of  $^{14}\text{C}$ -PP in the  $>10\ \mu\text{m}$  and  $2\text{--}10\ \mu\text{m}$  size fractions were significantly greater in the  $p\text{CO}_2$  treatments relative to the controls in the experiment conducted in August at Station ALOHA. These dimly-lit waters and larger phytoplankton size classes account for a relatively small fraction of the euphotic zone productivity in the NPSG (Li et al. 2011), so the resulting stimulation by  $p\text{CO}_2$  resulted in no significant change to euphotic zone (0–125 m) production in this experiment. The relatively small ( $\sim 20$  and  $\sim 50\%$ , for  $2\ \mu\text{m}$  and  $10\ \mu\text{m}$ , respectively) magnitude of the difference between control and perturbed rates requires caution in interpreting these results; however, the apparent stimulation of productivity among larger phytoplankton in the lower euphotic zone has potentially interesting ecological implications. Larger phytoplankton growing near the nitracline may contribute disproportionately to new production (Goldman & McGillicuddy 2003). The mechanism resulting in apparent stimulation of  $^{14}\text{C}$ -PP in the lower euphotic zone by  $p\text{CO}_2$  remains unknown; however, such observations may reflect carbon limitation of the Calvin cycle in the lower euphotic zone during summer months. Net production of oxygen in the sub-mixed layer waters results in accumulation of dissolved oxygen throughout the spring to early fall in the NPSG (Shulenberger & Reid 1981, Riser & Johnson 2008). In August 2010, dissolved oxygen at Station ALOHA was often supersaturated (percent oxygen saturation ranged 99–102%) between 50 and 110 m. Additionally, downwelling irradiances at 75 m for those wavelengths at which the relative absorption coefficient of chlorophyll *a* is greatest, were higher in August than in July. We speculate that the enhanced rates of  $^{14}\text{C}$ -PP in the presence of elevated  $p\text{CO}_2$  during this single experiment may be a consequence of elevated  $\text{O}_2:\text{CO}_2$  ratios in the water column. This could cause increased competitive binding of oxygen by RUBISCO, resulting in carbon limitation or increased photorespiration by these larger phytoplankton (Badger et al. 1998, Giordano et al. 2005). This explanation is strengthened by

observations that during the March sampling period, dissolved oxygen concentrations were below saturation (percent oxygen saturation ranged 93–97%) in the lower euphotic zone, and no enhancement of  $^{14}\text{C}$ -PP in the lower euphotic zone was observed during this time. In a mesocosm study conducted in coastal waters off Norway, Newbold et al. (2012) found that photosynthetic growth of smaller picoeukaryotes increased rapidly under conditions of elevated  $p\text{CO}_2$ ; at Station ALOHA, abundances of photosynthetic pico- and nanoeukaryotes are often maximal in the lower euphotic zone (Corno et al. 2007). The lack of a consistent response in  $^{14}\text{C}$ -PP rates to elevated  $p\text{CO}_2$  seawater across the other 4 experiments supports our results from the longer-term bubbling experiments, suggesting that these microbial assemblages are relatively resilient to rapid changes in the seawater carbonate system, even under conditions sufficient to produce elevated concentrations of chlorophyll *a*.

We also sought to examine the sensitivity of bacterial production to abrupt increases in seawater  $p\text{CO}_2$  during our depth-resolved experiments. While we observed no consistent response in rates of  $^3\text{H}$ -Leu<sub>Light</sub> or  $^3\text{H}$ -Leu<sub>Dark</sub> to the  $p\text{CO}_2$  treatments during the bubbling experiments, rates of  $^3\text{H}$ -Leu in our depth-resolved experiments frequently demonstrated differences between the controls and  $p\text{CO}_2$  treatments. In all five of the depth-resolved experiments, euphotic zone (0–125 m) rates of  $^3\text{H}$ -Leu<sub>Light</sub> were always lower in the enhanced  $p\text{CO}_2$  treatments than in control samples. In contrast, rates of  $^3\text{H}$ -Leu<sub>Dark</sub> did not vary in a consistent manner, with rates of  $^3\text{H}$ -Leu<sub>Dark</sub> greater in the control than the  $p\text{CO}_2$  treatments in one of five experiments. Several previous studies have reported increased rates of  $^3\text{H}$ -Leu<sub>Dark</sub> under elevated  $p\text{CO}_2$  (Grossart et al. 2006), suggesting a shift in the partitioning of primary production from the particulate to the dissolved pool (Engel 2002, Yoshimura et al. 2010, Kim et al. 2011), with subsequent increased growth by heterotrophic bacteria on this newly available DOM (Engel

et al. 2013, Endres et al. 2014). However, other studies that have specifically measured rates of dissolved organic carbon production under elevated  $p\text{CO}_2$  have reported inconsistent responses (MacGilchrist et al. 2014, Zark et al. 2015). In our experiments, based on both bubbling and depth-resolved experiments, rates of  $^3\text{H}\text{-Leu}_{\text{Dark}}$  was most often unchanged under conditions of elevated  $p\text{CO}_2$ . Similarly, in the near-surface waters (bubbling experiments) rates of  $^3\text{H}\text{-Leu}_{\text{Light}}$  were unaffected by increases in  $p\text{CO}_2$ , but in the deeper regions of the euphotic zone, rates of  $^3\text{H}\text{-Leu}_{\text{Light}}$  were often depressed under elevated  $p\text{CO}_2$  relative to the controls.

We incubated samples in both the light and dark to evaluate how elevated  $p\text{CO}_2$  might alter the known photostimulation of  $^3\text{H}\text{-Leu}$  previously reported in the euphotic zone of the NPSG (Church et al. 2004, 2006). In the present study rates of  $^3\text{H}\text{-Leu}_{\text{Light}}$  were up to  $\sim 2.5$ -fold greater than rates of  $^3\text{H}\text{-Leu}_{\text{Dark}}$  within the upper euphotic zone, consistent with these previous reports. Based on flow cytometric sorting of picoplankton populations, Björkman et al. (2015) determined that incorporation of  $^3\text{H}\text{-Leu}$  by *Prochlorococcus* in the light was a major factor controlling photostimulation. Given the large contribution of *Prochlorococcus* to rates of  $^{14}\text{C}\text{-PP}$  and  $^3\text{H}\text{-Leu}$  incorporation at Station ALOHA (Liu et al. 1997, Björkman et al. 2015), our results suggest *Prochlorococcus* growth may be relatively insensitive to, or perhaps negatively affected by, abrupt increases in  $p\text{CO}_2$ . These results are consistent with previous findings in culture that suggest that while *Synechococcus* growth responds positively to elevated  $p\text{CO}_2$ , *Prochlorococcus* growth appears largely insensitive to variations in  $p\text{CO}_2$  (Fu et al. 2007).

In general we found that abrupt increases in  $p\text{CO}_2$  have little or no influence on primary and bacterial productivity at Station ALOHA. On a single occasion, we did observe apparent stimulation of  $^{14}\text{C}\text{-PP}$  by larger phytoplankton dwelling in the lower euphotic zone, an observation we hypothesize may reflect seasonally-dependent carbon limitation or

photorespiration. However, the majority of our experiments suggest that contemporary microbial growth in the euphotic zone at Station ALOHA is relatively resilient to abrupt increases in  $p\text{CO}_2$ . Such results are somewhat surprising given the low temporal fluctuations in seawater  $p\text{CO}_2$  this habitat experiences; however, we suspect that in this persistently oligotrophic environment, both primary and bacterial production are strongly controlled by the availability of growth-limiting nutrients. As such, even large perturbations to the carbonate system have only weak influence on microbial growth. Hence, based on our observations together with those from previous reports, the response of marine microbial planktonic metabolic rates to elevated  $p\text{CO}_2$  displays considerable variability and likely depend on the types of organisms present and the conditions under which they grow (e.g. Krause et al. 2012, MacGilchrist et al. 2014, Richier et al. 2014). Our results suggest that contemporary microbial production in the NPSG is relatively insensitive to abrupt, short-term changes in  $p\text{CO}_2$ . Whether this reflects physiological flexibility by the resident microbial community in acclimating to changes in the carbonate system, or suggests that growth of these organisms is so tightly regulated by resource supply and any influence due to variations in the carbonate system are obscured by these other controlling factors remains unknown.

## Literature cited

- Badger M (2003) The roles of carbonic anhydrases in photosynthetic CO<sub>2</sub> concentrating mechanisms. *Photosynth Res* 77:83–94
- Badger M, Andrews T, Whitney S, Ludwig M, Yellowlees D, Leggat W, Price G (1998) The diversity and coevolution of Rubisco, plastids, pyrenoids, and chloroplast-based CO<sub>2</sub>-concentrating mechanisms in algae. *Can J Bot* 76:1052–1071
- Beman JM, Chow C-E, King AL, Feng Y, Fuhrman JA, Andersson A, Bates NR, Popp BN, Hutchins DA (2010) Global declines in oceanic nitrification rates as a consequence of ocean acidification. *Proc Natl Acad Sci USA* 108:208–213
- Björkman KM, Church MJ, Doggett JK, Karl DM (2015) Differential assimilation of inorganic carbon and leucine by *Prochlorococcus* in the oligotrophic North Pacific Subtropical Gyre. *Front Microbiol* 6:1401
- Böttjer D, Karl DM, Letelier RM, Viviani DA, Church MJ (2014) Experimental assessment of diazotroph responses to elevated seawater pCO<sub>2</sub> in the North Pacific Subtropical Gyre. *Global Biogeochem Cycles* 28:2013GB004690
- Church M, Ducklow H, Karl D (2004) Light dependence of [<sup>3</sup>H]leucine incorporation in the oligotrophic North Pacific ocean. *Appl Environ Microbiol* 70:4079–4087
- Church M, Ducklow H, Letelier R, Karl D (2006) Temporal and vertical dynamics in picoplankton photoheterotrophic production in the subtropical North Pacific Ocean. *Aquat Microb Ecol* 45:41–53
- Clayton TD, Byrne RH (1993) Spectrophotometric seawater pH measurements: total hydrogen ion concentration scale calibration of m-cresol purple and at-sea results. *Deep Sea Res I* 40:2115–2129
- Corno G, Karl D, Church M, Letelier R, Lukas R, Bidigare R, Abbott M (2007) Impact of climate forcing on ecosystem processes in the North Pacific Subtropical Gyre. *J Geophys Res* 112:C4
- Dickson AG (1990) Standard potential of the reaction: AgCl(s) + 1/2H<sub>2</sub>(g) = Ag(s) + HCl(aq), and the standard acidity constant of the ion HSO<sub>4</sub><sup>-</sup> in synthetic sea water from 273.15 to 318.15 K. *J Chem Thermodyn* 22:113–127
- Dickson AG, Sabine CL, Christian JR (2007) *Guide to best practices for ocean CO<sub>2</sub> measurements*. PICES Special Publication 3, 191 pp
- Doney SC, Fabry VJ, Feely RA, Kleypas JA (2009) Ocean acidification: the other CO<sub>2</sub> problem. *Annu Rev Mar Sci* 1:169–192

- Dore J, Lukas R, Sadler D, Church M, Karl D (2009) Physical and biogeochemical modulation of ocean acidification in the central North Pacific. *Proc Natl Acad Sci USA* 106:12235–12240
- Egge J, Thingstad T, Larsen A, Engel A, Wohlers J, Bellerby R, Riebesell U (2009) Primary production during nutrient-induced blooms at elevated CO<sub>2</sub> concentrations. *Biogeosciences* 6:877–885
- Endres S, Galgani L, Riebesell U, Schulz K-G, Engel A (2014) Stimulated bacterial growth under elevated pCO<sub>2</sub>: Results from an off-shore mesocosm study. *PLoS ONE* 9:e99228
- Engel A (2002) Direct relationship between CO<sub>2</sub> uptake and transparent exopolymer particles production in natural phytoplankton. *J Plankton Res* 24:49–53
- Engel A, Borchard C, Piontek J, Schulz KG, Riebesell U, Bellerby R (2013) CO<sub>2</sub> increases <sup>14</sup>C primary production in an Arctic plankton community. *Biogeosciences* 10:1291–1308
- Fu F, Warner M, Zhang Y, Feng Y, Hutchins D (2007) Effects of increased temperature and CO<sub>2</sub> on photosynthesis, growth, and elemental ratios in marine *Synechococcus* and *Prochlorococcus* (Cyanobacteria). *J Phycol* 43:485–496
- Gattuso J-P, Epitalon J-M, Lavigne H, Orr J, Gentili B, Hofmann A, Proye A, Soetaert K, Rae J (2015) seacarb: Seawater Carbonate Chemistry. R package version 3.0.8. <http://CRAN.R-project.org/package=seacarb>
- Giordano M, Beardall J, Raven JA (2005) CO<sub>2</sub> concentrating mechanisms in algae: Mechanisms, environmental modulation, and evolution. *Ann Rev Plant Biol* 56:99–131
- Goldman JC, McGillicuddy DJ (2003) Effect of large marine diatoms growing at low light on episodic new production. *Limnol Oceanogr* 48:1176–1182
- Grossart H, Allgaier M, Passow U, Riebesell U (2006) Testing the effect of CO<sub>2</sub> concentration on the dynamics of marine heterotrophic bacterioplankton. *Limnol Oceanogr* 51:1–11
- Hein M, Sand-Jensen K (1997) CO<sub>2</sub> increases oceanic primary production. *Nature* 388:526–527
- Hendriks IE, Duarte CM, Álvarez M (2010) Vulnerability of marine biodiversity to ocean acidification: A meta-analysis. *Estuarine, Coastal and Shelf Science* 86:157–164
- Hutchins D, Fu F, Zhang Y, Warner M, Feng Y, Portune K, Bernhardt P, Mulholland M (2007) CO<sub>2</sub> control of *Trichodesmium* N<sub>2</sub> fixation, photosynthesis, growth rates, and elemental ratios: Implications for past, present, and future ocean biogeochemistry. *Limnol Oceanogr* 52:1293–1304
- IPCC (2014) Summary for Policymakers. In: Field CB, Barros VR, Dokken DJ, Mach KJ, Mastrandrea MD, Bilir TE, Chatterjee M, Ebi KL, Estrada YO, Genova RC, Girma B, Kissel ES, Levy AN, MacCracken S, Mastrandrea PR, White LL (eds) *Climate Change 2014: Impacts, Adaptation, and Vulnerability. Part A: Global and Sectoral Aspects*.

*Contribution of Working Group II to the Fifth Assessment Report of the Intergovernmental Panel on Climate Change.* Cambridge University Press, Cambridge, United Kingdom, and New York, NY, USA, p 1–32

- Joint I, Doney SC, Karl DM (2011) Will ocean acidification affect marine microbes? *ISME J* 5:1–7
- Kim J-M, Lee K, Shin K, Yang EJ, Engel A, Karl DM, Kim H-C (2011) Shifts in biogenic carbon flow from particulate to dissolved forms under high carbon dioxide and warm ocean conditions. *Geophys Res Lett* 38:L08612
- Kirchman D, K'nees E, Hodson R (1985) Leucine incorporation and its potential as a measure of protein synthesis by bacteria in natural aquatic systems. *Appl Environ Microbiol* 49:599–607
- Krause E, Wichels A, Giménez L, Lunau M, Schilhabel MB, Gerdt G (2012) Small changes in pH have direct effects on marine bacterial community composition: a microcosm approach. *PLoS ONE* 7:e47035
- Langer G, Geisen M, Baumann K-H, Kläs J, Riebesell U, Thoms S, Young JR (2006) Species-specific responses of calcifying algae to changing seawater carbonate chemistry. *Geochem Geophys Geosyst* 7:Q09006
- Li B, Karl DM, Letelier RM, Church MJ (2011) Size-dependent photosynthetic variability in the North Pacific Subtropical Gyre. *Mar Ecol Prog Ser* 440:27–40
- Liu H, Nolla H, Campbell L (1997) *Prochlorococcus* growth rate and contribution to primary production in the equatorial and subtropical North Pacific Ocean. *Aquat Microb Ecol* 12:39–47
- Liu J, Weinbauer M, Maier C, Dai M, Gattuso J (2010) Effect of ocean acidification on microbial diversity and on microbe-driven biogeochemistry and ecosystem functioning. *Aquat Microb Ecol* 61:291–305
- Lomas MW, Hopkinson BM, Losh JL, Ryan DE, Shi DL, Xu Y, Morel FMM (2012) Effect of ocean acidification on cyanobacteria in the subtropical North Atlantic. *Aquat Microb Ecol* 66:211–222
- Lueker TJ, Dickson AG, Keeling CD (2000) Ocean  $p\text{CO}_2$  calculated from dissolved inorganic carbon, alkalinity, and equations for  $K_1$  and  $K_2$ : validation based on laboratory measurements of  $\text{CO}_2$  in gas and seawater at equilibrium. *Mar Chem* 70:105–119
- MacGilchrist GA, Shi T, Tyrrell T, Richier S, Moore CM, Dumousseaud C, Achterberg EP (2014) Effect of enhanced  $p\text{CO}_2$  levels on the production of dissolved organic carbon and transparent exopolymer particles in short-term bioassay experiments. *Biogeosciences* 11:3695–3706

- Newbold LK, Oliver AE, Booth T, Tiwari B, DeSantis T, Maguire M, Andersen G, Gast CJ van der, Whiteley AS (2012) The response of marine picoplankton to ocean acidification. *Environ Microbiol* 14:2293–2307
- Orr JC, Fabry VJ, Aumont O, Bopp L, Doney SC, Feely RA, Gnanadesikan A, Gruber N, Ishida A, Joos F, Key RM, Lindsay K, Maier-Reimer E, Matear R, Monfray P, Mouchet A, Najjar RG, Plattner G-K, Rodgers KB, Sabine CL, Sarmiento JL, Schlitzer R, Slater RD, Totterdell IJ, Weirig M-F, Yamanaka Y, Yool A (2005) Anthropogenic ocean acidification over the twenty-first century and its impact on calcifying organisms. *Nature* 437:681–686
- Perez FF, Fraga F (1987) Association constant of fluoride and hydrogen ions in seawater. *Mar Chem* 21:161–168
- Piontek J, Borchard C, Sperling M, Schulz KG, Riebesell U, Engel A (2013) Response of bacterioplankton activity in an Arctic fjord system to elevated  $p\text{CO}_2$ : results from a mesocosm perturbation study. *Biogeosciences* 10:297–314
- Piontek J, Lunau M, Händel N, Borchard C, Wurst M, Engel A (2010) Acidification increases microbial polysaccharide degradation in the ocean. *Biogeosciences* 7:1615–1624
- Raven J (1997) The role of marine biota in the evolution of terrestrial biota: Gases and genes - Atmospheric composition and evolution of terrestrial biota. *Biogeochemistry* 39:139–164
- R Development Core Team (2008) *R: A Language and Environment for Statistical Computing*. R Foundation for Statistical Computing, Vienna, Austria
- Richier S, Achterberg EP, Dumousseaud C, Poulton AJ, Suggett DJ, Tyrrell T, Zubkov MV, Moore CM (2014) Phytoplankton responses and associated carbon cycling during shipboard carbonate chemistry manipulation experiments conducted around Northwest European shelf seas. *Biogeosciences* 11:4733–4752
- Riebesell U, Zondervan I, Rost B, Tortell PD, Zeebe RE, Morel FMM (2000) Reduced calcification of marine plankton in response to increased atmospheric  $\text{CO}_2$ . *Nature* 407:364–367
- Riser S, Johnson K (2008) Net production of oxygen in the subtropical ocean. *Nature* 451:323–U5
- Sabine CL, Feely RA, Gruber N, Key RM, Lee K, Bullister JL, Wanninkhof R, Wong CS, Wallace DWR, Tilbrook B, Millero FJ, Peng T-H, Kozyr A, Ono T, Rios AF (2004) The oceanic sink for anthropogenic  $\text{CO}_2$ . *Science* 305:367–371
- Shulenberger E, Reid JL (1981) The Pacific shallow oxygen maximum, deep chlorophyll maximum, and primary productivity, reconsidered. *Deep Sea Res I* 28:901–919
- Simon M, Azam F (1989) Protein content and protein synthesis rates of planktonic marine bacteria. *Mar Ecol Prog Ser* 51:201–213

- Smith DC, Azam F (1992) A simple, economical method for measuring bacterial protein synthesis rates in seawater using  $^3\text{H}$ -leucine. *Mar Microb Food Webs* 6:107–114
- Tortell PD (2000) Evolutionary and ecological perspectives on carbon acquisition in phytoplankton. *Limnol Oceanogr* 45:744–750
- Tortell P, DiTullio G, Sigman D, Morel F (2002)  $\text{CO}_2$  effects on taxonomic composition and nutrient utilization in an Equatorial Pacific phytoplankton assemblage. *Mar Ecol Prog Ser* 236:37–43
- Tortell PD, Payne CD, Li Y, Trimborn S, Rost B, Smith WO, Riesselman C, Dunbar RB, Sedwick P, DiTullio GR (2008)  $\text{CO}_2$  sensitivity of Southern Ocean phytoplankton. *Geophys Res Lett* 35:L04605
- Uppström LR (1974) The boron/chlorinity ratio of deep-sea water from the Pacific Ocean. *Deep Sea Res I* 21:161–162
- Winn CD, Li Y-H, Mackenzie FT, Karl DM (1998) Rising surface ocean dissolved inorganic carbon at the Hawaii Ocean Time-series site. *Mar Chem* 60:33–47
- Wolf-Gladrow DA, Riebesell U, Burkhardt S, Bijma J (1999) Direct effects of  $\text{CO}_2$  concentration on growth and isotopic composition of marine plankton. *Tellus B* 51:461–476
- Yamada N, Suzumura M (2010) Effects of seawater acidification on hydrolytic enzyme activities. *J Oceanogr* 66:233–241
- Yoshimura T, Nishioka J, Suzuki K, Hattori H, Kiyosawa H, Watanabe YW (2010) Impacts of elevated  $\text{CO}_2$  on organic carbon dynamics in nutrient depleted Okhotsk Sea surface waters. *J Exp Mar Biol Ecol* 395:191–198
- Zark M, Riebesell U, Dittmar T (2015) Effects of ocean acidification on marine dissolved organic matter are not detectable over the succession of phytoplankton blooms. *Sci Adv* 1:e1500531
- Zeebe RE, Zachos JC, Caldeira K, Tyrrell T (2008) Carbon emissions and acidification. *Science* 321:51–52

**Table 4.1.** Near-surface ocean (5 m) temperatures, rates of  $^{14}\text{C}$ -PP, concentrations of chlorophyll *a*, nutrients, and carbonate system properties during those months when experiments were conducted for this study.

Month	Year	Station	T (°C)	Chl <i>a</i> ( $\mu\text{g L}^{-1}$ )	$^{14}\text{C}$ -PP ( $\mu\text{mol C L}^{-1} \text{d}^{-1}$ )	N+N ( $\text{nmol L}^{-1}$ )	SRP ( $\text{nmol L}^{-1}$ )	DIC ( $\mu\text{mol L}^{-1}$ )	TA ( $\mu\text{mol L}^{-1}$ )	pH	$p\text{CO}_2$ ( $\mu\text{atm}$ )
June	2010	ALOHA	24.7	0.06	0.26	3	62	2018	2336	8.069	376
August	2010	ALOHA	25.5	0.05	0.29	3	105	1997	2326	8.079	364
August	2010	S1	26.1	0.13	0.63	ND	ND	2041	2357	8.039	419
August	2010	S2	26.0	0.14	0.93	ND	ND	2009	2330	8.052	400
September	2010	ALOHA	25.6	0.07	ND	4	86	1998	2323	8.069	373
October	2010	ALOHA	26.0	0.08	0.42	3	65	1997	2323	8.065	377
January	2011	ALOHA	23.7	0.05	0.21	8	50	2012	2333	8.089	355
March	2011	ALOHA	24.4	0.07	0.43	3	68	1997	2324	8.092	351
April	2011	ALOHA	24.0	0.06	0.17	5	103	1993	2312	8.089	353
September	2012	ALOHA	25.5	0.06	0.32	8	123	1999	2306	8.048	377

**Table 4.2.** Percent differences between  $p\text{CO}_2$  elevated treatments (1100 ppm unless noted) and controls ( $[\text{CO}_2 \text{ perturbed} - \text{control}] / \text{control}$ ) in bubbling experiments for  $^{14}\text{C}\text{-PP}$ ,  $^3\text{H}\text{-Leu}_{\text{Dark}}$ , and  $^3\text{H}\text{-Leu}_{\text{Light}}$ . Differences between control and perturbed for the full experiment are reported as p-values (two-way ANOVA). NSD = not significantly different at  $p > 0.05$ , ND = no data.

Start date	time (hrs)	$^{14}\text{C}\text{-PP}$ (% difference)	p-value	$^3\text{H}\text{-Leu}_{\text{Dark}}$ (% difference)	p-value	$^3\text{H}\text{-Leu}_{\text{Light}}$ (% difference)	p-value
Aug. 6, 2010	0	14		ND		ND	
	24	94 ±34		ND		ND	
	48	58 ±147	NSD	ND		ND	
Aug. 21, 2010 (750 ppm)	0	0 ±33		19 ±16		-4 ±10	
	24	-27 ±26	NSD	143 ±62	<0.005	129 ±92	NSD
Aug. 21, 2010	0	37 ±35		31 ±57		19 ±52	
	24	-35 ±27	NSD	60 ±76	NSD	58 ±77	NSD
Aug. 23, 2010	0	10.2		153		97	
	24	-52 ±46	NSD	-4 ±15		-7 ±12	
	48	ND		-35 ±39	NSD	-30 ±17	NSD
Sep. 3, 2010	0	14		ND		ND	
	24	18 ±17		ND		ND	
	48	-7 ±45	NSD	ND		ND	
Oct. 3, 2010	0	-57		-19		ND	
	48	16 ±65		18 ±10		ND	
	72	-52 ±9	NSD	29 ±57	NSD	ND	
Jan. 11, 2011	0	-30		-13		11	
	48	-14		-3		27	
	96	121	NSD	-11		-16	
Mar. 3, 2011	0	-7		-1		-26	
	48	-14 ±20		3 ±8		2 ±8	
	72	-26 ±38	NSD	16 ±8	NSD	-4 ±5	NSD
Mar. 17, 2011	0	-4		-9		1	
	48	102 ±13		1 ±7		-26 ±14	
	96	123 ±48	NSD	9 ±16	NSD	11 ±5	NSD
Apr. 15, 2011	0	-5		ND		ND	
	24	-70 ±36		ND		ND	
	48	-50 ±58	0.039	ND		ND	
Sep. 6, 2012	0	-31 ±32		-35 ±23		-36 ±26	
	24	-52 ±46		7 ±36		3 ±44	
	72	-31 ±44	0.016	-26 ±6	NSD	-31 ±12	NSD

**Table 4.3.** Depth-integrated rates of  $^{14}\text{C}$ -PP measured under both ambient (<390 ppm at depths shallower than 45 m) and enhanced  $p\text{CO}_2$  (750 ppm) conditions in both upper (0–45 m) and lower euphotic zones (75–125 m) for three plankton size fractions, as well as the sum of the filter fractions. Significant differences between control and perturbed rates indicated by letters (two-sample t-Test).

Date - treatment	$^{14}\text{C}$ -PC	$^{14}\text{C}$ -PC	$^{14}\text{C}$ -PC	$^{14}\text{C}$ -PC	$^{14}\text{C}$ -PC	$^{14}\text{C}$ -PC	$^{14}\text{C}$ -PC	$^{14}\text{C}$ -PC	$^{14}\text{C}$ -PC	$^{14}\text{C}$ -PC
	10 $\mu\text{m}$ (mmol C $\text{m}^{-2} \text{d}^{-1}$ )	10 $\mu\text{m}$ (mmol C $\text{m}^{-2} \text{d}^{-1}$ )	10 $\mu\text{m}$ (mmol C $\text{m}^{-2} \text{d}^{-1}$ )	2 $\mu\text{m}$ (mmol C $\text{m}^{-2} \text{d}^{-1}$ )	2 $\mu\text{m}$ (mmol C $\text{m}^{-2} \text{d}^{-1}$ )	2 $\mu\text{m}$ (mmol C $\text{m}^{-2} \text{d}^{-1}$ )	0.2 $\mu\text{m}$ (mmol C $\text{m}^{-2} \text{d}^{-1}$ )	0.2 $\mu\text{m}$ (mmol C $\text{m}^{-2} \text{d}^{-1}$ )	0.2 $\mu\text{m}$ (mmol C $\text{m}^{-2} \text{d}^{-1}$ )	
	0-45	75-125	0-125	0-45	75-125	0-125	0-45	75-125	0-125	
Aug. 21, 2010										
390 ppm	1.6±0.1	A 0.3±0.0	B 2.5±0.1	2.6±0.2	0.5±0.0	C 4.6±0.2	A 3.9±0.7	4.5±0.1	A 11.8±1.0	
750 ppm	1.8±0.1	0.5±0.0	3.1±0.6	3.2±0.3	0.6±0.0	5.3±0.3	4.1±0.8	4.2±0.2	11.7±0.8	
Aug. 26, 2010										
390 ppm	14.0±1.0	A 0.2±0.0	16.8±1.0	A 5.9±0.3	0.4±0.0	8.0±0.3	8.8±1.0	3.4±0.3	16.7±1.0	
750 ppm	11.9±0.7	0.2±0.0	13.7±0.7	6.8±1.0	0.4±0.0	8.6±1.0	9.0±1.1	3.0±0.2	15.8±1.4	
Aug. 28, 2010										
390 ppm	17.5±2.3	0.4±0.5	18.8±2.3	3.5±0.5	0.5±0.1	5.2±0.5	13.2±0.6	A 3.2±0.1	20.8±0.6	A
750 ppm	17.7±1.5	0.3±0.1	18.7±1.5	3.1±0.1	0.5±0.0	4.7±0.2	11.2±0.8	2.9±0.2	18.1±0.9	
Mar. 14, 2011										
390 ppm	1.4±0.4	0.3±0.0	2.3±0.4	2.1±0.2	0.8±0.1	4.1±0.2	6.0±1.3	4.0±0.3	13.3±1.3	
750 ppm	1.3±0.2	0.3±0.0	2.2±0.2	2.2±0.3	0.9±0.1	4.4±0.3	4.5±0.6	4.4±0.3	13.1±1.2	
Mar. 16, 2011										
390 ppm	1.0±0.2	0.3±0.0	2.0±0.2	1.8±0.2	0.7±0.1	3.5±0.3	3.8±1.9	3.5±1.3	10.3±2.4	
750 ppm	1.0±0.2	0.3±0.0	1.8±0.2	1.6±0.1	0.8±0.1	3.6±0.3	5.9±1.0	2.4±0.6	11.9±1.6	

A:  $p < 0.05$

B:  $p < 0.0001$

C:  $P < 0.01$

**Table 4.4.** Depth-integrated rates of  $^3\text{H}$ -Leu (light and dark) incubated under both ambient (390 ppm) and enhanced  $p\text{CO}_2$  (750 ppm) for both the upper (0–45 m), lower (75–125 m), and full euphotic zone (0–125 m). Significant differences between control and perturbed rates indicated by letters (two-sample t-Test).

Date - treatment	$^3\text{H}$ -Leu <sub>Dark</sub> (nmol Leu $\text{m}^{-2} \text{h}^{-1}$ )		$^3\text{H}$ -Leu <sub>Dark</sub> (nmol Leu $\text{m}^{-2} \text{h}^{-1}$ )		$^3\text{H}$ -Leu <sub>Dark</sub> (nmol Leu $\text{m}^{-2} \text{h}^{-1}$ )		$^3\text{H}$ -Leu <sub>Light</sub> (nmol Leu $\text{m}^{-2} \text{h}^{-1}$ )		$^3\text{H}$ -Leu <sub>Light</sub> (nmol Leu $\text{m}^{-2} \text{h}^{-1}$ )		$^3\text{H}$ -Leu <sub>Light</sub> (nmol Leu $\text{m}^{-2} \text{h}^{-1}$ )	
	0-45 m	75-125 m	0-125 m	0-45 m	75-125 m	0-125 m	0-45 m	75-125 m	0-125 m			
Aug. 21, 2010												
390 ppm	272±9	A	216 ±6	643 ±11	B	321±12	271±10	A	849 ±16	C		
750 ppm	246±9		193±11	581±14		306±7	242±8		763 ±13			
Aug. 26, 2010												
390 ppm	574±27		106±2	923±28		776±12	D	234±1	C	732±18	C	
750 ppm	522±24		126±33	887 ±41		698 ±20		194±4		574±19		
Aug. 28, 2010												
390 ppm	611±23		130±4	926±24		825 ±36	A	252 ±3	E	720±35	C	
750 ppm	637±17		137±35	947±45		743±23		178±6		575±15		
Mar. 14, 2011												
390 ppm	176±4		119±4	389±6		286±6	D	272±17	A	1359 ±16	E	
750 ppm	173±13		118±1	391±15		208±16		190±2		1233±22		
Mar. 16, 2011												
390 ppm	193±9	A	96±4	387±11	C	305±33		223±7		1402±38	D	
750 ppm	156±12		99±5	330±13		232±7		218±3		1158±25		

A:  $p < 0.05$

B:  $p < 0.01$

C:  $p < 0.005$

D:  $p < 0.01$

E:  $p < 0.0005$

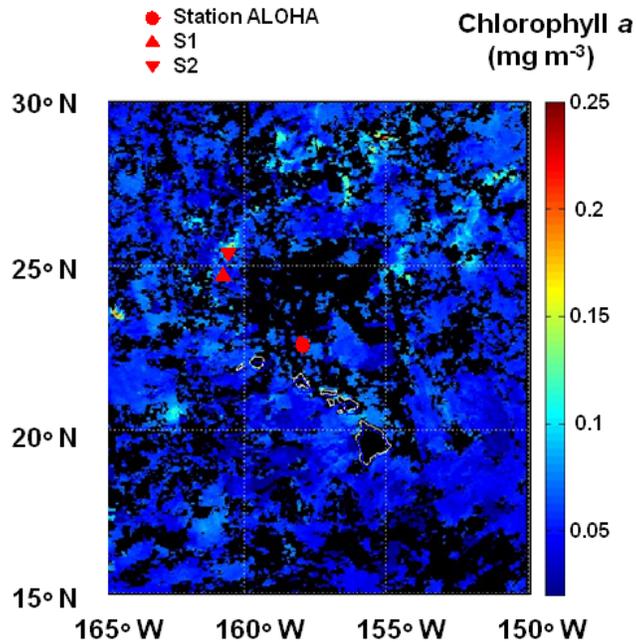


**Figure 4.1.** Satellite ocean color map depicting distributions and concentrations of near-surface ocean chlorophyll *a* (August 2010) in the proximity of the Hawaiian Islands. Image provided by Ricardo Letelier (Oregon State University; <http://omel-test.coas.oregonstate.edu/region/hawaii/satellite/>). Also shown are the locations of the three stations occupied in August 2010. Location of Station ALOHA is depicted as a red circle, while stations S1 and S2 are depicted by a red triangle and red inverted triangle, respectively.

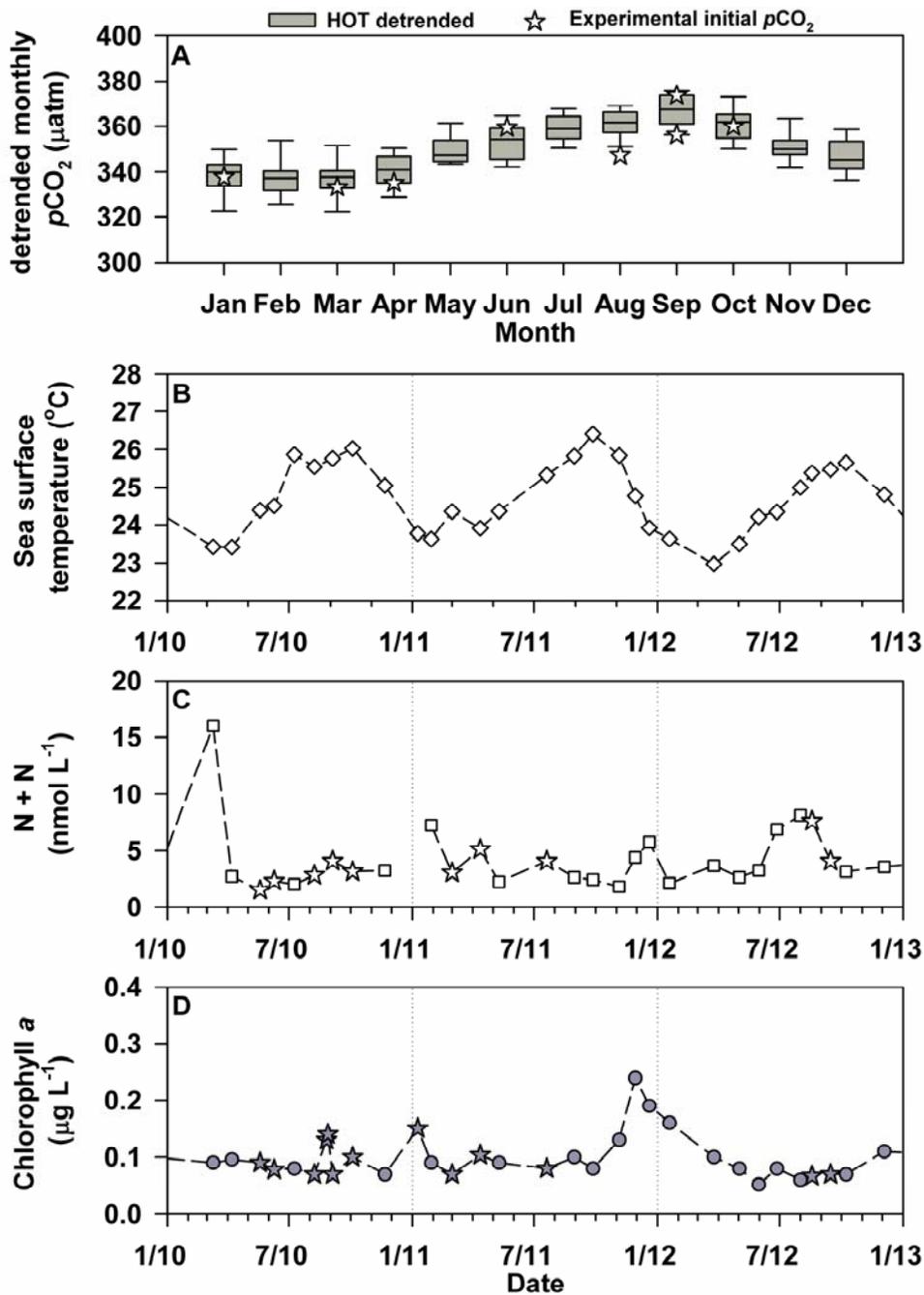


**Figure 4.2.** Long-term (multi-decadal) detrended monthly ALOHA surface ocean  $p\text{CO}_2$  (Dore et al. 2009) with stars depicting detrended  $p\text{CO}_2$  during months when experiments were conducted (panel A). Whiskers of boxes depict the 10<sup>th</sup> and 90<sup>th</sup> percentiles of the observations, box boundaries are 25<sup>th</sup> and 75<sup>th</sup> percentiles, and median value depicted by central line. Sea surface temperature (SST) at Station ALOHA during this study (2010–2012; panel B). Also shown are monthly concentrations of nitrate + nitrite (N+N; white symbols; panel C) and of chlorophyll *a* (dark grey symbols; panel D) at 5 meters. Stars indicate initial conditions when bubbling experiments were conducted.

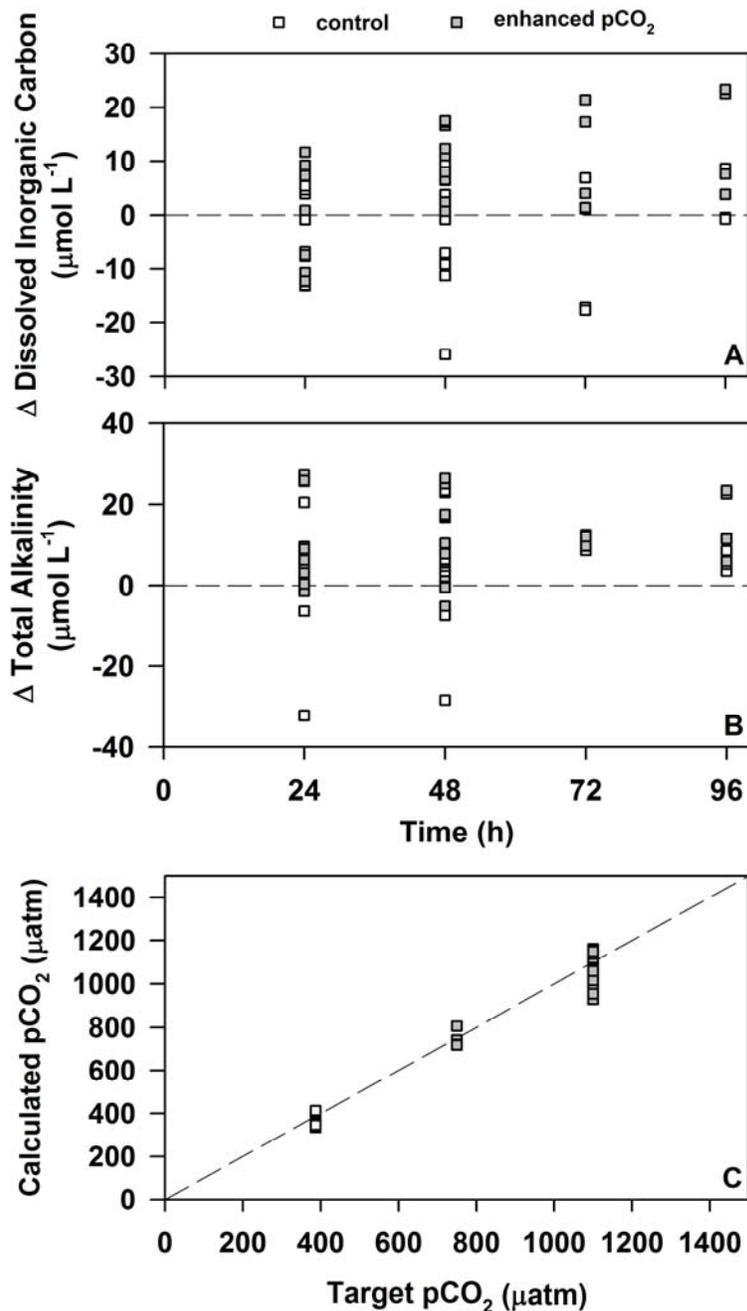


**Figure 4.3.** Comparison of seawater carbonate system properties during the time course experiments conducted for this study. Change in dissolved inorganic carbon (DIC) relative to time zero at each of the time points sampled during the bubbling experiments (panel A), as well as change in the total alkalinity (TA) between time zero and each of the time points (panel B) are shown for both control and enhanced  $p\text{CO}_2$  samples. Also shown are the differences between the target  $p\text{CO}_2$  and the  $p\text{CO}_2$  calculated from the DIC and TA measurements during the bubbling experiments (panel C).

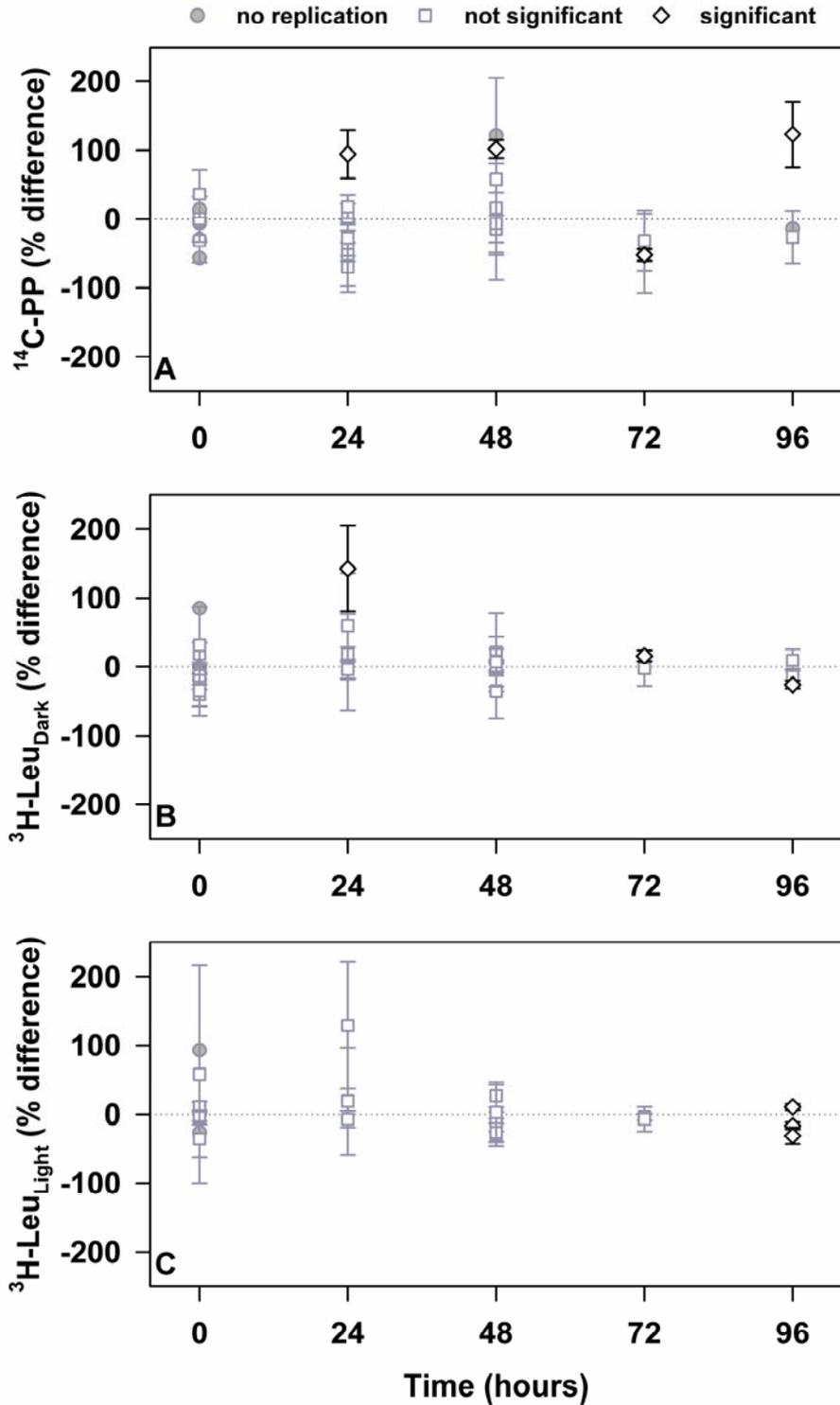


**Figure 4.4.** Percent differences ( $[(\text{perturbed} - \text{control}) / \text{control}]$ ) between control and perturbed treatments from all  $p\text{CO}_2$  bubbling experiments during this study for  $^{14}\text{C-PP}$  (panel A),  $^3\text{H-Leu}_{\text{Dark}}$  (panel B),  $^3\text{H-Leu}_{\text{Light}}$  (panel C) at each time point. Grey circle symbols indicate percent difference measurements that were not replicated, grey squares are percent differences that are not significantly different than 0, and black diamonds indicate the percent difference between control and perturbed was significantly above or below zero.

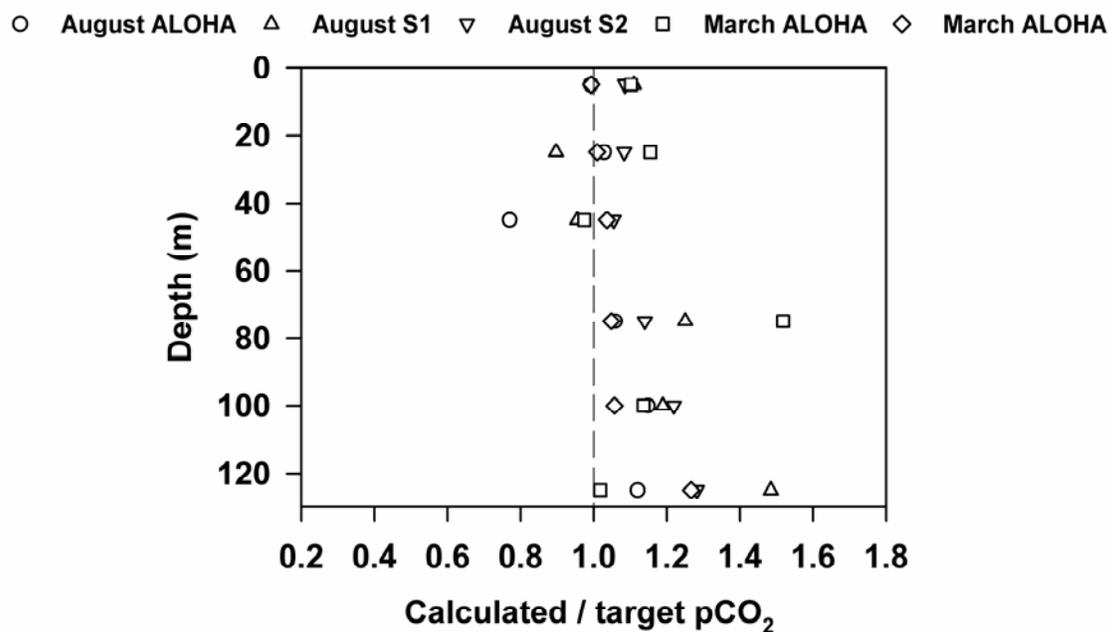


**Figure 4.5.** Ratio of calculated  $p\text{CO}_2$  versus the targeted  $p\text{CO}_2$  from the *in situ* array experiments. Dotted line depicts the 1:1 ratio.

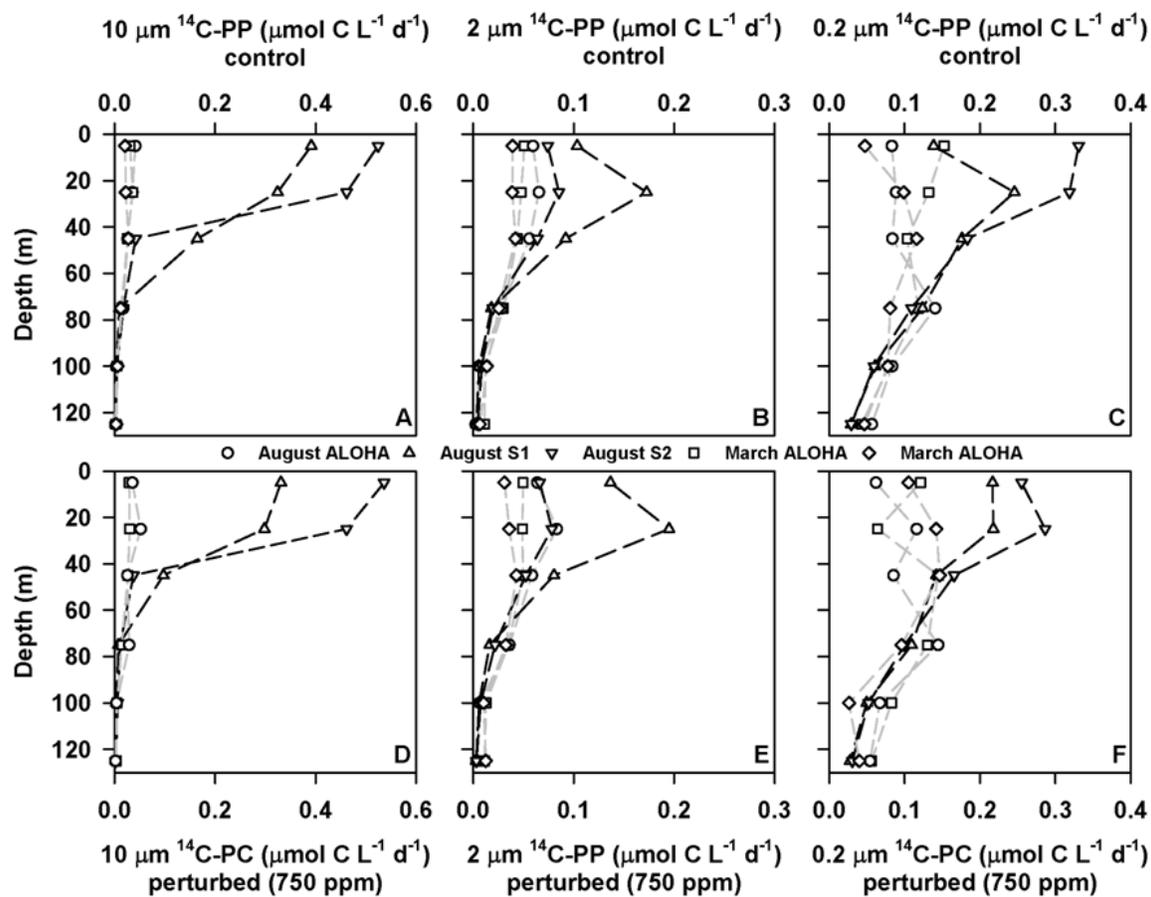


**Figure 4.6.** Depth-resolved measurements of size fractionated  $^{14}\text{C-PP}$  during cruises in August 2010 and March 2011. Rates of  $^{14}\text{C-PP}$  in the  $>10 \mu\text{m}$  size fraction under shown under ambient ( $<390 \text{ ppm}$ ; control) (panel A) and elevated  $p\text{CO}_2$  (750 ppm) conditions (panel D). Also shown, are rates of  $^{14}\text{C-PP}$  in the  $2\text{--}10 \mu\text{m}$  size class under ambient and elevated  $p\text{CO}_2$  (panels B and E, respectively). Also depicted are  $^{14}\text{C-PP}$  rates in the  $0.2\text{--}2 \mu\text{m}$  size class under ambient and elevated  $p\text{CO}_2$  (panels C and F, respectively).

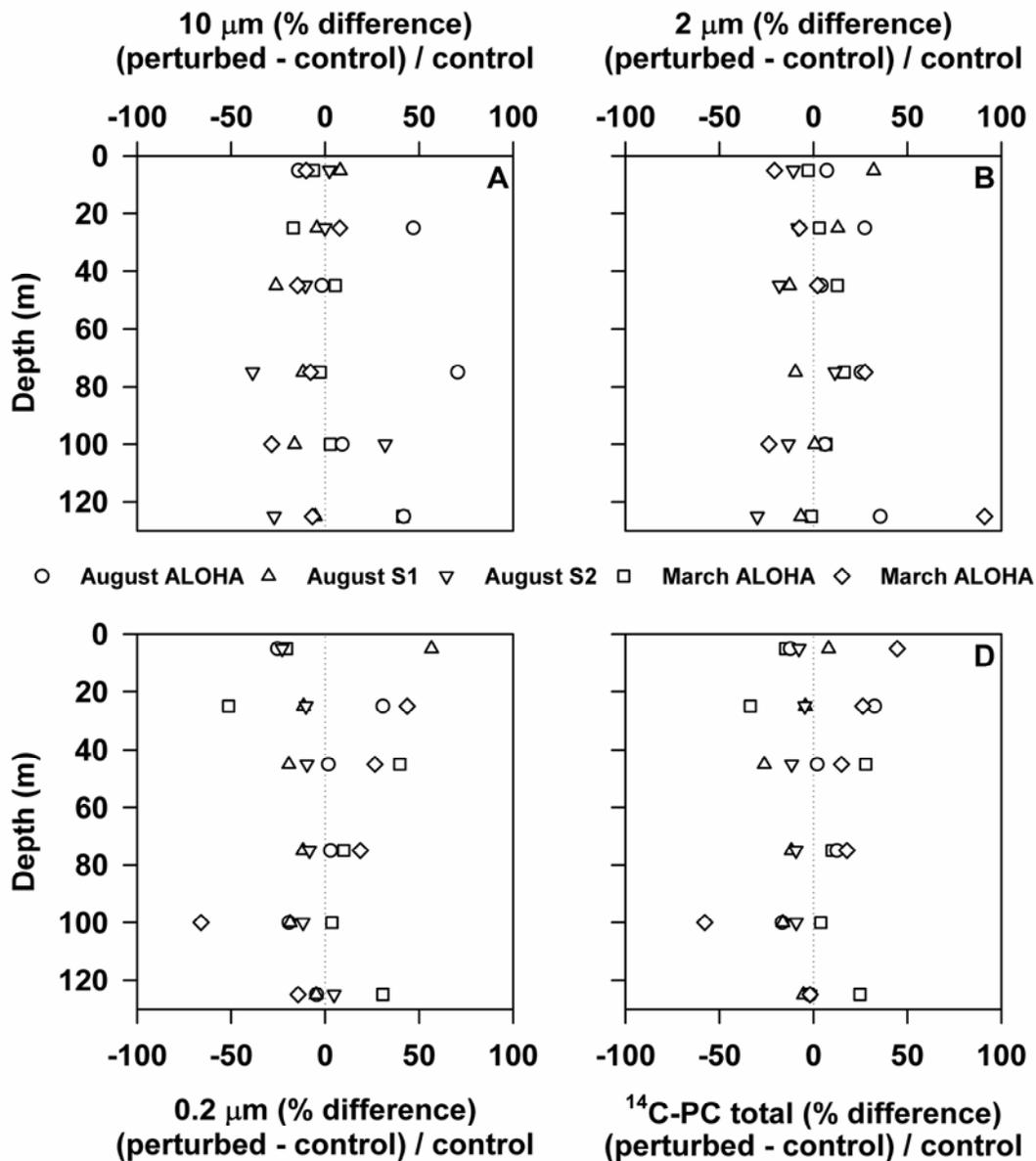


**Figure 4.7.** Shown are the relationships between control (<math>< 390 \text{ ppm}</math>) and elevated 10 \mu\text{m} size fraction (panel A), the  $2\text{--}10 \mu\text{m}$  size class (panel B), the  $0.2\text{--}2 \mu\text{m}$  size class (panel C), and the sum total of all size classes (panel D). Dotted line depicts no difference between treatments and controls.

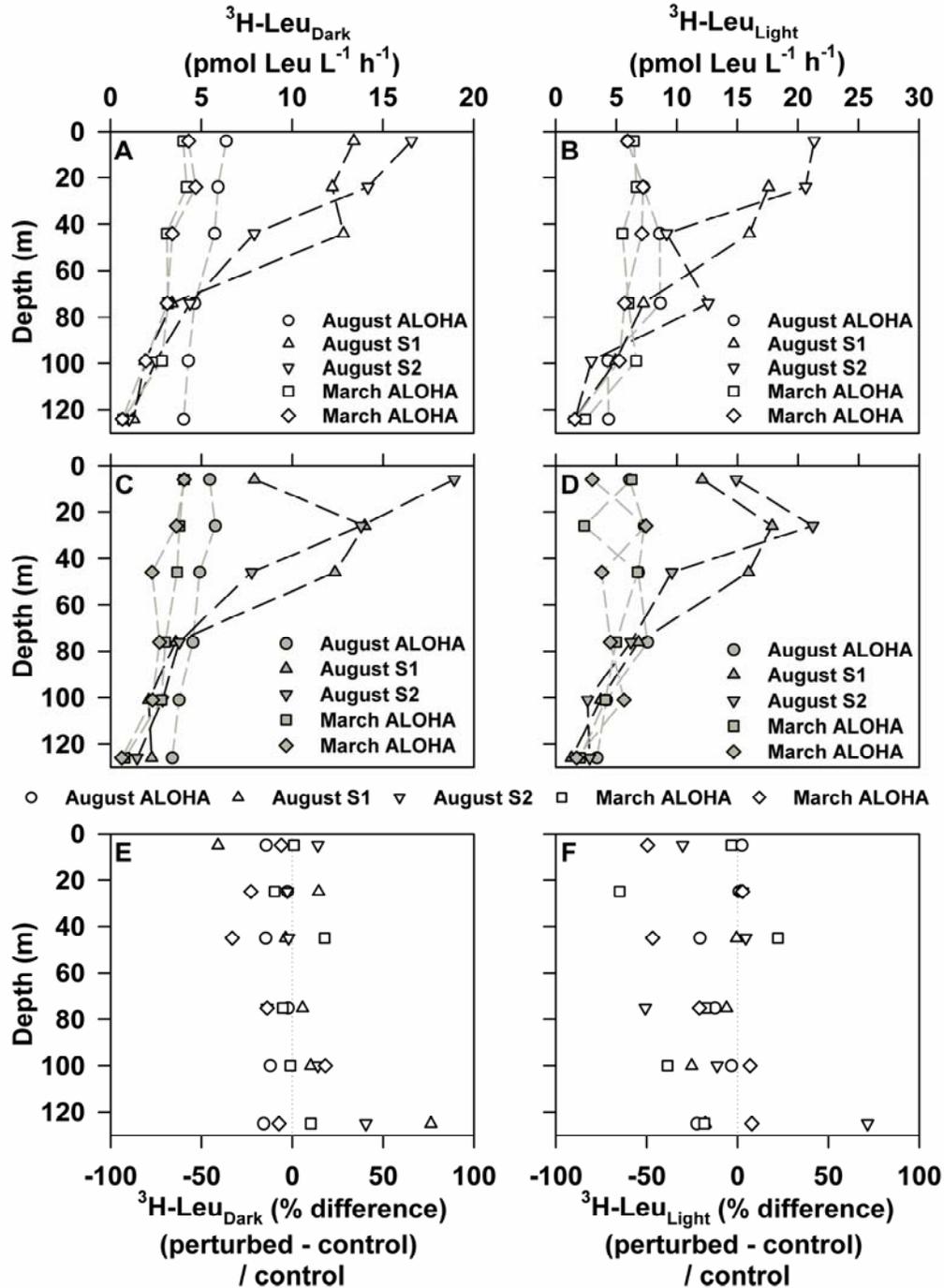


**Figure 4.8.** Rates of  $^3\text{H}$ -leucine incorporation (pmol Leu L<sup>-1</sup> h<sup>-1</sup>) in both light and dark for cruises in August 2010 and March 2011. Rates in the dark for both ambient and enhanced (750 ppm  $p\text{CO}_2$ ) are shown (panels A and C, respectively), as are rates in the light for both ambient and enhanced  $p\text{CO}_2$  (panels B and D, respectively). Also shown are percent differences between treatments ( $[\text{perturbed} - \text{control}] / \text{control}$ ) for  $^3\text{H}\text{-Leu}_{\text{Dark}}$  (panel E),  $^3\text{H}\text{-Leu}_{\text{Light}}$  (panel F).

## CHAPTER 5 - Conclusions

The overarching goals of my dissertation were to determine rates of photosynthetic carbon fixation and bacterial production (via leucine incorporation), and evaluate temporal variability and coupling between these rates in the contemporary oligotrophic North Pacific Subtropical Gyre (NPSG). In addition, I examined the sensitivity of these processes to abrupt changes in the seawater carbonate system. To pursue these goals, I designed and implemented three separate, but related projects described in the preceding chapters. Chapter 2 examined the partitioning of primary production between particulate and dissolved pools. For this project, I measured rates of particulate and dissolved organic carbon production at approximately monthly time scales *in situ* at Station ALOHA. Rates of primary production partitioned to the particulate phase showed depth-dependent behavior, with rates elevated in the well-lit regions of the euphotic zone and lower at depth. In contrast, rates of production partitioned to dissolved organic carbon (DOC) did not demonstrate depth-dependence. Similarly, use of a model fitting paired measurements of photosynthetically available radiation and rates of primary production (Platt et al. 1980) revealed information on the response of primary production to light, with rates of particulate matter production increasing linearly with light in the lower euphotic zone, and saturating in near-surface waters, while rates of DOC production demonstrated no significant relationship to changes in light intensity.

I also compared two different types of filters commonly used in aquatic ecology to separate dissolved and particulate phases of organic matter. Results from this comparison

revealed that rates of  $^{14}\text{C}$ -primary production measured using glass fiber filters (nominal pore size of  $0.7\ \mu\text{m}$ ) averaged 1.6-fold greater than coincident rates of  $^{14}\text{C}$ -primary production measured using polycarbonate membrane filters ( $0.2\ \mu\text{m}$  pore size). In contrast, concentrations of chlorophyll *a* did not demonstrate any significant differences among these filter types. Results from these experiments suggested that differences in rates of primary production measured on glass fiber versus polycarbonate membrane filters were a result of adsorption of DOC to the glass fiber filters, a finding consistent with previous studies evaluating retention characteristics of these filters (Maske & Garcia-Mendoza 1994, Karl et al. 1998, Morán et al. 1999).

The resulting depth-integrated (0–125 m) rates of  $^{14}\text{C}$ -primary production measured on glass fiber and polycarbonate membrane filters were well correlated in time. However, rates of dissolved organic carbon production did not co-vary in time with rates of production measured on either type of filter. Production of DOC represented  $\sim 18\%$  ( $\pm 10\%$ ) of total (i.e. particulate plus dissolved) primary production (Figure 5.1), but displayed significantly more temporal variability than rates of particulate production. In addition, while rates of particulate primary production were consistent between hourly rates measured during the morning and full photoperiod, declining at night, rates of DOC production were highest in the morning, and declined throughout the photoperiod and overnight. The decoupling of DOC and particulate primary production across various time scales, with depth, and with light, suggests that these rates are controlled by different factors. An obvious next step is to try to quantify the relative contributions to dissolved production of grazing, phytoplankton exudation, and viral lysis; it may be that time-variability in these processes (e.g. Winter et al. 2004, Boras et al. 2009) could explain the greater variability of dissolved production, as well as the decoupling between dissolved and particulate primary production.

Chapter 3 focused on the measurement of bacterial production at nested time scales of variability ranging from diel to daily to near-monthly to seasonal. For this study, I estimated rates of bacterial production based on  $^3\text{H}$ -leucine incorporation measured in both the light and dark. Rates of  $^3\text{H}$ -leucine were consistently photostimulated throughout the euphotic zone, with rates of production 1.5-fold greater (on average) in the light than in the dark. Rates of  $^3\text{H}$ -leucine incorporation were not significantly correlated to contemporaneous rates of primary production. Moreover, rates of bacterial production did not follow the same seasonal pattern as primary production, with bacterial production peaking in late summer or early fall and hence lagging primary production by several months.

During the summer of 2012, I also examined daily and diel scale changes in rates of bacterial production. During an intensive 62-day study where rates of  $^3\text{H}$ -leucine were measured at near-daily time scales, rates varied  $\sim 2$  and  $\sim 2.5$ -fold in the dark and light, respectively, but were not correlated with rates of primary production. The annual peak in bacterial production, when measured at monthly scales, corresponded with maximal sea surface temperatures, but over daily time scales rates of bacterial production declined during a period of time when sea surface temperature was still seasonally elevated. Over a two day period, rates of  $^3\text{H}$ -leucine incorporation were measured at  $\sim 4$  hour intervals, providing insight into diel scale changes in rates of bacterial production in the light and dark. When measured at diel time scales, rates of  $^3\text{H}$ -leucine incorporation measured in the light were greatest at midday, while rates measured in the dark were greatest at approximately sunset. On average, mean daily bacterial production represented  $\sim 46\%$  of average rate of DOC production (Figure 5.1). We still lack an explanation for the apparent temporal decoupling between rates of bacterial and primary production. New techniques that examine *in situ* patterns of gene transcription and enable the construction of

microbial community composition time-series may help shed light on the dynamics of these temporal lags between primary production and bacterial production. In particular, recent work conducted at in the NPSG suggests temporal synchronicity between phytoplankton and heterotrophic bacteria, where transcriptional maxima in *Prochlorococcus* photosystem genes were followed on the order of hours by a succession of transcript maxima in oxidative phosphorylation genes by heterotrophic bacteria (Ottesen et al. 2014, Aylward et al. 2015). These temporal lags at the transcriptional level could help explain why we observe temporal offsets in the measured rates.

Chapter 4 examined the effects of abrupt, large-scale changes to the seawater carbonate system. Included in this work were short-term (up to 96 hours) experiments where the  $p\text{CO}_2$  of near-surface seawater (5 m) was increased to 750 or 1100 ppm by gentle bubbling with a mixture of air and  $\text{CO}_2$ , and compared to controls bubbled with air. In these experiments, primary and bacterial production rates were measured approximately daily. The overall results of the bubbling experiments suggest that near-surface primary production and microbial growth rates are resilient to abrupt changes in the seawater carbonate system. Indeed, only 20% (2 of 10) of the experiments conducted as part of this study demonstrated any significant effect of elevated  $p\text{CO}_2$  on primary production. In both cases, these rates were depressed at elevated  $p\text{CO}_2$ . Similarly, only 14% (1 of 7) experiments demonstrated significant changes in rates of leucine incorporation, and in those experiments rates measured in the dark were elevated in the enhanced  $p\text{CO}_2$  treatment.

An additional 5 experiments were conducted to examine possible changes in  $^{14}\text{C}$ -primary production and  $^3\text{H}$ -leucine throughout the euphotic zone (0–125 m) to examine possible depth-dependent responses to elevated  $p\text{CO}_2$  over the course of the photoperiod. In contrast to the

bubbling experiments, in all the depth resolved experiments, rates of  $^3\text{H}$ -leucine incorporation (0–125 m) in the light were depressed in the elevated  $p\text{CO}_2$  treatments. Depth-integrated rates of leucine incorporation in the dark (0–125 m) were also depressed at elevated  $p\text{CO}_2$  in 2 of 5 experiments. Rates of size-fractionated (10, 2, and 0.2  $\mu\text{m}$ )  $^{14}\text{C}$ -primary production demonstrated less consistent patterns. On one array deployed at ALOHA in August, rates in the lower euphotic zone of the two larger size fractions (>10  $\mu\text{m}$  and 2–10  $\mu\text{m}$ ) were elevated at enhanced  $p\text{CO}_2$ , which may be related to super-saturation of oxygen in late summer below the mixed layer at Station ALOHA (Riser & Johnson 2008). Such results illustrate the importance of examining habitat conditions when assessing the effects of ocean acidification on rates measured from environmental samples. Also, while the >10 and 2–10  $\mu\text{m}$  size fraction rates ranged between depressed, elevated, and the more common no significant effect, primary production rates in the 0.2  $\mu\text{m}$  size fraction were only depressed or showed no significant effect. This result, combined with the inhibitory effect of elevated  $p\text{CO}_2$  on leucine incorporation in the light, suggests that the growth and metabolism of *Prochlorococcus* under elevated  $p\text{CO}_2$  may prove an interesting line of inquiry. In addition, future studies on the potential effects of changing  $p\text{CO}_2$  on rates of microbial community growth should also consider the effects of increasing temperature, as the literature (e.g. Rivkin & Legendre 2002), as well as my results from Chapter 3, suggest a relationship between bacterial growth and temperature.

The results from this dissertation suggest that photosynthetic production of DOC represents a significant, but highly variable fraction of total primary production in the NPSG. Rates of DOC and particulate primary production did not co-vary in time with each other. Neither of these rates of primary production co-vary in time with bacterial production, with the peak in yearly bacterial production appearing to lag primary production by one or two months.

Results from this dissertation also suggest that rates of primary production and bacterial growth in the NPSG are resilient to abrupt, large-scale changes to the seawater carbonate system.

## Literature cited

- Aylward FO, Eppley JM, Smith JM, Chavez FP, Scholin CA, DeLong EF (2015) Microbial community transcriptional networks are conserved in three domains at ocean basin scales. *Proc Natl Acad Sci* 112:5443–5448
- Boras JA, Sala MM, Vázquez-Domínguez E, Weinbauer MG, Vaqué D (2009) Annual changes of bacterial mortality due to viruses and protists in an oligotrophic coastal environment (NW Mediterranean). *Environ Microbiol* 11:1181–1193
- Karl D, Hebel D, Björkman K, Letelier R (1998) The role of dissolved organic matter release in the productivity of the oligotrophic North Pacific Ocean. *Limnol Oceanogr* 43:1270–1286
- Maske H, Garcia-Mendoza E (1994) Adsorption of dissolved organic matter to the inorganic filter substrate and its implications for <sup>14</sup>C uptake measurements. *Appl Environ Microbiol* 60:3887–3889
- Morán XAG, Gasol JM, Arin L, Estrada M (1999) A comparison between glass fiber and membrane filters for the estimation of phytoplankton POC and DOC production. *Mar Ecol Prog Ser* 187:31–41
- Ottesen EA, Young CR, Gifford SM, Eppley JM, Marin R, Schuster SC, Scholin CA, DeLong EF (2014) Multispecies diel transcriptional oscillations in open ocean heterotrophic bacterial assemblages. *Science* 345:207–212
- Platt T, Gallegos C, Harrison W (1980) Photoinhibition of photosynthesis in natural assemblages of marine phytoplankton. *J Mar Res* 38:687–701
- Riser S, Johnson K (2008) Net production of oxygen in the subtropical ocean. *Nature* 451:323–U5
- Rivkin RB, Legendre L (2002) Roles of food web and heterotrophic microbial processes in upper ocean biogeochemistry: Global patterns and processes. *Ecol Res* 17:151–159
- Winter C, Herndl GJ, Weinbauer MG (2004) Diel cycles in viral infection of bacterioplankton in the North Sea. *Aquat Microb Ecol* 35:207–216

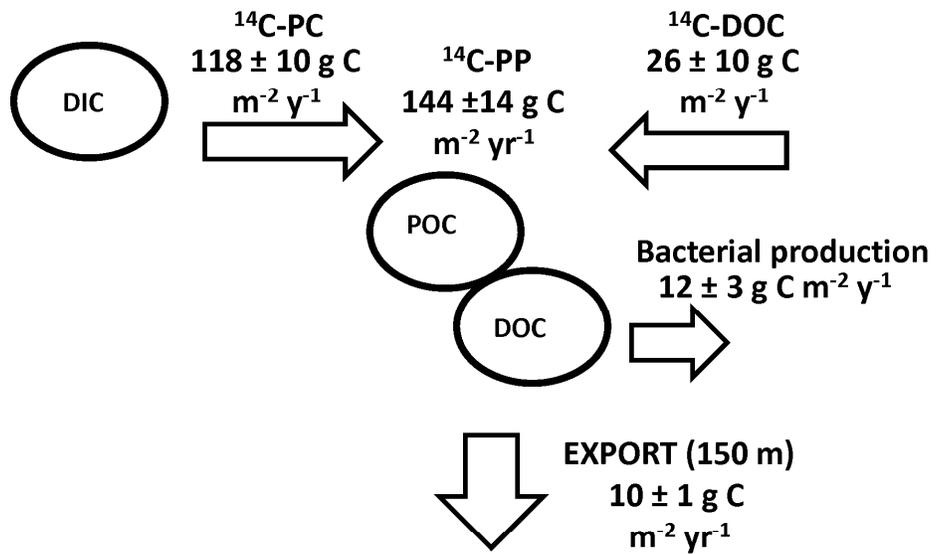


**Figure 5.1.** Schematic depicting rates of  $^{14}\text{C}$ -primary production constrained at Station ALOHA, both by the Hawaii Ocean Time-series program, and as part of this dissertation.